

A 4D IIB FLUX VACUUM AND SUPERSYMMETRY BREAKING

II. BOSONIC SPECTRUM AND STABILITY

J. MOURAD^a AND A. SAGNOTTI^b

^a*APC, UMR 7164-CNRS, Université Paris Cité
10 rue Alice Domon et Léonie Duquet
75205 Paris Cedex 13 FRANCE
e-mail: mourad@apc.univ-paris7.fr*

^b*Scuola Normale Superiore and INFN
Piazza dei Cavalieri, 7
56126 Pisa ITALY
e-mail: sagnotti@sns.it*

ABSTRACT

We recently constructed type-IIB compactifications to four dimensions depending on a single additional coordinate, where a five-form flux Φ on an internal torus leads to a constant string coupling. Supersymmetry is fully broken when the internal manifold includes a finite interval of length ℓ , which is spanned by a conformal coordinate in a finite range $0 < z < z_m$. Here we examine the low-lying bosonic spectra and their classical stability, paying special attention to self-adjoint boundary conditions. Special boundary conditions result in the emergence of zero modes, which are determined exactly by first-order equations. The different sectors of the spectrum can be related to Schrödinger operators on a finite interval, characterized by pairs of real constants μ and $\tilde{\mu}$, with μ equal to 1/3 or 2/3 in all cases and different values of $\tilde{\mu}$. The potentials behave as $\frac{\mu^2-1/4}{z^2}$ and $\frac{\tilde{\mu}^2-1/4}{(z_m-z)^2}$ near the ends and can be closely approximated by exactly solvable trigonometric ones. With vanishing internal momenta, one can thus identify a wide range of boundary conditions granting perturbative stability, despite the intricacies that emerge in some sectors. For the Kaluza-Klein excitations of non-singlet vectors and scalars the Schrödinger systems couple pairs of fields, and the stability regions, which depend on the background, widen as the ratio Φ/ℓ^4 decreases.

Contents

1	INTRODUCTION AND SUMMARY	4
2	SELF-ADJOINT EXTENSIONS AND SOLVABLE $(\mu, \tilde{\mu})$ POTENTIALS	11
2.1	ONE-DIMENSIONAL SECTORS	11
2.2	MATRIX GENERALIZATION OF THE SETUP	13
2.3	EXACTLY SOLVABLE HYPERGEOMETRIC POTENTIALS	16
2.4	A SIMPLE MATRIX GENERALIZATION OF THE HYPERGEOMETRIC MODEL	22
3	THE PERTURBED DILATON-AXION SYSTEM	24
4	THE PERTURBED TYPE-IIB THREE-FORMS	29
4.1	THE MODES ORIGINATING FROM $\mathcal{B}_{\mu\nu}$ AND $\mathcal{B}_{\mu r}$	33
4.2	THE MASSIVE SECTOR	35
4.3	THE MASSLESS SECTOR	38
4.3.1	THE CASE $d_4 U(x) = 0$	39
4.3.2	THE CASE $d_4 U(x) \neq 0$	40
4.4	The Modes Originating from $\mathcal{B}_{\mu i}$ and $\mathcal{B}_{r i}$	46
4.5	The Modes Originating from \mathcal{B}_{ij}	49
5	THE PERTURBED EINSTEIN - FIVE-FORM SYSTEM	51
5.1	PERTURBING THE TENSOR EQUATIONS	53
5.2	TENSOR GAUGE FIXING OF THE EINSTEIN-FIVE FORM SYSTEM	54
5.3	PERTURBING THE EINSTEIN EQUATIONS	56
6	TENSOR MODES DECOUPLED FROM GRAVITY PERTURBATIONS	58
6.1	$\mathbf{k} = 0$ TENSOR MODES	58
6.2	$\mathbf{k} \neq 0$ TENSOR MODES	63
7	SPIN-2 MODES FROM $h_{\mu\nu}$	66
8	SCALAR MODES FROM h_{ij}	67

9	SINGLET VECTOR MODES	68
9.1	$\mathbf{k} = 0$ MODES	69
9.2	$\mathbf{k} \neq 0$ MODES	70
10	NON-SINGLET VECTOR MODES	72
10.1	$\mathbf{k} = 0$ MODES	73
10.2	$\mathbf{k} \neq 0$ MODES	75
10.2.1	THE SCHRÖDINGER-LIKE SYSTEM	75
10.2.2	BOUNDARY CONDITIONS AND STABILITY ANALYSIS	77
11	NON-SINGLET SCALAR MODES	83
11.1	$\mathbf{k} = 0$ MODES	84
11.2	$\mathbf{k} \neq 0$ MODES	86
11.2.1	THE SCHRÖDINGER-LIKE SYSTEM	86
11.2.2	BOUNDARY CONDITIONS AND STABILITY ANALYSIS	89
12	SINGLET SCALAR MODES	91
13	CONCLUSIONS AND OPEN ISSUES	97
A	CONVENTIONS AND PROPERTIES OF THE BACKGROUND	102
B	INTERMEDIATE RESULTS FOR TENSOR PERTURBATIONS	106
C	INTERMEDIATE RESULTS FOR THE EINSTEIN EQUATIONS	108
C.1	INTERMEDIATE RESULTS FOR THE RICCI CURVATURE	108
C.2	THE PERTURBED ENERGY-MOMENTUM TENSOR	109
D	THE NON-SINGLET VECTOR MODES AS $\mathbf{k} \rightarrow 0$	110
E	SELF-ADJOINT VARIATIONAL TESTS	112

1 INTRODUCTION AND SUMMARY

Different scenarios for supersymmetry breaking in String Theory [1] have been explored over the years. The resulting pictures are captivating, but they all entail, in one way or another, strong back reactions on the vacuum. To wit, quantum corrections to Scherk–Schwarz compactifications [2, 3] lead to runaway potentials (and possibly to tachyonic modes), which also emerge, already at the (projective) disk level, in the three non-tachyonic ten-dimensional orientifolds [4] of [5, 6, 7]. While supersymmetry is absent in the first two, Sugimoto’s model in [7] rests on a non-linear realization of supersymmetry [8], and in fact it is the simplest setting for brane supersymmetry breaking [7]. Fluxed AdS vacua for the three non-tachyonic ten-dimensional strings of [5, 6, 7], where curvatures and string couplings are everywhere weak, do exist [9, 10, 11, 12], but they generally host unstable modes [13, 14]. In contrast with the standard Kaluza–Klein constructions that play a ubiquitous role for supersymmetric strings [1], the Dudas–Mourad vacua [15] rest on an internal interval, and are perturbatively stable [13, 14]. However, they include regions where the expected corrections sized by the string coupling, and/or by the space–time curvature, become unbounded.

This paper concerns a class of type IIB [16] compactifications to four-dimensional Minkowski space with internal fluxes [17] that avoid the emergence of regions where the string coupling becomes large ¹. It is a sequel of [19], where a number of properties of these vacua were elucidated, including the presence of an effective BPS orientifold at one end of the internal interval. Furthermore, supersymmetry is fully broken when this orientifold lies at a finite distance from another singularity, while it is partly recovered in the limit where the two ends are separated by an infinite distance. The analysis also showed that, for a natural choice of boundary conditions, the massless Fermi modes present in these vacua are those of $N = 4$ supergravity [20] coupled to five vector multiplets. Our task here is to investigate the nature of the corresponding bosonic modes, taking a close look at the available choices of self-adjoint boundary conditions [14], while also analyzing their implications for vacuum stability.

These backgrounds are characterized by a constant dilaton profile ϕ_0 , which we set to zero for

¹As in the original vacua of [15], the strong curvatures present in these types of vacua can be also confined to small portions of the internal space with suitable choices of their free parameters [17, 18].

simplicity, and by metric and five-form profiles that depend on a single coordinate r , and read

$$\begin{aligned}
ds^2 &= \frac{\eta_{\mu\nu} dx^\mu dx^\nu}{\left[2|H|\rho \sinh\left(\frac{r}{\rho}\right)\right]^{\frac{1}{2}}} + \left[2|H|\rho \sinh\left(\frac{r}{\rho}\right)\right]^{\frac{1}{2}} \left[e^{-\frac{\sqrt{10}}{2\rho}r} dr^2 + e^{-\frac{\sqrt{10}}{10\rho}r} (dy^i)^2\right], \\
\mathcal{H}_5^{(0)} &= H \left\{ \frac{dx^0 \wedge \dots \wedge dx^3 \wedge dr}{\left[2|H|\rho \sinh\left(\frac{r}{\rho}\right)\right]^2} + dy^1 \wedge \dots \wedge dy^5 \right\}.
\end{aligned} \tag{1.1}$$

The x^μ are coordinates of a four-dimensional Minkowski space, and positive values of the coordinate r parametrize the interior of an internal interval. The five y^i coordinates have a finite range,

$$0 \leq y^i \leq 2\pi R, \tag{1.2}$$

and parametrize an internal torus, which for simplicity we take to be the direct product of five circles of radius R . These vacua thus depend on the two constants H and ρ , and supersymmetry is fully broken for finite values of ρ . We shall often use the conformal coordinate

$$z(r) = z_0 \int_0^r d\xi \sinh \xi^{\frac{1}{2}} e^{-\frac{\sqrt{10}\xi}{4}}, \tag{1.3}$$

where

$$z_0 = (2H\rho^3)^{\frac{1}{2}}. \tag{1.4}$$

The upper bound for z , which will play a role in the ensuing discussion, is

$$z_m \simeq 2.24 z_0. \tag{1.5}$$

Half of the supersymmetries originally present in ten dimensions are recovered in the $\rho \rightarrow \infty$ limit [19], albeit within a curved spacetime that still includes the singularity at $r = 0$. After the coordinate transformation

$$\xi H = \frac{2}{5} (2Hr)^{\frac{5}{4}}, \tag{1.6}$$

the limiting behavior of the solution reads

$$\begin{aligned}
ds^2 &= \frac{\eta_{\mu\nu} dx^\mu dx^\nu}{\left(\frac{5}{2}H\xi\right)^{\frac{2}{5}}} + d\xi^2 + \left(\frac{5}{2}H\xi\right)^{\frac{2}{5}} (dy^i)^2, \\
\mathcal{H}_5^{(0)} &= H \left\{ \frac{dx^0 \wedge \dots \wedge dx^3 \wedge d\xi}{\left(\frac{5}{2}H\xi\right)^{\frac{9}{5}}} + dy^1 \wedge \dots \wedge dy^5 \right\},
\end{aligned} \tag{1.7}$$

and describes indeed a non-homogeneous curved background including an internal torus with an effective ξ -dependent size. As $\xi \rightarrow 0$, the volume of the internal torus shrinks to zero and the

scale factor of the spacetime coordinates blows up, while conversely as $\xi \rightarrow \infty$ the volume of the internal torus blows up while the scale factor of the spacetime coordinates shrinks to zero. Both limits are thus delicate within supergravity [20] although, as we saw in detail in [19], this limiting form of the vacuum does preserve half of the supersymmetries of ten-dimensional Minkowski space. One can also absorb the constant H , while rescaling the radius R of the internal torus by a factor $H^{\frac{1}{5}}$.

Alternatively, the backgrounds of eqs. (1.1) can be presented in the form

$$\begin{aligned} ds^2 &= \frac{\eta_{\mu\nu} dx^\mu dx^\nu}{[h \sinh(\tilde{r})]^{\frac{1}{2}}} + [\sinh(\tilde{r})]^{\frac{1}{2}} \left[\ell^2 e^{-\frac{\sqrt{10}}{2} \tilde{r}} d\tilde{r}^2 + (2\Phi\ell)^{\frac{2}{5}} e^{-\frac{\sqrt{10}}{10} \tilde{r}} (d\tilde{y}^i)^2 \right], \\ \mathcal{H}_5^{(0)} &= \frac{1}{2h} \frac{dx^0 \wedge \dots \wedge dx^3 \wedge d\tilde{r}}{[\sinh(\tilde{r})]^2} + \Phi d\tilde{y}^1 \wedge \dots \wedge d\tilde{y}^5, \end{aligned} \quad (1.8)$$

where $\tilde{r} > 0$ is a dimensionless variable, ℓ is the length scale of the interval, h is a dimensionless parameter and Φ is the five-form flux in the internal torus. Here

$$\tilde{r} = \frac{r}{\rho}, \quad \tilde{y}^i = \frac{y^i}{2\pi R}, \quad (1.9)$$

so that the \tilde{y}^i are dimensionless coordinates of unit range, and the new parameters are related to those in eqs. (1.1) according to

$$h = 2H\rho, \quad \ell = (2H)^{\frac{1}{4}} \rho^{\frac{5}{4}} = h^{\frac{1}{4}} \rho, \quad \Phi = H(2\pi R)^5, \quad z_0 = \ell h^{\frac{1}{4}}. \quad (1.10)$$

The volume of the six-dimensional internal space, which comprises the torus and the r -interval, scales as

$$V_6 \sim \Phi \ell^2 \sim H^{\frac{3}{2}} \rho^{\frac{5}{2}} R^5, \quad (1.11)$$

and similarly the volume of the internal torus, which can be defined as $\frac{V_6}{\ell}$, scales as

$$V_5 \sim \Phi \ell \sim H^{\frac{5}{4}} \rho^{\frac{5}{4}} R^5. \quad (1.12)$$

Both quantities diverge in the supersymmetric limit $\rho \rightarrow \infty$, which thus occurs in a ten-dimensional curved space with one singularity at the origin, as we had anticipated.

The fermionic zero modes present in these backgrounds were determined in [19]: for finite values of ρ or ℓ they are four Majorana gravitini and 20 Majorana spinors, the massless fermions of $N = 4$ supergravity coupled to *five* $N = 4$ vector multiplets, despite the breaking of supersymmetry². In the following sections we shall analyze in detail the corresponding bosonic zero

²More precisely, as explained in [19], this is the case if Fermi fields are subject to identical ‘‘ Λ projections’’ at the two ends of the r interval. Here we focus on this interesting option, but opposite ‘‘ Λ projections’’ would eliminate the massless Fermi modes.

modes and their excitations, with the aim of addressing the perturbative stability of these vacua at the classical level. As in [14], other parameters beyond those appearing in the background are generally encoded in the boundary conditions. Moreover, as we shall see, additional modes can be confined to boundaries. Only a subset of the possible self-adjoint boundary conditions grant stability, but in all cases we find an ample range of these choices.

The four-dimensional bosonic modes that we shall exhibit originate from the ten-dimensional fields of type-IIB supergravity [16, 20], and have r -profiles and discrete momenta \mathbf{k} in the internal torus. Linearized perturbations of the backgrounds can be characterized by their four-dimensional spin and their internal quantum numbers, and different representations of the residual symmetry groups can be studied independently. For example, starting from the ten-dimensional metric and the four-form gauge field, which can be decomposed as

$$g_{MN} = g_{MN}^{(0)} + h_{MN} , \quad B_{M_1 \dots M_4} = B_{M_1 \dots M_4}^{(0)} + \delta B_{M_1 \dots M_4} , \quad (1.13)$$

after a suitable gauge fixing the perturbations h_{MN} and $\delta B_{M_1 \dots M_4}$ give rise to tensor, vector and scalar modes of different types. The metric and the selfdual four-form are the only two fields with non-trivial vacuum profiles, and for this reason they generally mix, are more difficult to analyze and can affect other modes. In addition, the selfdual five-form is by itself somewhat unfamiliar. All modes afford Fourier decompositions in the internal space, so that for example the perturbations of the ten-dimensional metric can be decomposed according to

$$h_{MN}(x, r, y) = h_{MN}(x, r) + \sum_{\mathbf{k} \neq 0} h_{MN}^{(\mathbf{k})}(x, r) e^{i\mathbf{k} \cdot \mathbf{y}} . \quad (1.14)$$

The modes with vanishing internal momentum \mathbf{k} , and in particular $h_{MN}(x, r)$ in this example, fill effectively multiplets of a continuous $SO(5)$ symmetry. The $SO(5)$ tangent-space symmetry endows them with the internal quantum numbers that we alluded to above, although only a discrete subgroup of $SO(5)$ is actually an isometry of the torus. On the other hand, the remaining modes carry lattice momenta \mathbf{k} , and fill effectively $SO(4)$ multiplets corresponding to their stability groups. In practice, these will emerge as $SO(5)$ multiplets subject to orthogonality constraints. These properties will play an important role in our analysis, and the internal quantum numbers of the modes that we shall identify will correspond indeed to $SO(5)$ representations for $\mathbf{k} = 0$, and to $SO(4)$ representations for $\mathbf{k} \neq 0$. For brevity, however, we shall usually drop the superscript (\mathbf{k}) present in eq. (1.14) when discussing modes with non-vanishing internal momenta. It would be interesting to address generalizations of this type of setup where the internal torus is replaced by a more general Ricci-flat internal manifold.

Since the resulting spacetime is flat for the backgrounds of interest, the vacua of eq. (1.1) are perturbatively unstable if $m^2 < 0$ for some four-dimensional modes, and we shall perform a detailed scrutiny to this end. As in [13, 19, 14], the four-dimensional masses can be related to the eigenvalues of one-dimensional Schrödinger-like operators acting on one or two wavefunctions, whose potentials are determined by the background.

The field equations lead, in general, to operators that are not manifestly Hermitian, so that the replacement of the independent variable r with the “conformal” variable of eq. (1.3), whose range $0 \leq z \leq z_m$ is finite and proportional to z_0 , together with redefinitions of the different fields, will be instrumental to cast them into standard forms. Remarkably, as in the nine-dimensional vacua discussed in [14], in all cases the resulting potentials develop double poles at the two ends, where they behave as

$$V \sim \frac{\mu^2 - \frac{1}{4}}{z^2}, \quad V \sim \frac{\tilde{\mu}^2 - \frac{1}{4}}{(z - z_m)^2}. \quad (1.15)$$

The constants μ and $\tilde{\mu}$ depend on the mode sector, while the scale dependence is only encoded in z_m . Moreover, $\tilde{\mu}$ is zero for $h_{\mu\nu}$, h_{ij} , dilaton and axion perturbations, which share the same Schrödinger operator, while it is a real number between zero and about 2.3 in all other sectors. On the other hand, the parameter μ associated to the $z = 0$ end is curiously either $\frac{1}{3}$ or $\frac{2}{3}$ in all cases. The squared masses are eigenvalues of Hermitian operators and, as we saw in [19] for Fermi fields, these steps also determine the normalization conditions, a necessary ingredient to identify the actual physical modes. In most cases, these normalizations can be simply recovered from the four-dimensional kinetic terms determined by ten-dimensional action, but the self-dual tensor field does introduce some complications. However, despite its reduced manifest symmetry, the non-standard Henneaux–Teitelboim action of [21], when properly adapted, suffices to grant covariant descriptions in the backgrounds of eq. (1.1).

The completeness of the modes thus identified is essential to make statements on perturbative stability. It is granted if the Schrödinger-like operators are not only Hermitian but also self-adjoint, and this property demands judicious choices of boundary conditions. These are determined by the asymptotics of the wavefunctions at the ends of the interval [14], which reflects, in its turn, the singular behavior (1.15) of the potentials. Additional sets of parameters thus emerge, which impinge on the positivity of the Hermitian Schrödinger-like operators, and the stability of the resulting mass spectra generally places some constraints on them [14].

The massless modes are exactly calculable in most cases, with suitable boundary conditions, while in a few instances the allowed squared masses emerge as eigenvalues of operators that are

manifestly positive, again with suitable boundary conditions. Two sectors with $\mathbf{k} \neq 0$, the non-singlet vector modes of Section 10.2 and the non-singlet scalar modes of Section 11.2, did not allow exact statements, and approximation methods were necessary to address their stability. We thus relied on the variational principle of non-relativistic Quantum Mechanics, which can be adapted to the present setting and allows reliable numerical estimates of the lowest eigenvalues and of their dependence on \mathbf{k} and on the boundary conditions. In this fashion, we could identify background-dependent constraints on the boundary conditions that grant stability in both cases.

In general, different boundary conditions lead to different spectra, and the residual global symmetries required for the backgrounds of interest are instrumental to discriminate among them. These symmetries include infinitesimal translations and Lorentz rotations in spacetime, together with infinitesimal translations along the internal torus. The corresponding currents are already present in the background, and do not flow across the ends of the interval provided [22, 19]

$$\sqrt{-g} T^r{}_{\mu}|_{\partial\mathcal{M}} = 0, \quad \sqrt{-g} S^r{}_{\mu\nu}|_{\partial\mathcal{M}} = 0, \quad \sqrt{-g} T^r{}_i|_{\partial\mathcal{M}} = 0, \quad (1.16)$$

where $T^r{}_{\mu}$ and $T^r{}_i$ are components of the energy-momentum tensor and $S^r{}_{\mu\nu}$ are components of the spin portion of the angular momentum current. Enforcing eq. (1.16) selects special boundary conditions for the fields. The solutions of the linearized equations that we shall examine in detail, with special emphasis on the low-lying modes, determine the leading contributions to these no-flow conditions. One can thus use them independently for the different sectors of the spectrum to identify the boundary conditions compatible with them. While in a quantum theory of gravity global symmetries are expected not to be conserved [23], and therefore these requirements do not appear mandatory, they will prove nonetheless useful to characterize the choices of boundary conditions.

The contents of this paper are as follows. In Section 2 we briefly review the self-adjoint boundary conditions for Bose fields at the ends of the interval in the presence of singular potentials as in eq. (1.15). We also describe a class of exactly solvable trigonometric potentials related to hypergeometric functions that can closely approximate the Schrödinger potentials of all sectors in our background. In Section 3 we begin our detailed analysis of bosonic modes, starting from the dilaton-axion system. We examine the possible self-adjoint boundary conditions and the stability regions for the corresponding Schrödinger equation, and present an analytic solution for its zero mode. The same analysis applies to the axion, and to the spin-2 $h_{\mu\nu}$ and spin-0 h_{ij} modes of gravity. In section 4 we discuss the modes of the type-IIB three-forms. All these fields lack vacuum profiles, but their equations are affected by the five-form background via Chern-Simons

couplings. As a result, their massless modes require a special treatment, which finally leads to third-order equations and to some unfamiliar features for their spectra. We also determine the corresponding stability regions for the boundary conditions. In section 5 we first discuss a convenient parametrization for the components of the self-dual tensor field, and then present the perturbed self-duality equations, after making a convenient gauge choice. To the best of our knowledge, this is the first time that this type of detailed analysis is carried out, to this extent, for a self-dual tensor field. We then discuss the perturbed Einstein equations, including tensor contributions. To this end, we rely extensively on Appendices A, B and C, which contain a number of useful technical details on the background and on the perturbed equations for the various fields. In Sections 6, 7 and 8 we examine the modes arising from the self-dual tensor or from the ten-dimensional metric, with no mixings among them. The tensor modes of Section 6 arising from the five-form alone have some unfamiliar features, including the possible presence of zero modes within all possible Kaluza–Klein excitations. This would clearly seem unphysical, but actually the different occurrences correspond to different choices of boundary conditions, and thus to different vacua. These choices would also lead to tachyons for $\mathbf{k} = 0$, and are thus excluded a priori by the requirement of vacuum stability. In Sections 7 and 8 we discuss the spin-2 $h_{\mu\nu}$ and spin-0 h_{ij} modes, and show that the corresponding Schrödinger equations are identical to that of the dilaton–axion sector. In Section 9 we analyze the vector modes that are singlets under the internal symmetries and show that there are only massive excitations among them, since the zero mode is not normalizable. In Section 10 we consider non-singlet vector modes. The modes of this type with $\mathbf{k} = 0$, which are valued in the fundamental representation of $SO(5)$, lead to a one-dimensional Schrödinger system. We show that they are stable with suitable self-adjoint boundary conditions, and determine the corresponding zero mode. The sector with $\mathbf{k} \neq 0$ is more difficult to analyze, since it leads to a two-component Schrödinger system. After reducing it to a manifestly Hermitian form, we estimate the lowest allowed values for m^2 and their dependence on the lattice momentum \mathbf{k} and on the choice of self-adjoint boundary conditions, resorting to the variational principle. We show the existence of self-adjoint boundary conditions that grant stability also in this case. Their parameter space is background dependent, and widens as the ratio $\frac{\Phi}{\ell^4}$, or equivalently as the ratio $\frac{R}{\rho}$, decreases. In Section 11 we discuss non-singlet scalar perturbations. For $\mathbf{k} = 0$ these are valued in the fundamental representation of $SO(5)$, and with appropriate self-adjoint boundary conditions they are again stable, as in the preceding sectors. We also determine the corresponding massless mode. For $\mathbf{k} \neq 0$, the modes belonging to this sector are valued in the fundamental representation of $SO(4)$ and lead again to a two-component

Schrödinger system. After some redefinitions their squared mass can be related to the eigenvalues of an operator that, with proper self-adjoint boundary conditions, does not contain any unstable modes, but their parameter space is again background dependent, and widens as the ratio $\frac{\Phi}{\ell^4}$ decreases. In Section 12 we discuss singlet scalar modes. For $\mathbf{k} = 0$, after suitable redefinitions, their squared masses emerge from an operator that is strictly positive with proper self-adjoint boundary conditions. We show that stability persists within finite range of boundary conditions. We defer to a different publication the analysis of scalar singlets with $\mathbf{k} \neq 0$, which is more involved and requires different techniques, for reasons that we explain in Section 13, where we collect our conclusions and some perspectives for future work. Appendix D contains some details on small- \mathbf{k} limit for the modes discussed in Section 10.2, and finally Appendix E contains some details on our variational tests for Sections 10.2 and 11.2.

2 SELF-ADJOINT EXTENSIONS AND SOLVABLE $(\mu, \tilde{\mu})$ POTENTIALS

In the Introduction we stated that, as in the nine-dimensional cases analyzed in [14], the potentials for the various mode sectors in this class of vacua can be characterized by a pair of parameters $(\mu, \tilde{\mu})$ that determine their leading singularities at the ends of the internal interval. Let us first consider the sectors where the analysis of the fluctuations leads to a single second-order equation. This case was widely studied, over the years, in the Mathematical literature [24, 25, 26], and in [14] we formulated the whole setup in a way that seems particularly transparent to us, while also adapting it to the stability issue that is central to this work.

2.1 ONE-DIMENSIONAL SECTORS

We shall determine the values of μ and $\tilde{\mu}$ in the following sections, but for convenience we collect the results in Table 1. Note that the values of μ are either $\frac{1}{3}$ or $\frac{2}{3}$, while the values of $\tilde{\mu}$ range from 0 to about 2.3.

As explained in [14], the possible self-adjoint extensions of Schrödinger-like operators in an interval terminating at a pair of singular points can be characterized via the limiting behavior of the wavefunctions at the two ends. This is determined by μ and $\tilde{\mu}$, and the condition that $H\psi$ be in L^2 constrains in general the choice of the wavefunctions [24, 25, 26]. Referring to Table 1, two independent choices of limiting behaviors are thus allowed, in all cases of interest, at $z = 0$, while two choices are allowed at z_m when $0 \leq \tilde{\mu} < 1$ and a single one is allowed when $\tilde{\mu} \geq 1$. In

Case	Sector	μ	$\tilde{\mu}$
1	$\varphi, a, h_{\mu\nu}, h_{ij}$	$\frac{1}{3}$	0
2	$B_{\mu\nu}$	$\frac{2}{3}$	1.72
2	$b_{\mu\nu}{}^{ij}(g_1)$	$\frac{1}{3}$	1.09
2	V_μ	$\frac{1}{3}$	2.18
2	$h_{\mu i}$	$\frac{2}{3}$	1.18
2	ϕ_i	$\frac{2}{3}$	2.27
2	ϕ	$\frac{2}{3}$	1
3	$B_{\mu i}$	$\frac{1}{3}$	0.54
3	B_{ij}	$\frac{2}{3}$	0.63
3	$b^{(2)}{}_{\mu}{}^{ij}(g_2)$	$\frac{2}{3}$	0.09

Table 1: Values of μ and $\tilde{\mu}$ for the different sectors of Bose modes with $\mathbf{k} = 0$. The notation $b_{\mu\nu}{}^{ij}(g_1)$ and $b^{(2)}{}_{\mu}{}^{ij}(g_2)$ is meant to stress that the values of μ and $\tilde{\mu}$ refer to the Schrödinger-like equations for g_1 or g_2 in Section 6.

general, the asymptotic behavior at the left can be characterized by a pair of coefficients C_1 and C_2 , according to

$$\begin{aligned}
\psi &\sim \frac{C_1}{\sqrt{2\mu}} \left(\frac{z}{z_m}\right)^{\frac{1}{2} + \mu} + \frac{C_2}{\sqrt{2\mu}} \left(\frac{z}{z_m}\right)^{\frac{1}{2} - \mu} && \text{if } 0 < \mu < 1, \\
\psi &\sim C_1 \left(\frac{z}{z_m}\right)^{\frac{1}{2}} \log\left(\frac{z}{z_m}\right) + C_2 \left(\frac{z}{z_m}\right)^{\frac{1}{2}} && \text{if } \mu = 0
\end{aligned} \tag{2.1}$$

while at the other there are different options, depending of the value of $\tilde{\mu}$:

$$\begin{aligned}
\psi &\sim \frac{C_3}{\sqrt{2\tilde{\mu}}} \left(1 - \frac{z}{z_m}\right)^{\frac{1}{2} + \tilde{\mu}} + \frac{C_4}{\sqrt{2\tilde{\mu}}} \left(1 - \frac{z}{z_m}\right)^{\frac{1}{2} - \tilde{\mu}} && \text{if } 0 < \tilde{\mu} < 1; \\
\psi &\sim C_3 \left(1 - \frac{z}{z_m}\right)^{\frac{1}{2}} \log\left(1 - \frac{z}{z_m}\right) + C_4 \left(1 - \frac{z}{z_m}\right)^{\frac{1}{2}} && \text{if } \tilde{\mu} = 0; \\
\psi &\sim \frac{C_3}{\sqrt{2\tilde{\mu}}} \left(1 - \frac{z}{z_m}\right)^{\frac{1}{2} + \tilde{\mu}} && \text{if } \tilde{\mu} \geq 1.
\end{aligned} \tag{2.2}$$

When $\tilde{\mu} \geq 1$, the possible self-adjoint boundary conditions depend on a single parameter,

$$\frac{C_2}{C_1} = \tan\left(\frac{\alpha}{2}\right). \tag{2.3}$$

When $0 \leq \mu < 1$ and $0 \leq \tilde{\mu} < 1$, defining the two vectors

$$\underline{C}(0) = \begin{pmatrix} C_1 \\ C_2 \end{pmatrix}, \quad \underline{C}(z_m) = \begin{pmatrix} C_4 \\ C_3 \end{pmatrix}, \tag{2.4}$$

the self-adjointness condition becomes

$$\underline{C}(z_m) = \mathcal{U} \underline{C}(0), \tag{2.5}$$

where \mathcal{U} is a generic $U(1, 1)$ matrix, so that

$$\mathcal{U}^\dagger \sigma_2 \mathcal{U} = \sigma_2 . \quad (2.6)$$

\mathcal{U} is parametrized according to

$$\mathcal{U} = e^{i\beta} U , \quad (2.7)$$

where β is a phase and U is a generic $SL(2, R)$ matrix, and in the global $SL(2, R)$ parametrization

$$U(\rho, \theta_1, \theta_2) = \cosh \rho (\cos \theta_1 \underline{1} - i \sigma_2 \sin \theta_1) + \sinh \rho (\sigma_3 \cos \theta_2 + \sigma_1 \sin \theta_2) , \quad (2.8)$$

where $0 \leq \rho < \infty$, $-\pi \leq \theta_{1,2} < \pi$.

The Schrödinger equation determines in general the relation

$$\underline{C}(z_m) = V \underline{C}(0) , \quad (2.9)$$

where V is an $SL(2, R)$ matrix, consistently with our definitions and the constancy of the Wronskian, and the eigenvalue equation is in general [14]

$$\text{Tr} [U^{-1} V] = 2 \cos \beta . \quad (2.10)$$

The large- ρ limit of eq. (2.5) yields independent boundary conditions at the ends depending on the two parameters θ_1 and θ_2 , which can be cast in the form

$$\begin{aligned} \cos \left(\frac{\theta_1 - \theta_2}{2} \right) C_1 - \sin \left(\frac{\theta_1 - \theta_2}{2} \right) C_2 &= 0 , \\ \sin \left(\frac{\theta_1 + \theta_2}{2} \right) C_4 - \cos \left(\frac{\theta_1 + \theta_2}{2} \right) C_3 &= 0 \end{aligned} \quad (2.11)$$

when $0 \leq \mu < 1$ and $0 \leq \tilde{\mu} < 1$.

2.2 MATRIX GENERALIZATION OF THE SETUP

In some of the following sections we shall need a generalization of these results involving n -component states ψ and $n \times n$ matrix potentials, so that near the $z = 0$ boundary the Hamiltonian will have the limiting form

$$H = - \partial_z^2 + \frac{1}{z^2} V_0 , \quad (2.12)$$

with V_0 a Hermitian matrix with eigenvalues $[\mu_1^2 - \frac{1}{4}, \dots, \mu_n^2 - \frac{1}{4}]$. In a similar fashion, near the other end of the interval the Hamiltonian will have the limiting form

$$H = - \partial_z^2 + \frac{1}{(z_m - z)^2} V_m , \quad (2.13)$$

with V_m a Hermitian matrix with eigenvalues $[\tilde{\mu}_1^2 - \frac{1}{4}, \dots, \tilde{\mu}_n^2 - \frac{1}{4}]$. In general, the two matrices V_0 and V_m are diagonalized into D_0 and D_m by different unitary matrices U_0 and U_m , so that

$$V_0 = U_0 D_0 U_0^\dagger, \quad V_m = U_m D_m U_m^\dagger. \quad (2.14)$$

Consequently, if $0 < \mu_i < 1$ the limiting behavior of the wavefunction close to the left end of the interval has the general form

$$\psi \sim U_0 \begin{pmatrix} \frac{C_{11}}{\sqrt{2\mu_1}} z^{\frac{1}{2}+\mu_1} + \frac{C_{12}}{\sqrt{2\mu_1}} z^{\frac{1}{2}-\mu_1} \\ \dots \\ \frac{C_{n1}}{\sqrt{2\mu_n}} z^{\frac{1}{2}+\mu_n} + \frac{C_{n2}}{\sqrt{2\mu_n}} z^{\frac{1}{2}-\mu_n} \end{pmatrix}. \quad (2.15)$$

In complete analogy with the one-dimensional case, if some μ_i is larger than one the L^2 condition demands that the corresponding C_{i2} vanish. Finally, if some $\mu_i = 0$ the corresponding line becomes

$$C_{i1} z^{\frac{1}{2}} \log z + C_{i2} z^{\frac{1}{2}}. \quad (2.16)$$

The limiting behavior at the other end is similar, up to the replacement of μ_i with $\tilde{\mu}_i$, z with $z_m - z$ and $C_{i1,2}$ with new coefficients $C_{i3,4}$.

The Hamiltonian H is self-adjoint if

$$\left[\partial_z \psi^\dagger \chi - \psi^\dagger \partial_z \chi \right]_0^{z_m} = 0, \quad (2.17)$$

and therefore, if $0 \leq \mu_i < 1$,

$$\sum_i [C_{i1}^* D_{i2} - C_{i2}^* D_{i1} + C_{i3}^* D_{i4} - C_{i4}^* D_{i3}] = 0, \quad (2.18)$$

where we have denoted by C_{ij} and D_{ij} the coefficients of ψ and χ . One can now define the $2n$ -component vector $\underline{C}(0)_{ia}$, with $\underline{C}(0)_{i1} = C_{i1}$ and $\underline{C}(0)_{i2} = C_{i2}$ and $\underline{C}(z_m)_{ia}$, with $\underline{C}(z_m)_{i1} = C_{i4}$ and $\underline{C}(z_m)_{i2} = C_{i3}$ and $i = 1, \dots, n$, and the preceding condition becomes

$$\underline{C}^\dagger(0) 1_n \otimes \sigma_2 \underline{D}(0) = \underline{C}^\dagger(z_m) 1_n \otimes \sigma_2 \underline{D}(z_m). \quad (2.19)$$

Consequently the self-adjoint boundary conditions are parametrized by elements \mathcal{U} of $U(n, n)$ such that

$$C(z_m) = \mathcal{U} C(0), \quad (2.20)$$

together with a similar relation for the D coefficients. The independent boundary conditions are then obtained when both sides of eq. (2.19) vanish, which is the case if the linear conditions,

$$C(0) = \Lambda C(0), \quad (2.21)$$

hold, where Λ Hermitian, $\Lambda^2 = 1$, and

$$\{\Lambda, 1 \otimes \sigma_2\} = 0 . \quad (2.22)$$

One can thus write

$$\Lambda = \mathcal{M}_1 \otimes \sigma_1 + \mathcal{M}_3 \otimes \sigma_3 , \quad (2.23)$$

with $\mathcal{M}_{1,3}$ Hermitian matrices such that

$$\mathcal{M}_1^2 + \mathcal{M}_3^2 = 1 , \quad [\mathcal{M}_1, \mathcal{M}_3] = 0 . \quad (2.24)$$

The two matrices \mathcal{M}_1 and \mathcal{M}_3 can be simultaneously diagonalized, and can be cast in the form

$$\mathcal{M}_1 = \Omega^\dagger \text{diag}(\sin \alpha_1, \dots, \sin \alpha_n) \Omega , \quad \mathcal{M}_3 = \Omega^\dagger \text{diag}(\cos \alpha_1, \dots, \cos \alpha_n) \Omega , \quad (2.25)$$

with Ω a unitary $n \times n$ matrix of unit determinant. In detail, the boundary conditions (2.21) read

$$C_{ia} = \left[\mathcal{M}_{1i}^j \sigma_{1a}^b + \mathcal{M}_{3i}^j \sigma_{3a}^b \right] C_{jb} , \quad (2.26)$$

or regrouping the coefficients into a rectangular matrix

$$\Omega C = (D_1 \sigma_1 + D_3 \sigma_3) \Omega C , \quad (2.27)$$

where

$$D_1 = \text{diag}(\sin \alpha_1, \dots, \sin \alpha_n) \quad D_3 = \text{diag}(\cos \alpha_1, \dots, \cos \alpha_n) . \quad (2.28)$$

For an $n \times n$ second-order system, the general boundary conditions of this type thus involve $n(n+1) - 1$ parameters. Similar considerations apply at the other end, with n angles $\tilde{\alpha}_i$ and another unitary $n \times n$ matrix $\tilde{\Omega}$ of unit determinant. All in all, the independent boundary conditions are thus parametrized by $2n$ angles and a pair of special unitary $n \times n$ matrices. For $n = 1$, these considerations recover the choices of self-adjoint boundary conditions discussed in the preceding pages. However, only n of the $2n$ components of C are arbitrary, due to the condition (2.21), so that effectively one ends up with n parameters at each end. If some of the $\mu_i \geq 1$ (say, m of them), the number n is simply replaced by $n-m$ in the preceding considerations, and similarly for the $\tilde{\mu}_i$.

2.3 EXACTLY SOLVABLE HYPERGEOMETRIC POTENTIALS

Before exhibiting the actual potentials for the various sectors of our problem, is it convenient to introduce a family of exactly solvable Schrödinger systems that generalize those considered in [14], for which $\mu = \tilde{\mu}$, and share the same type of limiting behavior. These systems are characterized by the trigonometric potentials [26]

$$V(\mu, \tilde{\mu}, z) = \frac{\pi^2}{4 z_m^2} \left[\frac{\mu^2 - \frac{1}{4}}{\sin^2\left(\frac{\pi z}{2 z_m}\right)} + \frac{\tilde{\mu}^2 - \frac{1}{4}}{\cos^2\left(\frac{\pi z}{2 z_m}\right)} \right], \quad (2.29)$$

where $0 < z < z_m$, which can be obtained starting from the hypergeometric equation [27] and performing a change of independent variable followed by a redefinition of the function, in order to cast the result into the Schrödinger form

$$-\Psi''(z) + V(\mu, \tilde{\mu}, z) \Psi(z) = \frac{\pi^2 m^2}{z_m^2} \Psi(z). \quad (2.30)$$

For $\mu = \tilde{\mu}$ the potential reduces to

$$V(\mu, z) = \frac{\pi^2}{z_m^2} \frac{\mu^2 - \frac{1}{4}}{\sin^2\left(\frac{\pi z}{z_m}\right)}, \quad (2.31)$$

and the resulting spectra were discussed in detail in [14].

For $\mu \neq 0$, which is always the case in Table 1, the general solution of eq. (2.30) reads [27]

$$\Psi(z) = \frac{A w_1(z) + B w_2(z)}{u(z)^{\mu - \frac{1}{2}} v(z)^{-\tilde{\mu} - \frac{1}{2}}}, \quad (2.32)$$

where

$$\begin{aligned} w_1(z) &= {}_2F_1[a, b; c; u^2(z)], \\ w_2(z) &= u(z)^{2(1-c)} {}_2F_1[a - c + 1, b - c + 1; 2 - c; u^2(z)], \end{aligned} \quad (2.33)$$

and the ${}_2F_1$ are hypergeometric functions [27]. Moreover

$$\begin{aligned} u(z) &= \sin\left(\frac{\pi z}{2 z_m}\right), & v(z) &= \cos\left(\frac{\pi z}{2 z_m}\right), \\ a &= \frac{\tilde{\mu} - \mu + 1}{2} + m, & b &= \frac{\tilde{\mu} - \mu + 1}{2} - m, & c &= 1 - \mu, \end{aligned} \quad (2.34)$$

where, without loss of generality, one can assume that μ and $\tilde{\mu}$ be positive. The two functions

$$\begin{aligned} w_3(z) &= {}_2F_1[a, b; a + b - c + 1; v^2(z)], \\ w_4(z) &= v(z)^{2(c-a-b)} {}_2F_1[c - a, c - b; c - a - b + 1; v^2(z)] \end{aligned} \quad (2.35)$$

provide an alternative basis of solutions, and are related to previous pair according to [27]

$$\begin{aligned} w_1(z) &= \frac{\Gamma(c) \Gamma(c-a-b)}{\Gamma(c-a) \Gamma(c-b)} w_3(z) + \frac{\Gamma(c) \Gamma(a+b-c)}{\Gamma(a) \Gamma(b)} w_4(z) , \\ w_2(z) &= \frac{\Gamma(2-c) \Gamma(c-a-b)}{\Gamma(1-a) \Gamma(1-b)} w_3(z) + \frac{\Gamma(2-c) \Gamma(a+b-c)}{\Gamma(a-c+1) \Gamma(b-c+1)} w_4(z) . \end{aligned} \quad (2.36)$$

Even in this more general setting, one can introduce first-order operators $\mathcal{A}_{\epsilon_1, \epsilon_2}$ and $\mathcal{A}_{\epsilon_1, \epsilon_2}^\dagger$, where

$$\mathcal{A}_{\epsilon_1, \epsilon_2} = \partial_z + \frac{\pi}{4z_m} (2\epsilon_1 \mu + 1) \cot\left(\frac{\pi z}{2z_m}\right) + \frac{\pi}{4z_m} (2\epsilon_2 \tilde{\mu} - 1) \tan\left(\frac{\pi z}{2z_m}\right) . \quad (2.37)$$

which depend on the signs ϵ_1 and ϵ_2 . One can then show that

$$\mathcal{A}_{\epsilon_1, \epsilon_2} \mathcal{A}_{\epsilon_1, \epsilon_2}^\dagger = -\partial_z^2 + V_{\epsilon_1, \epsilon_2}(z) , \quad (2.38)$$

where

$$V_{\epsilon_1, \epsilon_2}(z) = V(z) - \frac{\pi^2}{4z_m^2} \left(1 + \epsilon_1 \mu - \epsilon_2 \tilde{\mu}\right)^2 . \quad (2.39)$$

The different Hamiltonians

$$H_{\epsilon_1, \epsilon_2} = -\partial_z^2 + V_{\epsilon_1, \epsilon_2}(z) \quad (2.40)$$

have the same eigenvectors as H but have shifted eigenvalues, so that

$$m_{\epsilon_1, \epsilon_2}^2 = m^2 - \frac{1}{4} \left(1 + \epsilon_1 \mu - \epsilon_2 \tilde{\mu}\right)^2 . \quad (2.41)$$

The solutions of

$$\mathcal{A}_{\epsilon_1, \epsilon_2}^\dagger \Psi_{\epsilon_1, \epsilon_2} = 0 , \quad (2.42)$$

are

$$\Psi_{\epsilon_1, \epsilon_2}(z) = C \left[\sin\left(\frac{\pi z}{2z_m}\right) \right]^{\frac{1}{2} + \epsilon_1 \mu} \left[\cos\left(\frac{\pi z}{2z_m}\right) \right]^{\frac{1}{2} - \epsilon_2 \tilde{\mu}} . \quad (2.43)$$

When they are normalizable, they are zero modes of $H_{\epsilon_1, \epsilon_2}$.

In order to discuss the possible self-adjoint boundary conditions for $V(z)$ in the different sectors of the spectrum, one must distinguish different ranges for $\tilde{\mu}$.

- The case $\mu > 1$ and $\tilde{\mu} > 1$ does not occur in Table 1, but it is simple and instructive. The L^2 condition at the origin implies that $A = 0$ in eq. (2.32), and the limiting behavior at the other end of the interval is determined by eqs.(2.36). The corresponding L^2 condition

demands that the coefficient of $w_4(z)$ vanish, so that $a - c + 1$ or $b - c + 1$ must be negative integers, which determine altogether the stable spectrum

$$m^2 = \left(\frac{\mu + \tilde{\mu} + 1}{2} + n \right)^2, \quad n = 0, 1, \dots \quad (2.44)$$

Consequently

$$m_{\epsilon_1, \epsilon_2}^2 = \frac{1}{4} [(1 + \epsilon_1)\mu + (1 - \epsilon_2)\tilde{\mu} + 2(n + 1)][(1 - \epsilon_1)\mu + (1 + \epsilon_2)\tilde{\mu} + 2n]. \quad (2.45)$$

In this case, among the zero mode wavefunctions (2.43), only Ψ_{+-} is normalizable, and the corresponding zero-mass eigenvalue is recovered for $n = 0$.

- If $0 < \mu < 1$ and $\tilde{\mu} \geq 1$, which corresponds to case 2 in Table 1, both solutions in eq. (2.32) are normalizable, but one must again demand that the resulting contribution proportional to $w_4(z)$ vanish near the other end of the interval. In this case, the allowed self-adjoint boundary conditions are related to the ratio of the two coefficients A and B and, according to eq. (2.3), they can be parametrized via an angle α , so that

$$\frac{A}{B} = \tan\left(\frac{\alpha}{2}\right) \left(\frac{\pi}{2}\right)^{2\mu}. \quad (2.46)$$

The resulting eigenvalue equation reads

$$\tan\left(\frac{\alpha}{2}\right) = \frac{C_2}{C_1} = - \left(\frac{\pi}{2}\right)^{-2\mu} \frac{\Gamma(1 + \mu) \Gamma\left(\frac{\tilde{\mu} - \mu + 1}{2} + m\right) \Gamma\left(\frac{\tilde{\mu} - \mu + 1}{2} - m\right)}{\Gamma(1 - \mu) \Gamma\left(\frac{\tilde{\mu} + \mu + 1}{2} + m\right) \Gamma\left(\frac{\tilde{\mu} + \mu + 1}{2} - m\right)}, \quad (2.47)$$

and can be solved graphically, as in fig. 1 for both real values of m , which correspond to stable modes, and for imaginary ones, which correspond to tachyonic modes.

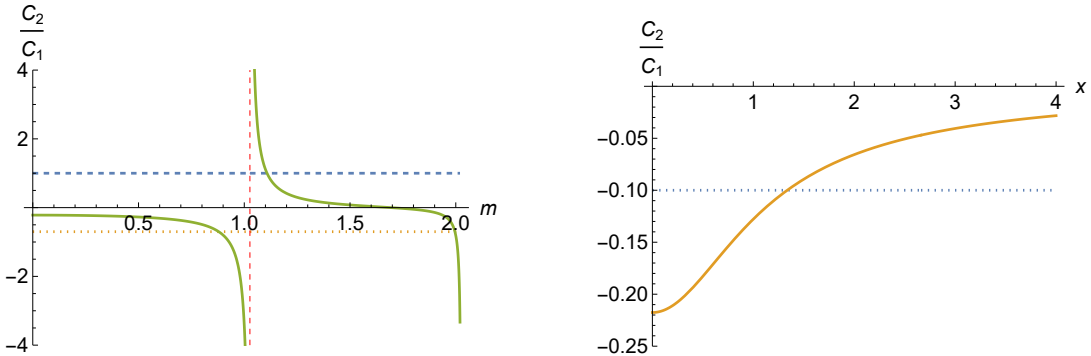


Figure 1: The left panel illustrates the first stable eigenvalues of the potential (2.29) for $\mu = \frac{2}{3}$, $\tilde{\mu} = 1.72$, $\tan\left(\frac{\alpha}{2}\right) = 1$ (blue dashed line) and for $\tan\left(\frac{\alpha}{2}\right) = -0.21$ (orange dotted line). The right panel illustrates the presence of a tachyonic mode for the same values of μ and $\tilde{\mu}$ and $-0.21 < \tan\left(\frac{\alpha}{2}\right) < 0$.

Some special cases are exactly solvable.

– For $\alpha = 0$ the denominator should have poles, so that the spectrum is given by

$$m^2 = \left(n + \frac{\tilde{\mu} + \mu + 1}{2} \right)^2, \quad (2.48)$$

which is stable, with no tachyons and no massless modes.

– For $\alpha = \pm\pi$ the numerator must have a pole, so that

$$m^2 = \left(n + \frac{\tilde{\mu} - \mu + 1}{2} \right)^2, \quad (2.49)$$

which is again stable, with no tachyons and no massless modes.

– For general values of α , one can solve the eigenvalue equation graphically, as illustrated in fig. 1, and there is an infinite spectrum of real m eigenvalues that correspond to stable modes with, in addition, at most one imaginary eigenvalue for m , which corresponds to a tachyonic mode. No tachyons are present if

$$\frac{C_2}{C_1} = \tan\left(\frac{\alpha}{2}\right) < -\left(\frac{\pi}{2}\right)^{-2\mu} \frac{\Gamma(1+\mu)}{\Gamma(1-\mu)} \frac{\Gamma^2\left(\frac{\tilde{\mu}-\mu+1}{2}\right)}{\Gamma^2\left(\frac{\tilde{\mu}+\mu+1}{2}\right)} \quad \text{or} \quad \frac{C_2}{C_1} > 0. \quad (2.50)$$

Two typical examples are displayed in fig. 1

- If $0 < \mu < 1$ and $0 < \tilde{\mu} < 1$, which corresponds to case 3 in Table 1, one is free to use arbitrary combinations of the independent solutions at the two ends of the interval, and the self-adjoint boundary conditions relate them by a $U(1,1)$ matrix, according to eq. (2.5). Taking eqs. (2.1), (2.2) and (2.32) into account, one can first conclude that

$$C_1 = B \sqrt{2\mu} \left(\frac{\pi}{2}\right)^{\frac{1}{2}+\mu}, \quad C_2 = A \sqrt{2\mu} \left(\frac{\pi}{2}\right)^{\frac{1}{2}-\mu}, \quad (2.51)$$

and then eqs. (2.36) determine C_4 and C_3 as

$$\begin{aligned} \frac{\left(\frac{\pi}{2}\right)^{\tilde{\mu}} \sqrt{\frac{\mu}{\tilde{\mu}}} C_4}{\Gamma(a+b-c)} &= C_1 \frac{\Gamma(2-c) \left(\frac{\pi}{2}\right)^{-\mu}}{\Gamma(a-c+1) \Gamma(b-c+1)} + C_2 \frac{\Gamma(c) \left(\frac{\pi}{2}\right)^{\mu}}{\Gamma(a) \Gamma(b)}, \\ \frac{\left(\frac{\pi}{2}\right)^{-\tilde{\mu}} \sqrt{\frac{\mu}{\tilde{\mu}}} C_3}{\Gamma(c-a-b)} &= C_1 \frac{\Gamma(2-c) \left(\frac{\pi}{2}\right)^{-\mu}}{\Gamma(1-a) \Gamma(1-b)} + C_2 \frac{\Gamma(c) \left(\frac{\pi}{2}\right)^{\mu}}{\Gamma(c-a) \Gamma(c-b)}. \end{aligned} \quad (2.52)$$

One can verify that the two pairs (C_1, C_2) and (C_4, C_3) are related by an $SL(2, R)$ transformation V , as in eq. (2.9). The boundary conditions can now be parametrized via eq. (2.8) and an additional phase β , and the eigenvalue equation (2.10) reads

$$\begin{aligned} &\xi(-\mu, \tilde{\mu}, m) (\cos \theta_1 \cosh \rho - \cos \theta_2 \sinh \rho) \\ &+ \xi(\mu, -\tilde{\mu}, m) (\cos \theta_1 \cosh \rho + \cos \theta_2 \sinh \rho) \\ &- \xi(\mu, \tilde{\mu}, m) (\sin \theta_1 \cosh \rho + \sin \theta_2 \sinh \rho) \\ &+ \xi(-\mu, -\tilde{\mu}, m) (\sin \theta_1 \cosh \rho - \sin \theta_2 \sinh \rho) = 2 \cos \beta, \end{aligned} \quad (2.53)$$

where

$$\xi(\mu, \tilde{\mu}, m) = \frac{\left(\frac{\pi}{2}\right)^{\mu-\tilde{\mu}} \sqrt{\left|\frac{\tilde{\mu}}{\mu}\right|} \Gamma(1-\mu) \Gamma(\tilde{\mu})}{\Gamma\left[\frac{1}{2}(-\mu+\tilde{\mu}+1)-m\right] \Gamma\left[m+\frac{1}{2}(-\mu+\tilde{\mu}+1)\right]} . \quad (2.54)$$

In the $\rho \rightarrow \infty$ limit, which translates into independent boundary conditions at the ends of the interval, this expression reduces to

$$\begin{aligned} & \xi(-\mu, \tilde{\mu}, m) (\cos \theta_1 - \cos \theta_2) + \xi(\mu, -\tilde{\mu}, m) (\cos \theta_1 + \cos \theta_2) \\ & - \xi(\mu, \tilde{\mu}, m) (\sin \theta_1 + \sin \theta_2) + \xi(-\mu, -\tilde{\mu}, m) (\sin \theta_1 - \sin \theta_2) = 0 . \end{aligned} \quad (2.55)$$

Some special cases are exactly solvable.

- If $\theta_1 = \theta_2 = 0$, eq. (2.55) reduces to $\xi(\mu, -\tilde{\mu}, m) = 0$, which is solved by

$$m^2 = \left(n - \frac{\mu + \tilde{\mu} - 1}{2}\right)^2 , \quad n = 0, 1, \dots . \quad (2.56)$$

There is a zero mode when $\mu + \tilde{\mu} = 1$, which is in principle possible within the ranges that concern this case, but never occurs in Table 1;

- In a similar fashion, if $\theta_1 = \theta_2 = \frac{\pi}{2}$, eq. (2.55) reduces to $\xi(\mu, \tilde{\mu}, m) = 0$, which is solved by

$$m^2 = \left(n - \frac{\mu - \tilde{\mu} - 1}{2}\right)^2 , \quad n = 0, 1, \dots . \quad (2.57)$$

- If $\theta_1 = -\theta_2 = \frac{\pi}{2}$, eq. (2.55) reduces to $\xi(-\mu, -\tilde{\mu}, m) = 0$, which is solved by

$$m^2 = \left(n + \frac{\mu - \tilde{\mu} + 1}{2}\right)^2 , \quad n = 0, 1, \dots . \quad (2.58)$$

- Finally, if $\theta_1 = 0$ and $\theta_2 = \pi$, eq. (2.55) reduces to $\xi(-\mu, \tilde{\mu}, m) = 0$, which is solved by

$$m^2 = \left(n + \frac{\mu + \tilde{\mu} + 1}{2}\right)^2 , \quad n = 0, 1, \dots . \quad (2.59)$$

- If $0 < \mu < 1$ and $\tilde{\mu} = 0$, both solutions in eq. (2.32) are normalizable, and the asymptotic behavior at the left end defines again the two coefficients C_1 and C_2 according to eq. (2.51), while C_3 and C_4 are defined according to

$$\psi \sim \sqrt{1 - \frac{z}{z_m}} \left[C_4 + C_3 \log \left(1 - \frac{z}{z_m} \right) \right] , \quad (2.60)$$

One can obtain the connection formulas as the $\tilde{\mu} \rightarrow 0$ limit of the preceding expressions in eqs. (2.35) and (2.36). Consequently, the behavior in the vicinity of the right end of the

interval is now

$$\begin{aligned} w_1(z) &\sim \xi_1(\mu, m) + \xi_2(\mu, m) \log \left(1 - \frac{z}{z_m} \right) , \\ w_2(z) &\sim \xi_1(-\mu, m) + \xi_2(-\mu, m) \log \left(1 - \frac{z}{z_m} \right) , \end{aligned} \quad (2.61)$$

where

$$\begin{aligned} \xi_1(\mu, m) &= - \frac{\left(\frac{\pi}{2}\right)^\mu \Gamma(1-\mu) \left[\psi\left(-m - \frac{\mu}{2} + \frac{1}{2}\right) + \psi\left(m - \frac{\mu}{2} + \frac{1}{2}\right) - 2\psi(1) + 2\log\left[\frac{\pi}{2}\right] \right]}{\sqrt{2|\mu|} \Gamma\left(-m - \frac{\mu}{2} + \frac{1}{2}\right) \Gamma\left(m - \frac{\mu}{2} + \frac{1}{2}\right)} \\ \xi_2(\mu, m) &= - \frac{2\left(\frac{\pi}{2}\right)^\mu \Gamma(1-\mu)}{\sqrt{2|\mu|} \Gamma\left(-m - \frac{\mu}{2} + \frac{1}{2}\right) \Gamma\left(m - \frac{\mu}{2} + \frac{1}{2}\right)} , \end{aligned} \quad (2.62)$$

with

$$\psi(z) = \frac{\Gamma'(z)}{\Gamma(z)} , \quad \psi(1) = -\gamma , \quad (2.63)$$

and $\gamma \sim 0.577$ the Euler–Mascheroni constant. The linear relations among the coefficients are now

$$\begin{aligned} C_4 &= C_2 \xi_1(\mu, m) + C_1 \xi_1(-\mu, m) , \\ C_3 &= C_2 \xi_2(\mu, m) + C_1 \xi_2(-\mu, m) . \end{aligned} \quad (2.64)$$

and consistently with [14] they define an $SL(2, R)$ transformation V . The resulting eigenvalue equation is

$$\begin{aligned} &(\cosh \rho \cos \theta_1 - \sinh \rho \cos \theta_2) \xi_1(-\mu, m) + (\cosh \rho \sin \theta_1 - \sinh \rho \sin \theta_2) \xi_2(-\mu, m) \\ &+ (\cosh \rho \cos \theta_1 + \sinh \rho \cos \theta_2) \xi_2(\mu, m) - (\cosh \rho \sin \theta_1 + \sinh \rho \sin \theta_2) \xi_1(\mu, m) \\ &- 2 \cos \beta = 0 . \end{aligned} \quad (2.65)$$

In the $\rho \rightarrow \infty$ limit, which translates into independent boundary conditions at the ends of the interval, this expression reduces to

$$\begin{aligned} &(\cos \theta_1 - \cos \theta_2) \xi_1(-\mu, m) + (\sin \theta_1 - \sin \theta_2) \xi_2(-\mu, m) \\ &+ (\cos \theta_1 + \cos \theta_2) \xi_2(\mu, m) - (\sin \theta_1 + \sin \theta_2) \xi_1(\mu, m) = 0 . \end{aligned} \quad (2.66)$$

Some special cases are exactly solvable:

– if $\theta_1 = \theta_2 = 0$, eq. (2.66) is solved by

$$m^2 = \left(n - \frac{\mu - 1}{2} \right)^2 , \quad n = 0, 1, \dots ; \quad (2.67)$$

– if $\theta_1 = 0$ and $\theta_2 = \pi$, the solution is

$$m^2 = \left(n + \frac{\mu + 1}{2} \right)^2, \quad n = 0, 1, \dots \quad (2.68)$$

Before turning to the different sectors of the actual spectrum, let us describe some features of the multi-dimensional case.

2.4 A SIMPLE MATRIX GENERALIZATION OF THE HYPERGEOMETRIC MODEL

One can generalize the preceding setup to cases when the wavefunction has n components, replacing μ and $\tilde{\mu}$ in eq. (2.29) by real diagonal matrices, so that

$$\mu \rightarrow \text{diag}(\mu_1, \dots, \mu_n), \quad (2.69)$$

and similarly for $\tilde{\mu}$. In this case there are n decoupled hypergeometric equations, whose solutions, however, can be mixed by the boundary conditions.

For simplicity, we can confine our attention to boundary conditions given independently at the two ends, and to the special cases of interest in this paper in Sections 10.2 and 11.2, where $n = 2$, $0 < \mu_{1,2} < 1$, while $0 < \tilde{\mu}_1 < 1$ and $\tilde{\mu}_2 > 1$. In these cases, the choice of self-adjoint boundary conditions involves five angles at the left end and one additional parameter at the right end.

Let us begin from the first end. Making use of eq. (2.27) and denoting the product ΩC by \tilde{C} , the independent boundary conditions at the left end can be cast in the form

$$\begin{aligned} \tilde{C}_{11} &= \cos \alpha_1 \tilde{C}_{11} + \sin \alpha_1 \tilde{C}_{12}, \\ \tilde{C}_{21} &= \cos \alpha_2 \tilde{C}_{21} + \sin \alpha_2 \tilde{C}_{22}, \end{aligned} \quad (2.70)$$

or equivalently

$$\tilde{C}_{11} = \cot \frac{\alpha_1}{2} \tilde{C}_{12}, \quad \tilde{C}_{21} = \cot \frac{\alpha_2}{2} \tilde{C}_{22}. \quad (2.71)$$

Now the actual C coefficients are related to the \tilde{C} by an $SU(2)$ matrix Ω^\dagger , and one can parametrize Ω as

$$\Omega = \begin{pmatrix} \cos \gamma e^{i\alpha} & \sin \gamma e^{i\beta} \\ -\sin \gamma e^{-i\beta} & \cos \gamma e^{-i\alpha} \end{pmatrix}, \quad (2.72)$$

so that finally

$$C_{i1} = \tilde{E}_{ij} C_{j2}, \quad (2.73)$$

with

$$\tilde{E} = \Omega^\dagger E \Omega, \quad E = \begin{pmatrix} \cot \frac{\alpha_1}{2} & 0 \\ 0 & \cot \frac{\alpha_2}{2} \end{pmatrix}. \quad (2.74)$$

For $\Omega = 1$ one recovers the boundary conditions for independent equations that encompass all cases with $\mathbf{k} = 0$. When $\alpha_1 = \alpha_2$, Ω commutes with E and disappears altogether, and a similar simplification occurs, for a generic E , when Ω is diagonal.

If $\tilde{\mu}_2 \geq 1$, as will be the case in Section 10.2, one must demand that at the right end $C_{24} = 0$, in order get L^2 solutions, and moreover the ratio

$$\frac{C_{13}}{C_{14}} = \cot \frac{\tilde{\alpha}_1}{2} \quad (2.75)$$

can be taken to parameterize the independent choices of self-adjoint boundary conditions there. The continuation to the right end of the interval of the hypergeometric solutions then yields the relations

$$\begin{aligned} \frac{\left(\frac{\pi}{2}\right)^{\tilde{\mu}_i} \sqrt{\frac{\mu_i}{\tilde{\mu}_i}} C_{i4}}{\Gamma(\tilde{\mu}_i)} &= C_{i1} \frac{\Gamma(1 + \mu_i) \left(\frac{\pi}{2}\right)^{-\mu_i}}{\Gamma\left(\frac{\tilde{\mu}_i + \mu_i + 1}{2} + m\right) \Gamma\left(\frac{\tilde{\mu}_i + \mu_i + 1}{2} - m\right)} \\ &+ C_{i2} \frac{\Gamma(1 - \mu_i) \left(\frac{\pi}{2}\right)^{\mu_i}}{\Gamma\left(\frac{\tilde{\mu}_i - \mu_i + 1}{2} + m\right) \Gamma\left(\frac{\tilde{\mu}_i - \mu_i + 1}{2} - m\right)}, \\ \frac{\left(\frac{\pi}{2}\right)^{-\tilde{\mu}_i} \sqrt{\frac{\mu_i}{\tilde{\mu}_i}} C_{i3}}{\Gamma(-\tilde{\mu}_i)} &= C_{i1} \frac{\Gamma(1 + \mu_i) \left(\frac{\pi}{2}\right)^{-\mu_i}}{\Gamma\left(\frac{\mu_i - \tilde{\mu}_i + 1}{2} + m\right) \Gamma\left(\frac{\mu_i - \tilde{\mu}_i + 1}{2} - m\right)} \\ &+ C_{i2} \frac{\Gamma(1 - \mu_i) \left(\frac{\pi}{2}\right)^{\mu_i}}{\Gamma\left(\frac{1 - \tilde{\mu}_i - \mu_i}{2} + m\right) \Gamma\left(\frac{1 - \tilde{\mu}_i - \mu_i}{2} - m\right)}, \end{aligned} \quad (2.76)$$

and taking eq. (2.73) into account, the *r.h.s* only involves the C_{j2} . These ingredients determine the eigenvalue equation as follows. One first expresses the C_{i1} in terms of the C_{i2} using eq. (2.73), so that the preceding relations become

$$\sqrt{\frac{\mu_i}{\tilde{\mu}_i}} C_{i4} = \mathcal{P}_{4ij} C_{j2}, \quad \sqrt{\frac{\mu_i}{\tilde{\mu}_i}} C_{i3} = \mathcal{P}_{3ij} C_{j2} \quad (2.77)$$

where

$$\begin{aligned} \mathcal{P}_{4ij} &= \frac{\tilde{E}_{ij} \Gamma(1 + \mu_i) \Gamma(\tilde{\mu}_i) \left(\frac{\pi}{2}\right)^{-\mu_i - \tilde{\mu}_i}}{\Gamma\left(\frac{\tilde{\mu}_i + \mu_i + 1}{2} + m\right) \Gamma\left(\frac{\tilde{\mu}_i + \mu_i + 1}{2} - m\right)} + \frac{\delta_{ij} \Gamma(1 - \mu_i) \Gamma(\tilde{\mu}_i) \left(\frac{\pi}{2}\right)^{\mu_i - \tilde{\mu}_i}}{\Gamma\left(\frac{\tilde{\mu}_i - \mu_i + 1}{2} + m\right) \Gamma\left(\frac{\tilde{\mu}_i - \mu_i + 1}{2} - m\right)}, \\ \mathcal{P}_{3ij} &= \frac{\tilde{E}_{ij} \Gamma(1 + \mu_i) \Gamma(-\tilde{\mu}_i) \left(\frac{\pi}{2}\right)^{-\mu_i + \tilde{\mu}_i}}{\Gamma\left(\frac{\mu_i - \tilde{\mu}_i + 1}{2} + m\right) \Gamma\left(\frac{\mu_i - \tilde{\mu}_i + 1}{2} - m\right)} + \frac{\delta_{ij} \Gamma(1 - \mu_i) \Gamma(-\tilde{\mu}_i) \left(\frac{\pi}{2}\right)^{\mu_i + \tilde{\mu}_i}}{\Gamma\left(\frac{1 - \tilde{\mu}_i - \mu_i}{2} + m\right) \Gamma\left(\frac{1 - \tilde{\mu}_i - \mu_i}{2} - m\right)}. \end{aligned} \quad (2.78)$$

One must now demand that $C_{24} = 0$, while also relating C_{13} and C_{14} according to eq. (2.75), and the resulting eigenvalue equation

$$\cot \frac{\tilde{\alpha}_1}{2} = \frac{P_{422} P_{311} - P_{421} P_{312}}{P_{422} P_{411} - P_{421} P_{412}} \quad (2.79)$$

depends on six parameter, the five parameters contained in \tilde{E} and $\tilde{\alpha}_1$.

The other case of interest, $\tilde{\mu}_1 = 0$ and $\tilde{\mu}_2 > 1$, will present itself in Section 11.2. Now the preceding equations (2.76) for $i = 1$ are replaced by

$$\begin{aligned} C_{14} &= C_{12} \xi_1(\mu_1, m) + C_{11} \xi_1(-\mu_1, m) , \\ C_{13} &= C_{12} \xi_2(\mu_1, m) + C_{11} \xi_2(-\mu_1, m) , \end{aligned} \quad (2.80)$$

where ξ_1 and ξ_2 are defined in eqs. (2.62), while they still hold for $i = 2$. The final form of the eigenvalue equation is then

$$\cot \frac{\tilde{\alpha}_1}{2} = \frac{P_{422} \left(\xi_2(\mu_1, m) - \xi_2(-\mu_1, m) \tilde{E}_{11} \right) - \xi_2(-\mu_1, m) \tilde{E}_{12} P_{421}}{P_{422} \left(\xi_1(\mu_1, m) + \xi_1(-\mu_1, m) \tilde{E}_{11} \right) - \xi_1(-\mu_1, m) \tilde{E}_{12} P_{421}} , \quad (2.81)$$

and the number of free parameters remains the same.

3 THE PERTURBED DILATON–AXION SYSTEM

In a generic metric of the form

$$ds^2 = e^{2A(r)} dx^2 + e^{2B(r)} dr^2 + e^{2C(r)} dy^2 , \quad (3.1)$$

and in the harmonic gauge

$$B = 4A + 5C , \quad (3.2)$$

the perturbed dilaton equation follows from the quadratic terms in the type–IIB effective action, which for manifolds without boundaries contains the terms

$$\mathcal{S} = - \frac{1}{4k_{10}^2} \int d^{10}x \left\{ e^{2(B-A)} \eta^{\mu\nu} \partial_\mu \varphi \partial_\nu \varphi + \epsilon^{2(B-C)} \delta^{ij} \partial_i \varphi \partial_j \varphi + (\partial_r \varphi)^2 \right\} , \quad (3.3)$$

and can be cast in the form

$$\square \varphi + e^{2(A-C)} \nabla^2 \varphi + e^{2(A-B)} \partial_r^2 \varphi = 0 . \quad (3.4)$$

Here \square and ∇^2 denote the d'Alembertian operator for four-dimensional Minkowski space and the Laplace operator for the internal torus. In the analysis of the different sectors we shall rely implicitly on the self-adjoint action discussed in [28], which differs from eq. (3.3) by the addition of boundary terms, in order to explore general self-adjoint boundary conditions. In this sector this action reduces to

$$\mathcal{S}_{s.a.} = \frac{1}{4k_{10}^2} \int d^{10}x \left\{ e^{2(B-A)} \varphi \square \varphi + e^{2(B-C)} \varphi \nabla^2 \varphi + \varphi \partial_r^2 \varphi \right\} , \quad (3.5)$$

and one can now separate variables letting

$$\varphi(x, r, y) = \varphi(x) f(r) e^{i\mathbf{k}\cdot\mathbf{y}} , \quad (3.6)$$

while also defining the four-dimensional squared mass via

$$\square \varphi(x) = m^2 \varphi(x) , \quad (3.7)$$

so that the perturbed dilaton equation becomes

$$f''(r) - \mathbf{k}^2 e^{2(B-C)} f(r) + m^2 e^{2(B-A)} f(r) = 0 . \quad (3.8)$$

This equation determines the allowed values of m^2 , and in fact one can recast it in a form where these become eigenvalues of a Hermitian second-order operator. We can now describe the procedure in detail, since it will recur in the following sections. The first step consists in trading r for the conformal variable z , defined via

$$dz = e^{B-A} dr , \quad (3.9)$$

with $z(0) = 0$. Note that z has a finite range for the background of eqs. (1.1), $0 \leq z \leq z_m$, with z_m given by

$$z_m = \int e^{B-A} dr \simeq 2.24 z_0 , \quad (3.10)$$

and

$$z_0 = \rho h^{\frac{1}{2}} = (2H\rho^3)^{\frac{1}{2}} . \quad (3.11)$$

Here and in the rest of the paper z -derivatives will be often denoted by a subscript, so that, for instance

$$A_z \equiv \frac{dA}{dz} = e^{A-B} A'(r) , \quad (3.12)$$

where $A'(r)$ denotes the derivative with respect to r . Performing this change of variable, the original equation (3.8) becomes

$$\frac{d^2 f}{dz^2} + (B_z - A_z) \frac{df}{dz} + \left[m^2 - \mathbf{k}^2 e^{2(A-C)} \right] f = 0 . \quad (3.13)$$

The second step entails, in this case, the field redefinition

$$f = e^{-\frac{1}{2}(B-A)} g , \quad (3.14)$$

which finally leads to the manifestly Hermitian Schrödinger-like equation

$$-\frac{d^2 g}{dz^2} + V g = m^2 g . \quad (3.15)$$

The potential is

$$V = \frac{1}{4}(B_z - A_z)^2 + \frac{1}{2}(B_{zz} - A_{zz}) + \mathbf{k}^2 e^{2(A-C)}, \quad (3.16)$$

and its detailed expression as a function of r , which can be obtained using results in Appendix A, reads

$$V = -\frac{e^{\frac{r}{\rho}} \sqrt{\frac{5}{2}}}{4 z_0^2 \sinh\left(\frac{r}{\rho}\right)^3} \left[1 + \frac{1}{4} \left(\cosh\left(\frac{r}{\rho}\right) - \sqrt{\frac{5}{2}} \sinh\left(\frac{r}{\rho}\right) \right)^2 \right] + \mathbf{k}^2 e^{2(A-C)}. \quad (3.17)$$

Note that

$$V = \frac{1}{z_0^2} \left[f_1\left(\frac{z}{z_0}\right) + (k\rho)^2 f_2\left(\frac{z}{z_0}\right) \right], \quad (3.18)$$

where

$$k = \frac{|\mathbf{n}|}{R}, \quad (3.19)$$

with $|\mathbf{n}|$ an integer-valued vector independent of R , and consequently for $\mathbf{k} = 0$ all squared masses are proportional to $\frac{1}{z_0^2}$, while in general they also depend on the ratio $\frac{\rho}{R}$.

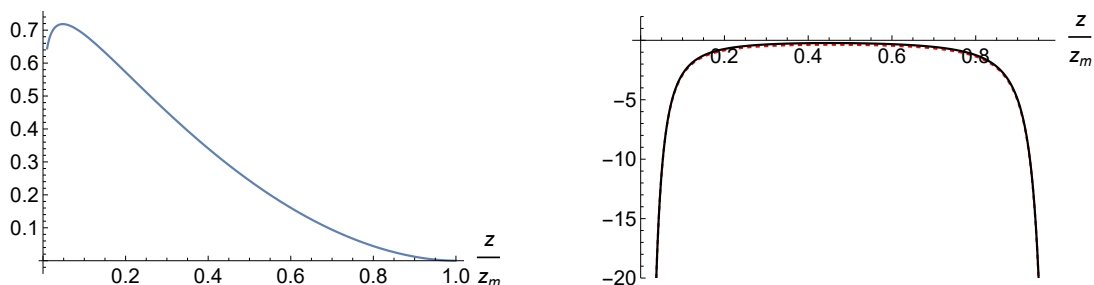


Figure 2: The left panel shows the normalized zero-mode wavefunction (3.25). The right panel compares the actual dilaton potential (black, solid) with its approximation (2.29) with $(\mu, \tilde{\mu}) = (\frac{1}{3}, 0)$ (red, dashed), which is almost superposed to it. They are in units of $\frac{1}{z_0^2}$, with z_m and z_0 defined in eqs. (3.10) and (3.11).

The \mathbf{k} -independent portion of the potential is displayed in fig. 2 as a function of $\frac{z}{z_0}$: it has the form of an inverted well, with singularities at the two ends $z = 0$ and $z = z_m$, where

$$V \sim \frac{\mu^2 - \frac{1}{4}}{z^2}, \quad V \sim \frac{\tilde{\mu}^2 - \frac{1}{4}}{(z - z_m)^2}, \quad (3.20)$$

with $\mu = \frac{1}{3}$ and $\tilde{\mu} = 0$, so that it belongs to case 1 in Section 2. The supersymmetric limit is recovered as $\rho \rightarrow \infty$, where the interval becomes of infinite length, and then V approaches

$$V_{susy} = -\frac{5}{36 z^2} + \frac{\mathbf{n}^2}{R^2} \left(\frac{1}{3|H|z} \right)^{\frac{2}{3}}. \quad (3.21)$$

One can actually recast eq. (3.15) in the form

$$\left[\mathcal{A} \mathcal{A}^\dagger + \mathbf{k}^2 e^{2(A-C)} \right] g = m^2 g, \quad (3.22)$$

where the operators \mathcal{A} and \mathcal{A}^\dagger are

$$\mathcal{A} = \partial_z + \frac{1}{2}(3A_z + 5C_z) , \quad \mathcal{A}^\dagger = -\partial_z + \frac{1}{2}(3A_z + 5C_z) . \quad (3.23)$$

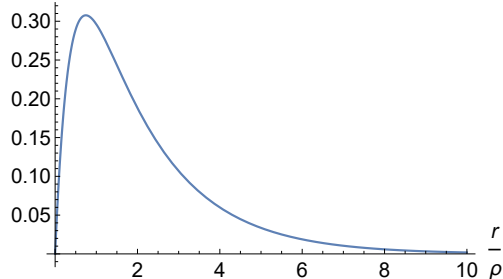


Figure 3: The distribution function $\Pi_\phi\left(\frac{r}{\rho}\right)$ for the dilaton zero mode, in units of $\frac{1}{\rho}$. The average value of r is about 2.1ρ .

One can thus find a massless mode for the dilaton, solving the first-order equation

$$\mathcal{A}^\dagger g = 0 . \quad (3.24)$$

The solution reads

$$g = g_0 e^{\frac{3A+5C}{2}} , \quad (3.25)$$

where g_0 a constant, and this wavefunction is normalizable, since

$$\int_0^{z_m} dz g^2 = \int_0^\infty dr e^{2(B-A)} g_0^2 \quad (3.26)$$

is clearly finite. The corresponding normalized r -distribution

$$\Pi_\phi(r) \simeq \frac{3}{2\rho} \sinh\left(\frac{r}{\rho}\right) e^{-\frac{r}{\rho}\sqrt{\frac{5}{2}}} , \quad (3.27)$$

which is localized in the vicinity of the effective BPS orientifold, is displayed in fig. 3. Note that the actual dilaton zero-mode wavefunction

$$\varphi(x, r, y) = \varphi(x) f_0 \quad (3.28)$$

has a constant r profile.

The behavior of the zero-mode wavefunction (3.27) near the right end of the interval is

$$g \sim \left(1 - \frac{z}{z_m}\right)^{\frac{1}{2}} , \quad (3.29)$$

without a log term, so that, in the notation of the previous section, $C_3 = 0$. In a similar fashion, the dominant behavior of the actual zero mode near the left end of the interval is

$$g \simeq \left(\frac{z}{z_m}\right)^{\frac{1}{6}} - 0.71 \left(\frac{z}{z_m}\right)^{\frac{5}{6}} . \quad (3.30)$$

The two limiting behaviors define the self-adjoint boundary conditions characterizing the zero mode. The argument presented in [14] shows that, with this choice of boundary conditions, no instabilities are present in this sector.

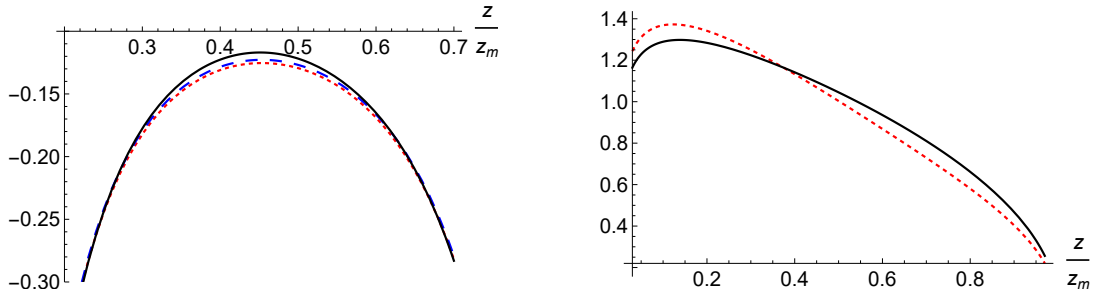


Figure 4: The left panel shows how shifting slightly eq. (2.29) can optimize the correspondence with the dilaton potential in the middle region. The potentials are multiplied by the ratio $\frac{z_m^2}{\pi^2}$ in order to enhance their differences. The dashed curve corresponds to a shift $a \simeq 0.26$, which is also suggested by perturbation theory, while the dotted curve corresponds to $a \simeq 0.255$. The right panel compares the normalized ground-state wavefunction (3.25) (black, solid) with its approximation obtained combining the two zero modes in eq. (2.43), in such a way that the leading behavior corresponds to eq. (3.30).

More general boundary conditions can be explored relying on the model potential (2.29) with $(\mu, \tilde{\mu}) = (\frac{1}{3}, 0)$

$$V \simeq \frac{\pi^2}{4 z_m^2} \left[\frac{-\frac{5}{36}}{\sin^2\left(\frac{\pi z}{2 z_m}\right)} - \frac{\frac{1}{4}}{\cos^2\left(\frac{\pi z}{2 z_m}\right)} \right] + \frac{\pi^2}{z_m^2} a^2, \quad (3.31)$$

where we have allowed for an overall shift determined by a . The preferred values are $a = 0.255$ (dashed curve) and $a = 0.26$ (dotted curve), as shown in fig. 4, and the latter is also suggested by perturbation theory. The resulting spectrum is now determined by eq. (2.66), but the actual masses m_{dil} are related to m according to

$$m_{dil}^2 = m^2 + a^2, \quad (3.32)$$

so that the massless mode corresponds to $m = ia$. The large- ρ boundary conditions leading to a massless mode are displayed in the left panel of fig. 5. Those corresponding to $C_3 = 0$ lie on the diagonal $\theta_1 = -\theta_2$, on account of the second of eqs. (2.11), while the second of eqs. (2.64), with $m \simeq 0.26 i$ gives

$$\frac{C_1}{C_2} = \tan \theta_1 = -\frac{\xi_2\left(\frac{1}{3}, ia\right)}{\xi_2\left(-\frac{1}{3}, ia\right)} \simeq -0.74, \quad (3.33)$$

to be compared with the coefficient 0.71 that enters eq. (3.30), which is thus captured up to an error of about 3%. The resulting stability region is displayed in the right panel of fig. 5. A large portion of the moduli space is excluded, but there is nonetheless a wide range of boundary

conditions that can make the dilaton massive. An alternative procedure to determine the shift a , which we shall favor in the following, is to determine it so that the ratio of C_1 and C_2 coincides with the result that can be deduced from the exact zero mode, which would be -0.71 in this case. This would lead to $a \simeq 0.3$, and to a very similar stability region.

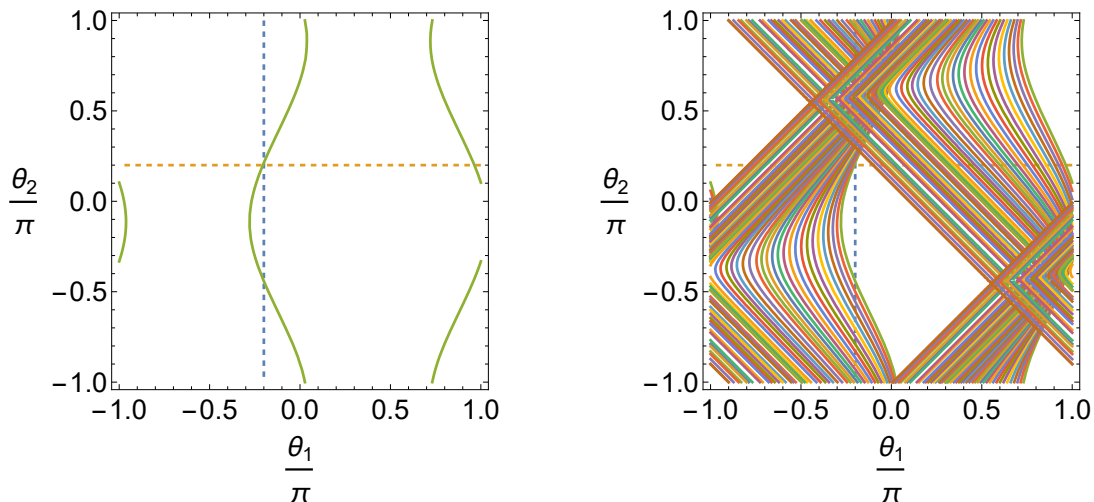


Figure 5: The curves in the left panel identify the boundary conditions leading to a massless mode. The zero mode (3.25) lies at the intersection of the vertical and horizontal dashed lines for $(\theta_1, \theta_2) \simeq (-0.2, 0.2)\pi$, on the line $\theta_1 + \theta_2 = 0$ that characterizes boundary conditions leading to $C_3 = 0$. The shaded regions in the right panel identify the boundary conditions leading to instabilities.

Summarizing, the requirement of stability removes a large portion of the moduli space of self-adjoint boundary conditions for the dilaton, and massless modes are only present on the curve in the left panel of fig. 5. There are two equivalent special points on this curve, which correspond to the solution of eq. (3.24). Using the same boundary conditions for the axion, which solves an identical equation, can thus lead to a pair of massless scalars. With this choice, no additional instabilities can emerge from the modes with $\mathbf{k} \neq 0$, since the corresponding spectrum is lifted in mass, as is manifest in eq. (3.17).

4 THE PERTURBED TYPE-IIB THREE-FORMS

We can now turn to the modes of the two type-IIB three-forms. This is a more intricate sector, with some unfamiliar features, as we are about to see. In the following, it will be convenient to work with the complex combination

$$\mathcal{H} \equiv d\mathcal{B} = d\mathcal{B}_2^1 + i d\mathcal{B}_2^2 \quad (4.1)$$

of the type-IIB three-form field strengths, so that \mathcal{B} will now denote the corresponding complex two-form gauge field. In this notation the self-adjoint action describing the quadratic fluctuations in this sector [16] becomes

$$\mathcal{S} = \frac{1}{4k_{10}^2} \int_{\mathcal{M}} \left[-\frac{1}{2} \bar{\mathcal{B}} \wedge d \star \mathcal{H} - \frac{1}{2} \mathcal{B} \wedge d \star \bar{\mathcal{H}} - i (\bar{\mathcal{B}} \wedge \mathcal{H} - \mathcal{B} \wedge \bar{\mathcal{H}}) \wedge \mathcal{H}_5^{(0)} \right], \quad (4.2)$$

and the corresponding field equations read ³

$$d \star \mathcal{H} = -2i \mathcal{H} \wedge \mathcal{H}_5^{(0)}, \quad (4.3)$$

or, in components

$$D^M \mathcal{H}_{MNP} = -\frac{2i}{3} \mathcal{H}_5^{(0)}{}_{NPQRS} \mathcal{H}^{QRS}. \quad (4.4)$$

These equations are clearly invariant under

$$\delta \mathcal{B} = d\Lambda, \quad (4.5)$$

while the boundary contributions to the variation of the action,

$$\delta \mathcal{S} = \frac{1}{4k_{10}^2} \int_{\partial \mathcal{M}} \left[-\frac{1}{2} \bar{\Lambda} \wedge \left(d \star \mathcal{H} + 2i \mathcal{H} \wedge \mathcal{H}_5^{(0)} \right) + \text{c.c.} \right], \quad (4.6)$$

only vanish on shell. Note that, even if one started from the conventional first-order action, the Chern–Simons term would still yield a non-vanishing contribution. There are two options to deal with this kind of problem: one can constrain the gauge parameter to vanish on the boundary, or alternatively one can introduce Stueckelberg fields living there that compensate the variation in eq. (4.6). In this case the second option would rest on a complex nine-dimensional one-form A living on the boundary such that

$$\delta A = -\Lambda|_{\partial \mathcal{M}}, \quad (4.7)$$

and on the modified action

$$\mathcal{S}_{\text{tot}} = \mathcal{S} - \frac{1}{4k_{10}^2} \int_{\partial \mathcal{M}} \left[\frac{1}{2} \bar{A} \wedge \left(d \star \mathcal{H} + 2i \mathcal{H} \wedge \mathcal{H}_5^{(0)} \right) + \text{c.c.} \right]. \quad (4.8)$$

Varying \bar{A} and its complex conjugate A one simply obtains eqs. (4.3) reduced to the boundary. Removing A via eq. (4.7) is possible, but at the cost of limiting the residual gauge transformations to those vanishing on the boundary, as we have said. When A is retained, one does not modify

³The factor 2 in this equation and the previous ones is consistent with the original work in [16], and the differences with respect to the excellent work in [29] reflect our different definition of \mathcal{H}_5 and our identical normalization for the three-forms.

the bulk equations provided the boundary term is stationary under variations of \mathcal{B} . The complete variation of the action (4.8) reads

$$\delta \mathcal{S}_{\text{tot}} = \frac{1}{4k_{10}^2} \int_{\mathcal{M}} \left[-\frac{1}{2} \delta \bar{\mathcal{B}} \left(d \star \mathcal{H} + 2i \mathcal{H} \wedge \mathcal{H}_5^{(0)} \right) + \text{c.c.} \right] + \delta \mathcal{S}_{\text{tot}}|_{\partial \mathcal{M}}, \quad (4.9)$$

and includes a boundary term, whose form we can now spell out after introducing the 9 + 1 dimensional decomposition

$$\mathcal{B} = \mathcal{C} + \mathcal{D} dr, \quad d = d_9 + dr \partial_r, \quad (4.10)$$

where \mathcal{C} is a nine-dimensional two-form and \mathcal{D} is nine-dimensional one-form. In terms of A and of these two quantities, one can see the total boundary term in eq. (4.9) is

$$\begin{aligned} \delta \mathcal{S}_{\text{tot}}|_{\partial \mathcal{M}} &= \frac{1}{4k_{10}^2} \int_{\partial \mathcal{M}} \left\{ \delta \mathcal{C} \left[-\frac{1}{2} e^{-B} \star_9 (d_9 \bar{\mathcal{D}} + \partial_r \bar{\mathcal{C}}) + i (\bar{\mathcal{C}} + d_9 \bar{A}) \wedge \mathcal{H}_5^{(0)} \right] \right. \\ &+ \frac{1}{2} e^{-B} \partial_r \delta \mathcal{C} \star_9 (\bar{\mathcal{C}} + d_9 \bar{A}) + \frac{1}{2} e^{-B} \delta \mathcal{D} d_9 \star_9 (\bar{\mathcal{C}} + d_9 \bar{A}) \\ &\left. - \delta \bar{A} \left[i d_9 \mathcal{C} \wedge \mathcal{H}_5^{(0)} + \frac{1}{2} e^{-B} d_9 \star_9 (d_9 \mathcal{D} + \partial_r \mathcal{C}) \right] + \text{c.c.} \right\}, \quad (4.11) \end{aligned}$$

where \star_9 denotes the nine-dimensional *curved* (r -dependent) Hodge dual.

The contribution involving $\delta \mathcal{D}$ vanishes provided

$$d_9 \star_9 (\mathcal{C} + d_9 A) = 0. \quad (4.12)$$

This is an equation of motion for A that describes a complex vector, massless in four dimensions, for which the divergence of C is a source. Moreover, the contribution proportional to δA is the induced equation of motion on the boundary for the original bulk fields, which is tantamount to eq. (4.3) if considered together with its r -component

$$e^B d_9 \star_9 d_9 \mathcal{C} + \partial_r (e^{-B} \star_9 \partial_r \mathcal{C}) + 2i (d_9 \mathcal{D} + \partial_r \mathcal{C}) \wedge \mathcal{H}_5^{(0)} = 0. \quad (4.13)$$

Finally, the vanishing of the remaining terms,

$$\delta \mathcal{C} \left[-\frac{1}{2} e^{-B} \star_9 (d_9 \bar{\mathcal{D}} + \partial_r \bar{\mathcal{C}}) + i (\bar{\mathcal{C}} + d_9 \bar{A}) \wedge \mathcal{H}_5^{(0)} \right] + \frac{1}{2} \partial_r \delta \mathcal{C} \star_9 (\bar{\mathcal{C}} + d_9 \bar{A}), \quad (4.14)$$

is a gauge-invariant counterpart of the self-adjoint condition

$$\left(\partial_z \Psi \delta \Psi - \Psi \partial_z \delta \Psi \right) \Big|_{\partial \mathcal{M}} = 0, \quad (4.15)$$

discussed at length in [28] for a scalar field, together with the corresponding expression for gravity.

Let us now address the gauge fixing of this formulation, taking into account that the gauge parameter Λ can be decomposed according to

$$\Lambda = \Lambda_2 + \Lambda_1 dr , \quad (4.16)$$

where we have distinguished in it a nine-dimensional two-form Λ_2 and a nine-dimensional one-form Λ_1 . Then, taking eq. (4.10) into account, one can conclude that

$$\delta \mathcal{C} = d_9 \Lambda_2 , \quad \delta \mathcal{D} = d_9 \Lambda_1 + \partial_r \Lambda_2 , \quad \delta A = - \Lambda_2 |_{\partial \mathcal{M}} . \quad (4.17)$$

There are two options at this point.

- A first option is removing \mathcal{D} altogether, which leaves a residual gauge symmetry associated to Λ_2 gauge parameters satisfying the condition

$$\partial_r d_9 \Lambda_2 = 0 . \quad (4.18)$$

The bulk equations of motion then become

$$\begin{aligned} e^B d_9 \star_9 d_9 \mathcal{C} + \partial_r (e^{-B} \star_9 \partial_r \mathcal{C}) + 2i \partial_r \mathcal{C} \wedge \mathcal{H}_5^{(0)} &= 0 , \\ d_9 \left[i \mathcal{C} \wedge \mathcal{H}_5^{(0)} + \frac{1}{2} e^{-B} \star_9 \partial_r \mathcal{C} \right] &= 0 . \end{aligned} \quad (4.19)$$

A complex massless vector field A lives on the boundary, and the solution for \mathcal{C} is a source for it. Strictly speaking, it might seem that two different A fields are left at the two ends of the interval, but the residual gauge symmetry with an r -independent Λ_2 can be used to remove one of them.

- There is a second option, which is less convenient. It consists in enforcing the Lorentz gauge condition $d \star \mathcal{B} = 0$, which becomes

$$d_9 \star_9 \mathcal{D} = 0 , \quad \star_9 \partial_r \mathcal{D} - d_9 \star_9 \mathcal{C} = 0 \quad (4.20)$$

in the 9+1 decomposition. This turns eq. (4.3) into

$$\square_{10} \mathcal{B} - 2i \star \left(d \mathcal{B} \wedge \mathcal{H}_5^{(0)} \right) = 0 , \quad (4.21)$$

so that the kinetic contribution becomes simpler, but the equations still involve both \mathcal{C} and \mathcal{D} .

In order to make progress, it is now important to take into account the detailed form of the background. To this end, it is useful to distinguish the spacetime and toroidal coordinates among the nine residual ones. In this fashion, one can identify in \mathcal{B} a four-dimensional two-form, two types of one-forms and scalars, according to

$$b = \frac{1}{2} \mathcal{B}_{\mu\nu} dx^\mu dx^\nu, \quad a = \mathcal{B}_{\mu r} dx^\mu, \quad a_i = \mathcal{B}_{\mu i} dx^\mu, \quad \mathcal{B}_{ri}, \quad \mathcal{B}_{ij}, \quad (4.22)$$

and one can similarly decompose Λ into a four-dimensional one-form λ and scalars Λ_r and Λ_i , so that

$$\begin{aligned} \delta b &= d_4 \lambda, & \delta a &= d_4 \Lambda_r - \partial_r \lambda, & \delta \mathcal{B}_{ij} &= i(k_i \Lambda_j - k_j \Lambda_i), \\ \delta a_i &= d_4 \Lambda_i - i k_i \lambda, & \delta \mathcal{B}_{ri} &= \partial_r \Lambda_i - i k_i \Lambda_r. \end{aligned} \quad (4.23)$$

For $\mathbf{k} \neq 0$, in the spirit of what we said in the Introduction, one can eliminate the longitudinal parts of \mathcal{B}_{ij} , \mathcal{B}_{ri} and a_i . Both for $\mathbf{k} \neq 0$ and for $\mathbf{k} = 0$, in view of the preceding discussion, a and \mathcal{B}_{ri} could be eliminated using the gauge parameters λ and Λ_i . However, in all cases one should retain on the boundary the A field, within which one can distinguish a complex four-dimensional one-form A_4 and five complex scalars A_i . There is however a further simplification: the Chern–Simons term plays a role only in the equations for $\mathcal{B}_{\mu\nu}$ and $\mathcal{B}_{\mu r}$, on account of the special form of the five-form field strength present in the background of eqs. (1.1).

We can now examine the available modes, treating separately those corresponding to different $SO(5)$ representations since, as we have stressed in the Introduction, this is an internal symmetry for the $\mathbf{k} = 0$ sector, on which our analysis is largely focused.

4.1 THE MODES ORIGINATING FROM $\mathcal{B}_{\mu\nu}$ AND $\mathcal{B}_{\mu r}$

The modes originating from $\mathcal{B}_{\mu\nu}$ and $\mathcal{B}_{\mu r}$ entail some complications, due to the role played by the Chern–Simons term that, as we have seen, contributes to the small fluctuations due to the five-form background profile (1.1). Let us now focus on the modes of this type with $\mathbf{k} = 0$. In this case there are only two types of curvature components, $\mathcal{H}_{\mu\nu\rho}$ and $\mathcal{H}_{\mu\nu r}$, so that the decomposition

$$\mathcal{B} = b + a dr, \quad (4.24)$$

where b is a four-dimensional complex two-form and a is a four-dimensional complex one-form, translates into

$$\mathcal{H} = d_4 b + (\partial_r b + d_4 a) dr, \quad (4.25)$$

with d_4 the four-dimensional exterior derivative. The gauge transformations act on a and b as

$$\delta a = d_4 \Lambda_r - \partial_r \Lambda, \quad \delta b = d_4 \Lambda, \quad (4.26)$$

and allow one to remove a altogether, but at the expense of introducing an A field on the boundary, as we have stressed. One is thus left with the system

$$\begin{aligned} d_4 \left[e^{-4A} \star_4 \partial_r b - \frac{i\hbar}{\rho} b \right] &= 0, \\ e^{2A+10C} d_4 \star_4 d_4 b + \partial_r \left[e^{-4A} \star_4 \partial_r b - \frac{i\hbar}{\rho} b \right] &= 0 \end{aligned} \quad (4.27)$$

in the bulk, and on the boundary

$$e^{5C} \left[d_4 \star_4 d_4 A + d_4 \star_4 b \right] = 0. \quad (4.28)$$

Here \star_4 denotes the four-dimensional *flat* Hodge dual, and we have used the harmonic gauge condition (3.2) for the background. As we have seen, a residual r -independent gauge transformation can remove A from one of the two boundaries, where the last equation still sets to zero the divergence of b .

It is now convenient to define

$$u = e^{-4A} \star_4 \partial_r b, \quad (4.29)$$

so that eqs. (4.27) become

$$\begin{aligned} d_4 u - \frac{i\hbar}{\rho} d_4 b &= 0, \\ e^{2A+10C} d_4 \star_4 d_4 b + \partial_r u + \frac{i\hbar}{\rho} \star_4 e^{4A} u &= 0, \end{aligned} \quad (4.30)$$

and combining them leads to an equation for u that is of first order in r :

$$\partial_r u - \frac{i\rho}{\hbar} e^{2A+10C} d_4 \star_4 d_4 u + \frac{i\hbar}{\rho} e^{4A} \star_4 u = 0. \quad (4.31)$$

Note that, using eqs. (4.25), (4.29) and the first of eqs. (4.30), one can link \mathcal{H} to u according to

$$\mathcal{H} = -\frac{i\rho}{\hbar} d_4 u - e^{4A} \star_4 u dr, \quad (4.32)$$

or

$$\mathcal{H} = -\frac{i\rho}{\hbar} (\partial_r u dr + d_4 u) - \left(\frac{\rho}{\hbar}\right)^2 e^{2A+10C} d_4 \star_4 d_4 u dr. \quad (4.33)$$

One can now exhibit different modes within u , making use of the key identity

$$\star_4 d_4 \star_4 d_4 + d_4 \star_4 d_4 \star_4 = -\square = -m^2, \quad (4.34)$$

which defines the four-dimensional mass-shell condition. To this end, one can apply d_4 and then $d_4 \star_4$ to eq. (4.31), and combining the result with the d_4 of eq. (4.34) leads to the system

$$\begin{aligned} \partial_r d_4 u + \frac{i\hbar}{\rho} e^{4A} d_4 \star_4 u &= 0, \\ \partial_r d_4 \star_4 u + \frac{i m^2 \rho}{h} e^{2A+10C} d_4 u - \frac{i\hbar}{\rho} e^{4A} d_4 u &= 0. \end{aligned} \quad (4.35)$$

The first equation can now be solved for $d_4 \star_4 u$, and substituting the result into the second gives a second-order equation in r involving only $d_4 u$ and not $d_4 \star_4 u$:

$$\partial_r (e^{-4A} \partial_r d_4 u) + m^2 e^{2A+10C} d_4 u - \left(\frac{\hbar}{\rho}\right)^2 e^{4A} d_4 u = 0. \quad (4.36)$$

One can now separate variables in eq. (4.36), letting

$$d_4 u(x, r) = d_4 U(x) f(r), \quad (4.37)$$

which is equivalent to

$$u(x, r) = U(x) f(r) + d_4 \Lambda(x, r), \quad (4.38)$$

with $\Lambda(x, r)$ a four-dimensional one-form also depending on r , which is not necessarily separable. This decomposition should be consistent with the initial equation (4.31), and substituting in it eq. (4.38) leads to

$$\begin{aligned} \partial_r d_4 \Lambda(x, r) + \frac{i\hbar}{\rho} e^{4A} \star_4 d_4 \Lambda(x, r) &= -\frac{i\hbar}{\rho} e^{4A} \star_4 U(x) f(r) - U(x) f'(r) \\ + \frac{i\rho}{h} e^{2A+10C} f(r) d_4 \star_4 d_4 U(x). & \end{aligned} \quad (4.39)$$

The parameter Λ of eq. (4.38) is defined up to an exact form, and consequently it can be chosen to be transverse. The exterior derivative of this equation then gives

$$d_4 \star_4 U(x) f(r) - m^2 \star_4 \Lambda(x, r) = \frac{i\rho}{h} e^{-4A} d_4 U f', \quad (4.40)$$

which determines Λ algebraically for the modes with $m^2 \neq 0$. One can verify that eq. (4.39) is identically satisfied if one makes use of this solution for $\Lambda(x, r)$. Therefore, the massive spectrum can be analyzed referring solely to a Schrödinger system, as in Section 3, starting from eq. (4.36).

4.2 THE MASSIVE SECTOR

As we have seen, all the preceding equations are consistent with the separation of variables (4.38) in the massive case, where Λ is determined algebraically by eq. (4.40). One can then focus on

eq. (4.36), assuming that $d_4 u \neq 0$. In fact, if $d_4 u = 0$, eqs. (4.35) imply that $d_4 \star_4 u = 0$, and taking these results into account eq. (4.34) implies that $m = 0$. We shall return to this case later.

For the time being, let us thus concentrate on modes with $d_4 u \neq 0$, which are complex massive two-forms and are dual to complex massive vectors in the resulting four-dimensional spacetime. In view of eq. (4.36) f satisfies

$$\partial_r (e^{-4A} \partial_r f) + m^2 e^{2A+10C} f - \left(\frac{h}{\rho}\right)^2 e^{4A} f = 0. \quad (4.41)$$

In terms of the conformal variable z defined in eq. (3.9), this equation takes the form

$$-(\partial_z + B_z - 5A_z) \partial_z f + \left(\frac{h}{\rho}\right)^2 e^{2(A-5C)} f = m^2 f, \quad (4.42)$$

and the further redefinition

$$f(r) = e^{\frac{5A-B}{2}} \Psi(z) \quad (4.43)$$

finally yields the Schrödinger-like equation

$$\tilde{\mathcal{A}} \tilde{\mathcal{A}}^\dagger \Psi = m^2 \Psi. \quad (4.44)$$

The two operators

$$\tilde{\mathcal{A}} = \partial_z + \frac{7}{2} A_z + \frac{5}{2} C_z, \quad \tilde{\mathcal{A}}^\dagger = -\partial_z + \frac{7}{2} A_z + \frac{5}{2} C_z, \quad (4.45)$$

can be identified after making use of the identities for the background in eqs. (A.19), and the resulting Schrödinger potential,

$$V = \frac{1}{64 z_0^2} \frac{e^{\sqrt{\frac{5}{2}} \frac{r}{\rho}}}{\sinh\left(\frac{r}{\rho}\right)^3} \left[2\sqrt{10} \sinh\left(\frac{2r}{\rho}\right) + \cosh\left(\frac{2r}{\rho}\right) + 27 \right], \quad (4.46)$$

is displayed in fig. 6.

Eq. (4.44) now implies that

$$\Psi = C e^{\frac{7A+5C}{2}} \quad (4.47)$$

is an exact normalizable zero mode of the Schrödinger system. Note that this result translates into

$$f(r) = C e^{4A} = \frac{C}{h \sinh\left(\frac{r}{\rho}\right)}, \quad (4.48)$$

in view of eq. (4.43), consistently with eq. (4.105). Taking the measure into account, the zero mode (4.48) corresponds to the normalized r -distribution

$$\Pi_f(r) = \frac{1}{\rho} \sqrt{\frac{5}{2}} e^{-\frac{r}{\rho} \sqrt{\frac{5}{2}}}. \quad (4.49)$$

The arguments presented in [14] show that the self-adjoint boundary conditions satisfied by this zero mode would identify a complete spectrum of excitations for the Schrödinger operator (4.44) that is free from tachyonic instabilities. However, we originally assumed that $m \neq 0$, and in fact this expression for $f(r)$ *does not* satisfy eq. (4.40) if $m = 0$, unless the two conditions

$$d_4 \star_4 U(x) = 0, \quad d_4 U(x) = 0 \quad (4.50)$$

hold. Moreover, even if these conditions hold, one should make sure that the original equation (4.31) be satisfied. This condition will be spelled out in detail in the next two sections, where the actual nature of the zero modes will emerge. In contrast, when $m \neq 0$ the Schrödinger problem is *equivalent* to the original equation.

Summarizing, from the Schrödinger system one can retain, without further ado, the whole spectrum aside from the zero mode that can possibly be present. When a zero mode is present, it must be handled with care, as we shall see. Nonetheless, the zero mode profile (4.48) will now prove useful in characterizing the optimal shift of the hypergeometric approximation of the actual potential (4.46).

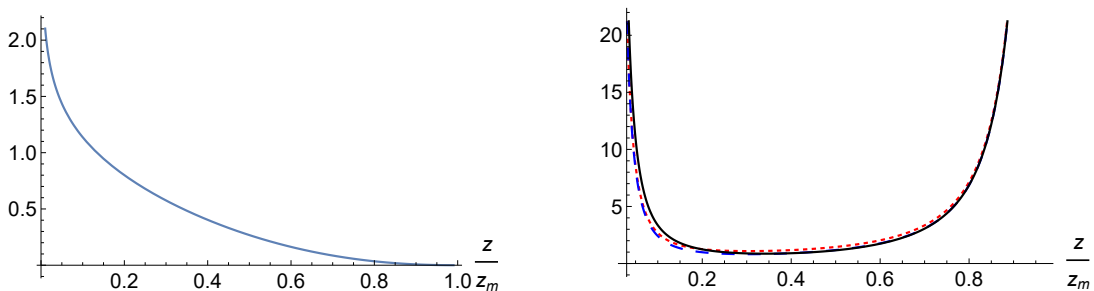


Figure 6: The left panel shows the normalized zero-mode wavefunction (4.47). The right panel compares the actual $B_{\mu\nu}$ potential (black, solid), its approximation (2.29) with $(\mu, \tilde{\mu}) = (\frac{2}{3}, 1.72)$ (red, dotted) and the improvement of the latter obtained with a slight negative shift, all in units of $\frac{1}{z_0^2}$. z_m and z_0 are defined in eqs. (3.10) and (3.11).

At the two ends the potential is dominated once more by the behavior in eq. (1.15), with $\mu = \frac{2}{3}$ and $\tilde{\mu} = 1.72$. Consequently, we are now in case 2 of Table 1, so that the limiting behavior near the left end is given by the first of eqs. (2.1), while near z_m it is given by the last of eqs. (2.2), and is actually fixed to be

$$\psi \sim \left(1 - \frac{z}{z_m}\right)^{2.22}. \quad (4.51)$$

Self-adjoint boundary conditions thus depend on a single parameter characterizing, close to the

origin, the relative weight of the two independent contributions

$$\psi \sim C_1 \left(\frac{z}{z_m} \right)^{\frac{7}{6}} + C_2 \left(\frac{z}{z_m} \right)^{-\frac{1}{6}}, \quad (4.52)$$

which can be identified with the ratio between C_2 and C_1 . For the zero mode (4.47) the self-adjoint boundary conditions are determined by

$$\frac{C_2}{C_1} \sim -2.85. \quad (4.53)$$

This result can determine an optimal shift of the hypergeometric approximation (2.29) of the potential. One can see from fig. 1 that, in the hypergeometric model, the ground state should correspond to $m \simeq 0.99$, so that the optimal potential for this sector is

$$V \simeq V \left(\frac{2}{3}, 1.72, z \right) - \frac{\pi^2}{z_m^2} (0.99)^2. \quad (4.54)$$

Taking the shift into account, the hypergeometric eigenvalue equation becomes in general

$$\frac{C_2}{C_1} \simeq - \left(\frac{2}{\pi} \right)^{\frac{4}{3}} \frac{\Gamma \left(\frac{5}{3} \right) \Gamma \left(1.03 + \sqrt{m_{B\mu\nu}^2 + (0.99)^2} \right) \Gamma \left(1.03 - \sqrt{m_{B\mu\nu}^2 + (0.99)^2} \right)}{\Gamma \left(\frac{1}{3} \right) \Gamma \left(1.69 + \sqrt{m_{B\mu\nu}^2 + (0.99)^2} \right) \Gamma \left(1.69 - \sqrt{m_{B\mu\nu}^2 + (0.99)^2} \right)}. \quad (4.55)$$

This approximation reveals the presence of an instability region corresponding to

$$-2.85 < \frac{C_2}{C_1} < 0. \quad (4.56)$$

On the other hand, outside this region, if $\frac{C_2}{C_1}$ differs from the “critical” value -2.85 , the spectrum consists of purely massive complex two-forms, which are dual to complex massive vectors, as we have stressed.

For $\mathbf{k} \neq 0$, one can gauge away all excitations that are longitudinal in \mathbf{k} , and then these perturbations continue not to mix with others. The resulting masses increase, as dictated by the additional positive potential $\mathbf{k}^2 \epsilon^{2(A-C)}$.

We can now turn to a detailed analysis of the zero modes that can be contained in u .

4.3 THE MASSLESS SECTOR

When the boundary conditions allow a massless sector, the resulting setup is rather peculiar. In analyzing it, we shall explore two solutions of the massless equations of increasing complexity.

4.3.1 THE CASE $d_4 U(x) = 0$

If $d_4 U(x) = 0$, eq. (4.40) implies that $d_4 \star_4 U(x) = 0$, and then $f(r)$ is arbitrary. Letting

$$d_4 \Lambda = -U(x) f(r) + d_4 g(x, r) , \quad (4.57)$$

so that

$$d_4 g(x, r) = u(x, r) . \quad (4.58)$$

Eq. (4.39), or equivalently (4.31), leads to

$$\partial_r d_4 g(x, r) + \frac{i h}{\rho} e^{4A} \star_4 d_4 g(x, r) = 0 . \quad (4.59)$$

Decomposing now the complex two-form $d_4 g$ into selfdual and anti-selfdual parts according to

$$d_4 g = (d_4 g)^+ + (d_4 g)^- , \quad (4.60)$$

with

$$(d_4 g)^\pm = \frac{1}{2} (1 \mp i \star_4) d_4 g , \quad (4.61)$$

leads to

$$(d_4 g)^\pm = (d_4 g)^\pm(x) \left[\tanh \left(\frac{r}{2\rho} \right) \right]^{\pm 1} , \quad (4.62)$$

and finally to

$$u = (d_4 g)^+(x) \tanh \left(\frac{r}{2\rho} \right) + (d_4 g)^-(x) \coth \left(\frac{r}{2\rho} \right) \quad (4.63)$$

or

$$u = d_4 g = d_4 g(x) \coth \left(\frac{r}{\rho} \right) + \frac{i \star_4 d_4 g(x)}{\sinh \left(\frac{r}{\rho} \right)} . \quad (4.64)$$

The condition $d_4 u = 0$, which was our starting point, demands that

$$d_4 \star_4 d_4 g(x) = 0 . \quad (4.65)$$

Making use of eq. (4.64) gives

$$b = -\frac{i\rho}{h} u , \quad (4.66)$$

up to an r -independent two-form that is pure gauge, and using eqs. (4.32), (4.64) and (4.65) gives

$$\mathcal{H} = \frac{i}{h \sinh \left(\frac{r}{\rho} \right)} \left[i \star_4 d_4 g(x) \coth \left(\frac{r}{\rho} \right) + \frac{d_4 g(x)}{\sinh \left(\frac{r}{\rho} \right)} \right] dr . \quad (4.67)$$

The norm is determined by the sum of the two contributions

$$\begin{aligned} \int \bar{\mathcal{H}} \wedge \star \mathcal{H} &= V_5 \int \frac{dr d_4 \bar{g} \wedge \star_4 d_4 g}{h \sinh\left(\frac{r}{\rho}\right)}, \\ \int 2 \operatorname{Im}(\bar{b} \wedge \mathcal{H}) \wedge \mathcal{H}_5^{(0)} &= -V_5 \int \frac{dr dV_5 d_4 \bar{g} \wedge \star_4 d_4 g}{h \sinh\left(\frac{r}{\rho}\right)}. \end{aligned} \quad (4.68)$$

These terms cancel, and actually they are both total derivatives if eq. (4.65), which is a constraint in this case, is used. Therefore, the modes obtained in this fashion have vanishing norm, and must be rejected. In the next section we shall recover eq. (4.65), but as an equation of motion, not as a consistency condition.

4.3.2 THE CASE $d_4 U(x) \neq 0$

If $d_4 U(x) \neq 0$, eq. (4.40) with $m = 0$ implies that

$$f'(r) = \gamma e^{4A} f(r), \quad d_4 \star_4 U(x) = \frac{i \rho \gamma}{h} d_4 U(x), \quad (4.69)$$

where γ is a constant. Substituting in eq. (4.36) now leads to

$$d_4 U \left[\gamma^2 - \left(\frac{h}{\rho} \right)^2 \right] e^{4A} f = 0, \quad (4.70)$$

so that

$$\gamma = \pm \frac{h}{\rho}. \quad (4.71)$$

There are thus two solutions of this type,

$$\begin{aligned} f^+(r) &= \tanh\left(\frac{r}{2\rho}\right), & d_4(1 + i \star_4) U^+(x) &= 0, \\ f^-(r) &= \coth\left(\frac{r}{2\rho}\right), & d_4(1 - i \star_4) U^-(x) &= 0, \end{aligned} \quad (4.72)$$

where the overall constants are included in $U^\pm(x)$, which are both consistent with the separation of variables (4.38). Consequently one can conclude that

$$U^+(x) = U^{++}(x) + A^{+-}(x), \quad U^-(x) = U^{--}(x) + A^{-+}(x), \quad (4.73)$$

where U^{++} and A^{-+} are selfdual two-forms, U^{--} and A^{+-} are anti-selfdual two-forms, and furthermore

$$d_4 A^{+-} = 0, \quad d_4 A^{-+} = 0. \quad (4.74)$$

In general, a complex (anti-)selfdual two-form \mathcal{G}_2^\pm , such that

$$\star_4 \mathcal{G}_2^\pm = \pm i \mathcal{G}_2^\pm \quad (4.75)$$

can be expressed in terms of a real two-form G_2 according to

$$\mathcal{G}_2^\pm = (1 \mp i \star_4) G_2 . \quad (4.76)$$

Consequently one can write

$$\begin{aligned} U^{++} &= (1 - i \star_4) u^+ , & A^{+-} &= (1 + i \star_4) a^+ , \\ U^{--} &= (1 + i \star_4) u^- , & A^{-+} &= (1 - i \star_4) a^- , \end{aligned} \quad (4.77)$$

where u^\pm and a^\pm are real two-forms, with

$$d_4 a^\pm = 0 , \quad d_4 \star_4 a^\pm = 0 . \quad (4.78)$$

Collecting all these contributions, the general massless u profile of this type, obtained combining the two separable solutions that we started from, reads

$$\begin{aligned} u(x, r) &= [a^+ + u^+ + i \star_4 (a^+ - u^+)] \tanh\left(\frac{r}{2\rho}\right) \\ &+ [a^- + u^- - i \star_4 (a^- - u^-)] \coth\left(\frac{r}{2\rho}\right) + d_4 \Lambda(x, r) , \end{aligned} \quad (4.79)$$

where $d_4 \Lambda$ is determined by eq. (4.31). One can thus conclude that

$$d_4 u(x, r) = d_4 (1 - i \star_4) u^+ \tanh\left(\frac{r}{2\rho}\right) + d_4 (1 + i \star_4) u^- \coth\left(\frac{r}{2\rho}\right) . \quad (4.80)$$

In particular, for a divergence-free u with $u^+ = -u^-$ this expression recovers the zero mode of the Schrödinger system.

In order to determine Λ , taking eqs. (4.78) into account, one can let

$$d_4 \Lambda(x, r) = - (1 + i \star_4) a^+ \tanh\left(\frac{r}{2\rho}\right) - (1 - i \star_4) a^- \coth\left(\frac{r}{2\rho}\right) + d_4 \lambda(x, r) , \quad (4.81)$$

thus eliminating all terms involving a^\pm from $u(x, r)$, which becomes

$$u(x, r) = (1 - i \star_4) u^+ \tanh\left(\frac{r}{2\rho}\right) + (1 + i \star_4) u^- \coth\left(\frac{r}{2\rho}\right) + d_4 \lambda(x, r) , \quad (4.82)$$

and now $d_4 \lambda$ can be determined by eq. (4.31). Decomposing it into selfdual and anti-selfdual portions according to

$$d_4 \lambda(x, r) = (d_4 \lambda(x, r))^+ + (d_4 \lambda(x, r))^- , \quad (4.83)$$

and using the identity

$$(1 - i \star_4) d_4 \star_4 d_4 (1 - i \star_4) = 0 \quad (4.84)$$

for massless modes, one can see that $(d_4 \lambda)^\pm(x, r)$ satisfy the decoupled first-order equations

$$\partial_r (d_4 \lambda(x, r))^\pm \mp \frac{h}{\rho} e^{4A} (d_4 \lambda(x, r))^\pm = \frac{i\rho}{h} e^{2A+10C} f^\mp(r) d_4 \star_4 d_4 U^{\mp\mp}(x). \quad (4.85)$$

These are solved by

$$(d_4 \lambda)^\pm = \left[\tanh\left(\frac{r}{2\rho}\right) \right]^{\pm 1} \left[C^\pm(x) + \frac{igh}{4} \int_{r_0}^r ds e^{-\frac{5s}{\rho\sqrt{10}}} \left(e^{\frac{s}{2\rho}} \pm e^{-\frac{s}{2\rho}} \right)^4 \xi^\mp(x) \right], \quad (4.86)$$

where the $C^\pm(x)$ are proportional to $(d_4 \lambda)^\pm$ at $r = r_0$, and

$$\xi^\mp(x) = d_4 \star_4 d_4 U^{\mp\mp}(x) = d_4 \star_4 d_4 (1 \pm i \star_4) u^\mp(x). \quad (4.87)$$

In fact, given the different r dependence of $(d_4 \lambda)^\pm$, the decomposition (4.83) is only consistent if

$$d_4 C^\pm = 0, \quad (4.88)$$

and consequently

$$d_4 \star_4 d_4 \lambda = 0, \quad (4.89)$$

so that $d_4 \lambda$ is also co-closed. One finally obtains

$$\begin{aligned} u(x, r) &= (1 - i \star_4) u^+ \tanh\left(\frac{r}{2\rho}\right) + (1 + i \star_4) u^- \coth\left(\frac{r}{2\rho}\right) \\ &+ \left[\tanh\left(\frac{r}{2\rho}\right) \right] \left[C^+(x) + \frac{igh}{4} \int_{r_0}^r ds e^{-\frac{5s}{\rho\sqrt{10}}} \left(e^{\frac{s}{2\rho}} + e^{-\frac{s}{2\rho}} \right)^4 \xi^-(x) \right] \\ &+ \left[\coth\left(\frac{r}{2\rho}\right) \right] \left[C^-(x) + \frac{igh}{4} \int_{r_0}^r ds e^{-\frac{5s}{\rho\sqrt{10}}} \left(e^{\frac{s}{2\rho}} - e^{-\frac{s}{2\rho}} \right)^4 \xi^+(x) \right], \end{aligned} \quad (4.90)$$

which is consistent with the decomposition (4.80).

We can now compute the gauge-invariant field strength \mathcal{H} , whose expression in terms of $u(x, r)$ is given in eq. (4.32). One thus finds

$$\begin{aligned} \mathcal{H} &= -\frac{i\rho}{h} d_4 (1 - i \star_4) u^+ \tanh\left(\frac{r}{2\rho}\right) - \frac{i\rho}{h} d_4 (1 + i \star_4) u^- \coth\left(\frac{r}{2\rho}\right) \\ &- e^{4A} i dr (1 - i \star_4) u^+ \tanh\left(\frac{r}{2\rho}\right) + e^{4A} i dr (1 + i \star_4) u^- \coth\left(\frac{r}{2\rho}\right) \\ &- e^{4A} dr \star_4 d_4 \lambda, \end{aligned} \quad (4.91)$$

and

$$\begin{aligned} b &= -\frac{i\rho}{h} (1 - i \star_4) u^+ \tanh\left(\frac{r}{2\rho}\right) - \frac{i\rho}{h} (1 + i \star_4) u^- \coth\left(\frac{r}{2\rho}\right) \\ &- \star_4 d_4 \int e^{4A} \lambda(x, r). \end{aligned} \quad (4.92)$$

Let us begin by analyzing the asymptotic behavior of these quantities as $r \rightarrow \infty$. To this end, it is important to note that in this limit the second contribution on the left-hand side of eqs. (4.85) can be neglected, and consequently

$$d_4 \lambda \sim \frac{i \rho^2 h}{4 \left(2 - \sqrt{\frac{5}{2}}\right)} e^{\frac{r}{\rho} \left(2 - \sqrt{\frac{5}{2}}\right)} d_4 \star_4 d_4 \left[(1 + i \star_4) u^- + (1 - i \star_4) u^+ \right] , \quad (4.93)$$

while

$$\mathcal{H} \sim - \frac{i \rho}{h} \left[d_4 (1 - i \star_4) u^+ + d_4 (1 + i \star_4) u^- \right] , \quad (4.94)$$

or

$$\mathcal{H} \sim - \frac{i \rho}{h} d_4 \mu , \quad (4.95)$$

where

$$\mu = u^+ + u^- - i \star_4 (u^+ - u^-) , \quad (4.96)$$

since the other contributions are sub-dominant in the limit.

Near the right end of the interval the leading behavior of b is

$$b \sim - \frac{i \rho}{h} u , \quad (4.97)$$

and the only two-derivative contribution to the kinetic action integral thus originates from the first term in eq. (4.2), and is proportional to

$$\int e^{\left(2 - \sqrt{\frac{5}{2}}\right) \frac{r}{\rho}} d_4 \bar{\mu} \wedge \star_4 d_4 \mu . \quad (4.98)$$

Consequently, a finite result only obtains if the two conditions

$$d_4 (u^+ + u^-) = 0 , \quad d_4 \star_4 (u^+ - u^-) = 0 . \quad (4.99)$$

hold for normalizable massless modes. These conditions are solved letting

$$u^\pm = d_4 \gamma \pm \star_4 d_4 \delta , \quad (4.100)$$

where γ and δ are two real one-forms, which could be taken to be divergence-free. Consequently, the overall content of u^\pm corresponds at most to a pair of real vectors, and

$$\xi^\mp(x) = \pm d_4 \star_4 d_4 \star_4 d_4 (\delta - i \gamma) . \quad (4.101)$$

Making use of eq. (4.100), one can conclude that

$$\begin{aligned}
\mathcal{H} &= \frac{2\rho}{h} \frac{d_4 \star_4 d_4 (\gamma + i\delta)}{\sinh\left(\frac{r}{\rho}\right)} - \frac{2dr \left[\cosh\left(\frac{r}{\rho}\right) \star_4 - i \right]}{h \sinh^2\left(\frac{r}{\rho}\right)} d_4 (\gamma + i\delta) - e^{4A} dr \star_4 d_4 \lambda, \\
\star\mathcal{H} &= 2\rho h dr dV_5 \star_4 d_4 \star_4 d_4 (\gamma + i\delta) \sinh\left(\frac{r}{\rho}\right) e^{-\frac{r}{\rho}\sqrt{\frac{5}{2}}} \\
&\quad - \frac{2dV_5 \left[\cosh\left(\frac{r}{\rho}\right) \star_4 - i \right]}{\sinh\left(\frac{r}{\rho}\right)} \star_4 d_4 (\gamma + i\delta) + d_4 \lambda, \\
b &= -\frac{2i\rho}{h \sinh\left(\frac{r}{\rho}\right)} \left[1 + i \star_4 \cosh\left(\frac{r}{\rho}\right) \right] (d_4 \gamma + \star_4 d_4 \delta) - \star_4 d_4 \int e^{4A} \lambda(x, r),
\end{aligned} \tag{4.102}$$

but taking eq. (4.89) into account one can see all terms involving λ do not contribute to the action (4.2). Consequently

$$\begin{aligned}
\int \overline{\mathcal{H}} \wedge \star\mathcal{H} &= 4\rho^2 \int dr dV_5 d_4 \star_4 d_4 (\gamma - i\delta) \wedge \star_4 d_4 \star_4 d_4 (\gamma + i\delta) e^{-\frac{r}{\rho}\sqrt{\frac{5}{2}}} \\
&\quad - \int \frac{4dr dV_5}{h \sinh\left(\frac{r}{\rho}\right)} \left(d_4 \gamma \wedge \star_4 d_4 \gamma + d_4 \delta \wedge \star_4 d_4 \delta \right), \\
-2 \int \text{Im}(b \wedge \overline{\mathcal{H}}) \wedge \mathcal{H}_5^{(0)} &= \int \frac{4dr dV_5}{h \sinh\left(\frac{r}{\rho}\right)} d_4 \delta \wedge \star_4 d_4 \delta.
\end{aligned} \tag{4.103}$$

The terms involving δ that are singular at the origin cancel among the two contributions above, so that finiteness only demands that $\gamma = 0$. One is thus left with a real vector δ , whose contribution to the action, in the first term, is finite but contains higher derivatives.

The corresponding measure is precisely the one captured by the Schrödinger system for the massive modes. Keeping only δ one finds indeed

$$\begin{aligned}
\mathcal{H} &= \frac{2i\rho}{h} \frac{d_4 \star_4 d_4 \delta}{\sinh\left(\frac{r}{\rho}\right)} - 2 \frac{dr \left[1 + i \star_4 \cosh\left(\frac{r}{\rho}\right) \right]}{h \sinh^2\left(\frac{r}{\rho}\right)} d_4 \delta, \\
u &= 2 \frac{i \cosh\left(\frac{r}{\rho}\right) - \star_4}{\sinh\left(\frac{r}{\rho}\right)} d_4 \delta, \\
b &= \frac{2\rho}{h \sinh\left(\frac{r}{\rho}\right)} \left[\star_4 - i \cosh\left(\frac{r}{\rho}\right) \right] d_4 \delta,
\end{aligned} \tag{4.104}$$

so that

$$d_4 u = -2 \frac{d_4 \star_4 d_4 \delta}{\sinh\left(\frac{r}{\rho}\right)}. \tag{4.105}$$

We have thus recovered for $d_4 u$ the r profile of the massless mode of the Schrödinger system in eq. (4.48). However, the x dependence of u is determined by a real vector δ . The results of the preceding section are recovered if

$$d_4 \star_4 d_4 \delta = 0 , \quad (4.106)$$

so that δ reduces to the field g introduced there. The novelty here is the absence of this constraint.

The equation for δ in four dimensions,

$$d_4 \star_4 d_4 \star_4 d_4 \delta = 0 , \quad (4.107)$$

follows if one substitutes eqs. (4.104) in the ten-dimensional equations (4.27). It has a peculiar form, and contains an odd number of derivatives. However, it is consistent with the four-derivative equation that follows from the effective action

$$\mathcal{S}_4 = \int d_4 \star_4 d_4 \delta \wedge \star_4 d_4 \star_4 d_4 \delta . \quad (4.108)$$

Note also that only $d_4 u$ has a separable form in x and r .

Denoting $d_4 \delta$ by F , eq. (4.107) can be cast in the form

$$\partial_{[\mu} \partial^\rho F_{\nu]\rho} = 0 , \quad (4.109)$$

which is equivalent to

$$\partial^\rho F_{\nu\rho} = \partial_\nu \sigma , \quad \square \sigma = 0 , \quad (4.110)$$

where σ is a massless scalar field. All in all, one is thus left with a real massless vector and a real massless scalar in this sector. To these massless modes one must add a complex massless vector that lives generically in the boundary.

Summarizing, as we have seen in Section 4.2, the massive modes of this sector are complex two-forms, which in four dimensions are dual to complex massive vectors. Naively, when massless modes are present, what happens in circle compactification would suggest the presence of a complex scalar from $\mathcal{B}_{\mu\nu}$ and a complex vector from $\mathcal{B}_{\mu r}$. The surprise is that the peculiar system (4.31) actually leads to a third-order equation, which results in the halving of the massless modes, in a way that resonates with chiral projections of Fermi systems. In addition, in an interval, as we have seen, another vector mode lives on the boundary, in a way reminiscent of what is familiar for twisted sectors in orbifolds [30] or orientifolds [4] in String Theory, or from the Horava–Witten construction [31].

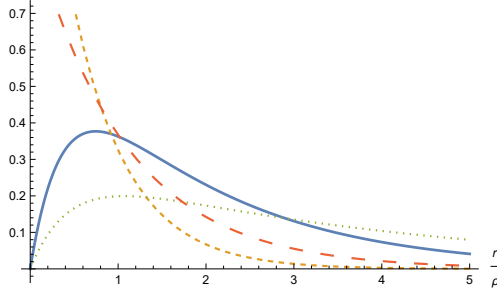


Figure 7: The r -distributions $\Pi_\phi\left(\frac{r}{\rho}\right)$ of eq. (3.27) (blue, solid), $\Pi_f\left(\frac{r}{\rho}\right)$ of eq. (4.48) (yellow, dashed), $\Pi_{B_{\mu i}}\left(\frac{r}{\rho}\right)$ of eq. (4.121) (green, dotted), $\Pi_{B_{ij}}\left(\frac{r}{\rho}\right)$ of eq. (4.139) (red, long-dashed), in units of $\frac{1}{\rho}$. The corresponding mean values of $\frac{r}{\rho}$ are about 2.1, 0.6, 4.2 and 1.1.

4.4 The Modes Originating from $\mathcal{B}_{\mu i}$ and \mathcal{B}_{ri}

For this mode sector, one can start from

$$\mathcal{B} = a_i(x)f(r) dy^i, \quad (4.111)$$

where the a_i are five 4D complex one-forms since. As we already stressed after eq. (4.23), Λ_i can be used to remove the \mathcal{B}_{ri} , but as in the previous section this is at the cost of introducing a set of complex scalars A_i living in the boundary. The field strength corresponding to \mathcal{B} is in this case

$$\mathcal{H} = f d_4 a_i dy^i + f' a_i dy^i dr, \quad (4.112)$$

and the equations of motion give

$$f' d_4 * a_i = 0, \quad m^2 f e^{B+3C} + (f' e^{-2C-2A})' = 0. \quad (4.113)$$

Letting

$$f = g e^{-\frac{A+3C}{2}}, \quad (4.114)$$

one obtains a manifestly Hermitian Schrödinger-like equation

$$\left(\partial_z + \frac{(A_z + 3C_z)}{2}\right) \left(-\partial_z + \frac{(A_z + 3C_z)}{2}\right) g = m^2 g, \quad (4.115)$$

of the familiar $\mathcal{A}\mathcal{A}^\dagger$ form, with the potential

$$V = -\frac{1}{4}(A_z + 3C_z)(5A_z + 7C_z) - 4\mathcal{W}_5^2. \quad (4.116)$$

This is displayed in fig. 8 as a function of z , together with the corresponding hypergeometric approximation. In terms of r its detailed form is

$$V = \frac{e^{\sqrt{\frac{5}{2}}\frac{r}{\rho}}}{32 z_0^2 \sinh\left(\frac{r}{\rho}\right)} \left[\sqrt{10} \sinh\left(\frac{2r}{\rho}\right) - \frac{31}{10} \cosh\left(\frac{2r}{\rho}\right) - \frac{69}{10} \right]. \quad (4.117)$$

At the two ends of the interval, this potential has the singular limiting behavior of eq. (1.15), with $\mu = \frac{1}{3}$ and $\tilde{\mu} = 0.54$, and thus belongs to case 3 of Section 2. As for the dilaton-axion pair, there are boundary conditions given independently at the two ends that are parametrized by a pair on angles (θ_1, θ_2) .

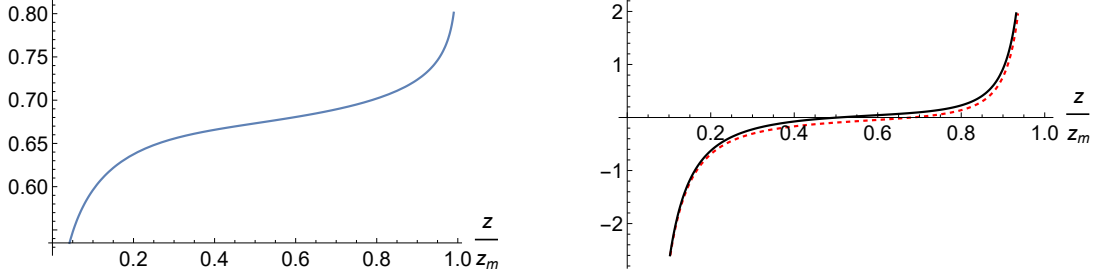


Figure 8: The left panel shows the normalized zero-mode wavefunction (4.118). The right panel compares the actual $B_{\mu i}$ potential (black, solid) with its approximation (2.29) with $(\mu, \tilde{\mu}) = (\frac{1}{3}, 0.54)$ (red, dashed), both in units of $\frac{1}{z_0^2}$. z_m and z_0 are defined in eqs. (3.10) and (3.11).

Before examining the possible choices of boundary conditions, let us remark that the \mathcal{AA}^\dagger form of the Schrödinger system implies the presence of the zero mode

$$g = g_0 e^{\frac{A+3C}{2}}, \quad (4.118)$$

which corresponds to

$$f = g_0, \quad (4.119)$$

where g_0 is a constant. This zero mode is normalizable, since

$$\int_0^{z_m} dz e^{A+3C} = \int_0^\infty dr e^{4(A+2C)} < \infty, \quad (4.120)$$

and the corresponding normalizable r -distribution is

$$\Pi_{B_{\mu i}} = \frac{3}{5\rho} \left[\sinh\left(\frac{r}{\rho}\right) \right] e^{-\frac{4r}{\rho\sqrt{10}}}. \quad (4.121)$$

Note that the zero-mode wavefunction has the dominant behaviors

$$g \sim \left(\frac{z}{z_m}\right)^{\frac{1}{6}} - 0.35 \left(\frac{z}{z_m}\right)^{\frac{5}{6}} \quad (4.122)$$

close to $z = 0$, and

$$g \sim \left(1 - \frac{z}{z_m}\right)^{-0.04} - 0.14 \left(1 - \frac{z}{z_m}\right)^{1.04} \quad (4.123)$$

close to $z = z_m$.

The arguments of [14] lead one to conclude that this whole sector is stable with the boundary conditions of this zero mode, which correspond to $(\theta_1, \theta_2) = \pi(-0.15, 0.06)$, in the notation of Section 2, in view of eqs. (2.11). The comparison with the hypergeometric potentials of eq. (2.29) requires a slight shift of the latter, as can be seen from fig. 8. The precise shift can be determined demanding that the exact zero mode lie on the resulting massless curve, and amounts to adding to the hypergeometric potential the constant

$$\Delta V \simeq (0.22)^2 \frac{\pi^2}{z_m^2} . \quad (4.124)$$

Once this is done, one can rely on the hypergeometric approximation, and in particular on the corresponding exact eigenvalue equation (2.55), to identify the boundary conditions resulting in stable modes, which correspond to the unshaded region displayed in fig. 9

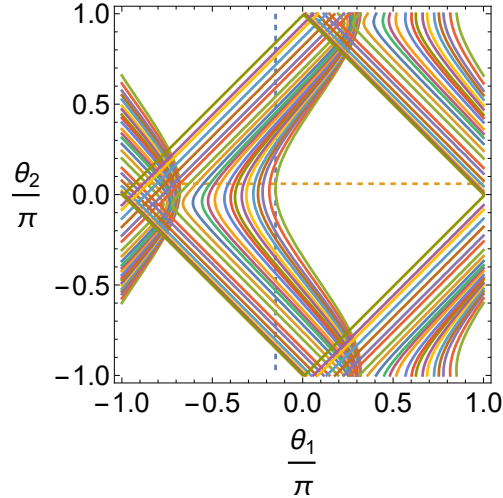


Figure 9: The point $(\theta_1, \theta_2) = (-0.15, 0.06)\pi$ identifies the special boundary conditions for $\mathcal{B}_{\mu i}$ corresponding to the zero mode (4.118). The shaded regions identify the boundary conditions leading to instabilities.

In conclusion, this sector can yield altogether, *ten massless real Abelian vectors* in the bulk, with suitable boundary conditions, which are accompanied by ten real massless scalars living in the boundary. When allowing for nonzero values of \mathbf{k} , it is convenient not to eliminate B_{ri} but rather to impose the transversality of all fields to \mathbf{k} . In this fashion, one can see that B_{ri} is set to zero by the equations of motion while m^2 , as usual, is replaced by $m^2 - e^{2(A-C)} \mathbf{k}^2$, and the whole spectrum is lifted in this sector, which thus contains no unstable modes for suitable boundary conditions.

4.5 The Modes Originating from \mathcal{B}_{ij}

Turning now to the modes that are scalar fields valued in the antisymmetric of $SO(5)$, let us first note that the two-form is in this case

$$\mathcal{B} = \frac{1}{2} \mathcal{B}_{ij} dy^i dy^j , \quad (4.125)$$

while the corresponding field strength is

$$\mathcal{H} = \frac{1}{2} (d_4 \mathcal{B}_{ij} + \partial_r \mathcal{B}_{ij} dr) dy^i dy^j \quad (4.126)$$

for $\mathbf{k} = 0$. The non-trivial equation is in this case

$$m^2 e^{6A+6C} \mathcal{B}_{ij} + \partial_r (e^{-4C} \partial_r \mathcal{B}_{ij}) = 0 , \quad (4.127)$$

and in terms of the z variable it becomes

$$m^2 \mathcal{B}_{ij} + (\partial_z + 3A_z + C_z) \partial_z \mathcal{B}_{ij} = 0 . \quad (4.128)$$

The redefinition

$$\mathcal{B}_{ij} = e^{-\frac{1}{2}(3A+C)} g(z) b_{ij}(x) \quad (4.129)$$

leads once more to a manifestly Hermitian Schrödinger-like equation of the $\mathcal{A}\mathcal{A}^\dagger$ form,

$$\left(\partial_z + \frac{(3A_z + C_z)}{2} \right) \left(-\partial_z + \frac{(3A_z + C_z)}{2} \right) g = m^2 g , \quad (4.130)$$

with the potential

$$V = \frac{1}{4} (3A_z + C_z)^2 + \frac{1}{2} \partial_z (3A_z + C_z) , \quad (4.131)$$

which is displayed in fig. 10 as a function of z . In terms of r its detailed form is

$$V = \frac{e^{\sqrt{\frac{5}{2}} \frac{r}{\rho}}}{320 z_0^2 \sinh\left(\frac{r}{\rho}\right)} \left[-6\sqrt{10} \sinh\left(\frac{2r}{\rho}\right) + 21 \cosh\left(\frac{2r}{\rho}\right) + 119 \right] . \quad (4.132)$$

Close to $z = 0$ the potential has the singular limiting behaviors of eq. (1.15), with $\mu = \frac{2}{3}$ and $\tilde{\mu} = 0.63$, so that it corresponds to case 3 in Table 1, as for the previous sector. There is a normalizable ground state, which corresponds to

$$g = g_0 e^{\frac{3A+C}{2}} , \quad (4.133)$$

with a constant g_0 , and thus to \mathcal{B}_{ij} independent of r :

$$\mathcal{B}_{ij} = g_0 b_{ij}(x) . \quad (4.134)$$

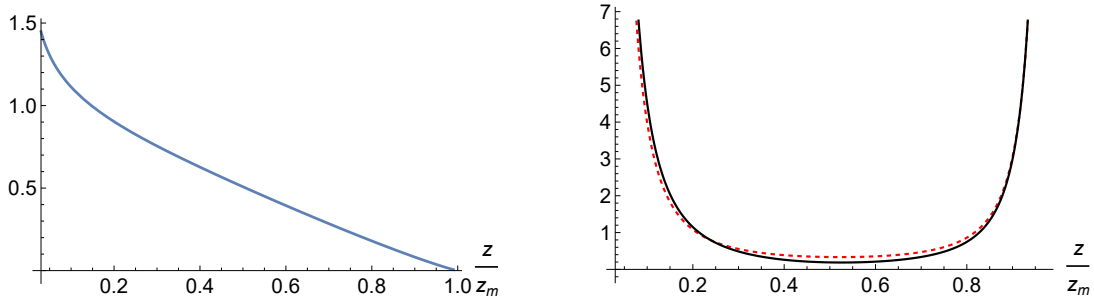


Figure 10: The left panel shows the normalized zero-mode wavefunction (4.133). The right panel compares the actual B_{ij} potential (black, solid) with its approximation (2.29) with $(\mu, \tilde{\mu}) = (\frac{2}{3}, 0.63)$ (red, dashed), both in units of $\frac{1}{z_0^2}$. z_m and z_0 are defined in eqs. (3.10) and (3.11).

Note that the zero-mode wavefunction has the dominant behaviors

$$g \sim \left(\frac{z}{z_m}\right)^{-\frac{1}{6}} - 0.35 \left(\frac{z}{z_m}\right)^{\frac{7}{6}} \quad (4.135)$$

close to $z = 0$, and

$$g \sim \left(1 - \frac{z}{z_m}\right)^{-0.13} + 0.18 \left(1 - \frac{z}{z_m}\right)^{1.13} \quad (4.136)$$

close to $z = z_m$. The arguments of [14] lead one to conclude that this whole sector is stable with the boundary conditions of this zero mode, which correspond to $(\theta_1, \theta_2) = \pi(-0.16, 0.05)$, in the notation of Section 2. The comparison with the hypergeometric potentials of eq. (2.29) requires a slight shift of the latter. The shift can be determined demanding that the exact zero mode lie on the resulting massless curve, and amounts to adding to the hypergeometric potential the constant

$$\Delta V \simeq - (0.08)^2 \frac{\pi^2}{z_m^2}. \quad (4.137)$$

Once this is done, one can rely on the hypergeometric approximation, and in particular on the corresponding exact eigenvalue equation (2.55), to identify the boundary conditions for \mathcal{B}_{ij} resulting in stable modes, which correspond to the unshaded region displayed in fig. 11

The Schödinger system also indicates that the norm would be proportional to

$$\int dz e^{3A+C} = \int_0^\infty dr e^{6(A+C)}, \quad (4.138)$$

which is finite, as we have anticipated. This expression identifies the r -distribution

$$\Pi_{B_{ij}}(r) = \frac{1}{\rho} \frac{3}{\sqrt{10}} e^{-\frac{r}{\rho} \frac{3}{\sqrt{10}}}. \quad (4.139)$$

Only $\mathcal{H}_{\mu ij}$ is present for these zero modes, and therefore the no-flow conditions of [22] are identically satisfied.

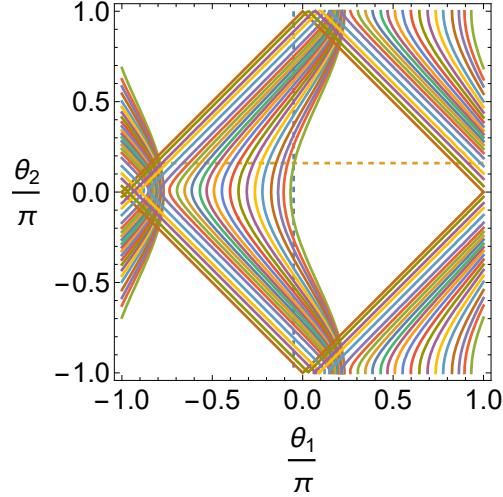


Figure 11: The point $(\theta_1, \theta_2) = \pi(-0.05, 0.16)$ identifies the special boundary conditions corresponding to the zero mode (4.118). The shaded regions identify the boundary conditions leading to instabilities.

With non-vanishing internal momenta \mathbf{k} , the Chern–Simons term still does not contribute while, once more, m^2 is replaced by $m^2 - e^{2(A-C)} \mathbf{k}^2$. All the preceding choices of boundary conditions remain possible, once the wavefunctions are modified by the addition of suitable \mathbf{k} -dependent corrections. Once this restriction is taken into account, the \mathbf{k}^2 term lifts the mass spectrum further, and no instabilities emerge with suitable boundary conditions.

5 THE PERTURBED EINSTEIN - FIVE-FORM SYSTEM

A peculiar feature of type–IIB supergravity [16] is the presence of a four–form gauge field whose field strength satisfies the self–duality condition

$$\mathcal{H}_5 = \star \mathcal{H}_5 . \quad (5.1)$$

We have already seen its crucial role in the class of backgrounds at stake, and now we want to explore its perturbations. Eq. (5.1) is indeed the complete four–form equation of motion, together with the Bianchi identity for \mathcal{H}_5 , once the field strength is properly dressed with fermionic terms and Chern–Simons forms, which are however irrelevant for the linearized analysis.

Linear perturbations of the four–form gauge field in eq. (5.1) mix with metric perturbations, and eq. (5.1) is to be combined with the linearized Einstein equations, which can be deduced starting from

$$R_{MN} = \frac{1}{24} (\mathcal{H}_5^2)_{MN} . \quad (5.2)$$

The type of system one is confronted with is rather unfamiliar and, as we shall see, is somewhat complicated. In organizing the analysis, it is always useful to distinguish various sectors of modes relying on an internal symmetry, whenever this is present. The internal toroidal directions are helpful in this respect, and it will be important, as in the preceding sections, to distinguish matters according to whether or not the toroidal momentum \mathbf{k} vanishes.

As we have already seen, the modes with $\mathbf{k} = 0$ have an $SO(5)$ internal symmetry inherited from the internal space. In flat space, after a IIB compactification on $S^1 \times T^5$, the original 35 modes of the 10D self-dual five-form field strength would translate, within this sector, into 35 massless modes independent of the r coordinate. They would build a multiplet of Abelian vectors in the 10 of $SO(5)$, together with two scalar multiplets in the 10 and 5 representations of $SO(5)$. This can be seen in the four-dimensional light-cone gauge, leaving aside the components along r , which are linked to the others by the self-duality relations (5.1). In this fashion, one must deal with three types of four-dimensional modes, B_{ijkl} , B_{ijka} and B_{ijab} . Here $(i, j, k) = 1, \dots, 5$ correspond to the internal directions and $(a, b) = 1, 2$ correspond to the two four-dimensional directions transverse to the light cone. If massless in four dimensions, these three sets of fields, up to internal and spacetime dualities, would indeed describe a 5 of scalars, a 10 of vectors and an additional 10 of two-tensors, which are dual to scalars. These modes would add to 35 other modes originating from the metric field. These are the two graviton polarizations from $h_{\mu\nu}$, a multiplet of vectors $h_{\mu i}$ in the 5 of $SO(5)$, an additional singlet vector $h_{\mu r}$, a 5 of scalars h_{ri} , a singlet, h_{rr} , and finally a 14 and a singlet scalar from h_{ij} . In the present context, one expects to find, in general, a subset of these massless modes emerging in the bulk.

Although some of these massless modes will disappear in our background, the comparison with this benchmark will often prove a convenient tool in the following. When modes become massive due to the behavior along r but still correspond to $\mathbf{k} = 0$, the $SO(5)$ remains manifest, but the ten scalars from the five form can be eaten by the corresponding 10 vectors, or equivalently the vectors can be eaten by the ten two-forms. On the gravity side, the pattern is more familiar from Kaluza-Klein theory.

For any given choice of $\mathbf{k} \neq 0$, the relevant symmetry is the $SO(4)$ associated to the four internal directions orthogonal to it, as we have already stated. While so far we have largely confined our attention to $\mathbf{k} = 0$ modes, reserving only brief comments to sectors with non-vanishing internal momenta, here it will be important to also scrutinize perturbations with $\mathbf{k} \neq 0$, since they will entail special subtleties and, as we saw in detail in [13], can host instabilities as a

result of mixings.

5.1 PERTURBING THE TENSOR EQUATIONS

Perturbing eqs. (5.1) around the background leads to

$$\begin{aligned} \delta \mathcal{H}_{P_1 \dots P_5} &= h_{[P_1}{}^{M_1} \mathcal{H}_{5 P_2 \dots P_5] M_1}^{(0)} - \frac{1}{2} h_M{}^M \mathcal{H}_{5 P_1 \dots P_5}^{(0)} \\ &+ \frac{g_{P_1 M_1}^{(0)} \dots g_{P_5 M_5}^{(0)}}{5! \sqrt{-g^{(0)}}} \epsilon^{M_1 \dots M_5 N_1 \dots N_5} \delta \mathcal{H}_{N_1 \dots N_5}, \end{aligned} \quad (5.3)$$

where the antisymmetrizations have unit coefficients, quantities bearing the superscript (0) refer to the background, $\delta \mathcal{H}$ denotes perturbations of the tensor field strength and h denotes perturbations of the metric, defined in eq. (1.13). Moreover, $\mathcal{H}_5^{(0)}$ is defined in eq. (1.1), and here the Levi–Civita tensor, such that $\epsilon^{01\dots 9} = -1$, will be lowered with the Minkowski metric.

The perturbation $\delta \mathcal{H}$ is to be expressed in terms of the four–form gauge field, whose independent components can be conveniently parametrized as follows:

$$\begin{aligned} \delta B_{\mu\nu\rho\sigma} &= \epsilon_{\mu\nu\rho\sigma} b, & \delta B_{\mu\nu\rho r} &= \epsilon_{\mu\nu\rho}{}^\sigma b_\sigma, & \delta B_{\mu\nu\rho i} &= \epsilon_{\mu\nu\rho}{}^\sigma b_{\sigma i}, \\ \delta B_{\mu\nu r i} &= b_{\mu\nu i}, & \delta B_{\mu\nu i j} &= b_{\mu\nu i j}, & \delta B_{\mu r i j} &= b_{\mu i j}^{(1)}, \\ \delta B_{\mu i j k} &= \frac{1}{2} \epsilon_{ijklm} b_\mu^{(2)lm}, & \delta B_{r i j k} &= \frac{1}{2} \epsilon_{ijklm} b^{lm}, & \delta B_{ijkl} &= \epsilon_{ijklm} b^m. \end{aligned} \quad (5.4)$$

Using eqs. (5.3) and the results collected in Appendix B, and in particular eqs. (B.4), one can see that the independent self–duality conditions reduce to

$$\begin{aligned} \partial_{[\mu} b^{(2)}{}_{\nu]}{}^{lm} + \frac{1}{2} \epsilon^{pqrilm} \partial_p b_{\mu\nu qr} &= -\frac{e^{-4A-4C}}{2} \epsilon_{\mu\nu\rho\sigma} \\ &\times \left(\partial^{[\rho} b^{(1)\sigma]lm} + \partial_r b^{\rho\sigma lm} - \partial^{[l} b^{\rho\sigma]m} \right), \\ \partial_\mu b^{lm} - \partial_r b^{(2)}{}_\mu{}^{lm} + \frac{1}{2} \epsilon^{pqslm} \partial_p b^{(1)}{}_{\mu qs} &= -e^{2A+6C} \left(\partial^{[l} b_\mu{}^{m]} + \frac{1}{2} \epsilon^{\alpha\beta\gamma}{}_\mu \partial_\alpha b_{\beta\gamma}{}^{lm} \right), \\ \partial_\mu b^m - \partial_n b^{(2)}{}_\mu{}^{mn} &= e^{-2C} \left[\frac{h}{2\rho} h_\mu{}^m \right. \\ &+ \left. e^{-6A} \left(\partial^m b_\mu - \partial_r b_\mu{}^m - \frac{1}{2} \epsilon^{\alpha\beta\gamma}{}_\mu \partial_\alpha b_{\beta\gamma}{}^m \right) \right], \\ \partial_r b^m - \partial_n b^{mn} &= e^{-2C} \left[\frac{h}{2\rho} h_r{}^m - e^{10C} (\partial^m b - \partial_\mu b^{\mu m}) \right], \\ \partial_p b^p &= \left[\frac{h}{4\rho} (-e^{-2A} h_\alpha{}^\alpha - e^{-2B} h_{rr} + e^{-2C} h_i{}^i) \right. \\ &+ \left. e^{-8A} (\partial_r b - \partial_\tau b^\tau) \right], \end{aligned} \quad (5.5)$$

where we expressed the background metric in terms of the three functions $A(r)$, $B(r)$ and $C(r)$, as in eq. (3.1).

5.2 TENSOR GAUGE FIXING OF THE EINSTEIN–FIVE FORM SYSTEM

In order to analyze the modes arising from the Einstein–five-form sector, one must perform a gauge fixing of the resulting equations.

Diffeomorphisms act on metric fluctuations h_{MN} as

$$\delta_\xi h_{MN} = \nabla_M \xi_N + \nabla_N \xi_M ,$$

and consequently the Ricci curvature perturbations transform according to

$$\delta_\xi (\delta R_{NR}) = \nabla_N \xi^P R^{(0)}_{PR} + \nabla_R \xi^P R^{(0)}_{NP} , \quad (5.6)$$

where $R^{(0)}_{MN}$ is the background Ricci curvature. They are thus covariant under diffeomorphisms, albeit not invariant as would be the case when working around flat space.

The four–form gauge potential is also affected by tensor gauge transformations, and a convenient presentation of their combined action with diffeomorphisms is

$$\begin{aligned} \delta_{\xi,\Lambda} (\delta B_{MNPQ}) &= \xi^R \mathcal{H}_5^{(0)}{}_{RMNPQ} + \partial_{[M} \Lambda_{NPQ]} , \\ \delta_\xi (\delta \mathcal{H}_{SMNPQ}) &= (\nabla_{[S} \xi^R) \mathcal{H}_5^{(0)}{}_{MNPQ|R} + 5 \xi^R \nabla_R \mathcal{H}_5^{(0)}{}_{SMNPQ} . \end{aligned} \quad (5.7)$$

Here Λ is a three–form gauge parameter and, as in other portions of this paper, square brackets denote antisymmetrizations without overall factors. The independent components of Λ_{MNP} can be conveniently parametrized as

$$\begin{aligned} \Lambda_{\nu\rho\sigma} &= \epsilon_{\nu\rho\sigma\tau} \Lambda^\tau , & \Lambda_{\nu\rho r} &= \Lambda_{\nu\rho} , & \Lambda_{\nu\rho i} &, & \Lambda_{\nu r i} &= \Lambda_{\nu i} , \\ \Lambda_{r i j} &= \Lambda^{(1)}{}_{ij} , & \Lambda_{\mu i j} &, & \Lambda_{i j k} &= \frac{1}{2} \epsilon_{ijklm} \Lambda^{(2)lm} . \end{aligned} \quad (5.8)$$

Diffeomorphisms and tensor gauge transformation thus act on the independent fields according to

$$\begin{aligned} \delta h_{\mu\nu} &= \partial_\mu \xi_\nu + \partial_\nu \xi_\mu + 2 \eta_{\mu\nu} A' e^{2(A-B)} \xi_r , \\ \delta h_{\mu r} &= \partial_\mu \xi_r + (\partial_r - 2A') \xi_\mu , & \delta h_{\mu i} &= \partial_\mu \xi_i + \partial_i \xi_\mu , \\ \delta h_{rr} &= 2(\partial_r - B') \xi_r , & \delta h_{r i} &= (\partial_r - 2C') \xi_i + \partial_i \xi_r , \\ \delta h_{ij} &= \partial_i \xi_j + \partial_j \xi_i + 2 \delta_{ij} C' e^{2(C-B)} \xi_r , \\ \delta b &= \frac{\hbar}{2\rho} e^{-10C} \xi_r - \partial_\mu \Lambda^\mu , & \delta b_i &= \frac{\hbar}{2\rho} e^{-2C} \xi_i + \partial^j \Lambda_{ij}^{(2)} , \\ \delta b_\mu &= -\frac{\hbar}{2\rho} e^{6A} \xi_\mu - \frac{1}{2} \epsilon_{\mu\nu\rho\sigma} \partial^\nu \Lambda^{\rho\sigma} - \partial_r \Lambda_\mu , \end{aligned} \quad (5.9)$$

while the remaining tensor components are invariant under diffeomorphisms and have the tensor gauge transformations

$$\begin{aligned}
\delta b_{\mu i} &= -\frac{1}{2}\epsilon_{\mu\nu\rho\sigma}\partial^\nu\Lambda^{\rho\sigma i} - \partial_i\Lambda_\mu, & \delta b_{\mu\nu i} &= \partial_{[\mu}\Lambda_{\nu]i} + \partial_r\Lambda_{\mu\nu i} - \partial_i\Lambda_{\mu\nu}, \\
\delta b_{\mu\nu ij} &= \partial_{[\mu}\Lambda_{\nu]ij} + \partial_{[i}\Lambda_{\mu\nu]j}, & \delta b_{\mu ij}^{(1)} &= \partial_\mu\Lambda^{(1)}_{ij} - \partial_r\Lambda_{\mu ij} + \partial_{[i}\Lambda_{\mu]j}, \\
\delta b_{\mu ij}^{(2)} &= \partial_\mu\Lambda^{(2)}_{ij} - \frac{1}{2}\epsilon_{ijklm}\partial^k\Lambda_\mu{}^{lm}, & \delta b_{ij} &= \partial_r\Lambda^{(2)}_{ij} - \frac{1}{2}\epsilon_{ijklm}\partial^k\Lambda^{(1)lm}.
\end{aligned} \tag{5.10}$$

Using the tensor gauge transformations one can now set

$$B_{rMNP} = 0, \tag{5.11}$$

for all choices of M , N and P , thus removing all fields whose gauge transformations involve the radial derivative of a parameter with the same Lorentz structure. In analogy with what we said for the two-forms, this gauge fixing brings along other modes living in the boundary, which can be associated to a nine-dimensional three form.

The gauge condition (5.11) translates into

$$b_\mu = 0, \quad b_{\mu\nu i} = 0, \quad b^{(1)}_{\mu ij} = 0, \quad b_{ij} = 0, \tag{5.12}$$

and reduces the system of tensor equations to

$$\begin{aligned}
\partial_{[\mu}b^{(2)}_{\nu]}{}^{lm} + \frac{1}{2}\epsilon^{lmnpq}\partial_n b_{\mu\nu pq} &= -\frac{e^{-4A-4C}}{2}\epsilon_{\mu\nu\rho\sigma}\partial_r b^{\rho\sigma lm}, \\
\partial_r b^{(2)}_{\mu}{}^{lm} &= e^{2A+6C}\left[\partial^{[l}b_\mu{}^{m]} + \frac{1}{2}\epsilon^{\alpha\beta\gamma}{}_\mu\partial_\alpha b_{\beta\gamma}{}^{lm}\right], \\
\partial_\mu b^m - \partial_n b^{(2)}_{\mu}{}^{mn} &= e^{-2C}\left[\frac{h}{2\rho}h_\mu{}^m - e^{-6A}\partial_r b_\mu{}^m\right], \\
\partial_r b^m &= e^{-2C}\left[\frac{h}{2\rho}h_r{}^m - e^{10C}(\partial^m b - \partial_\mu b^{\mu m})\right], \\
\partial_p b^p &= \frac{h}{4\rho}\left[-e^{-2A}h_\alpha{}^\alpha - e^{-2B}h_{rr} + e^{-2C}h_i{}^i\right] + e^{-8A}\partial_r b.
\end{aligned} \tag{5.13}$$

This simpler system is still invariant under some residual gauge transformations, with arbitrary parameters $\Lambda_{\rho\sigma}$, $\Lambda_{\mu i}$ and $\Lambda^{(1)}_{ij}$, while the radial dependence of the others is determined by

$$\begin{aligned}
\partial_r\Lambda_\mu &= -\frac{1}{2}\epsilon_{\mu\nu\rho\sigma}\partial^\nu\Lambda^{\rho\sigma} - \frac{h}{2\rho}e^{6A}\xi_\mu, & \partial_r\Lambda_{\mu\nu i} &= \partial_i\Lambda_{\mu\nu} - \partial_{[\mu}\Lambda_{\nu]i}, \\
\partial_r\Lambda_{\mu ij} &= \partial_\mu\Lambda^{(1)}_{ij} + \partial_{[i}\Lambda_{\mu]j}, & \partial_r\Lambda^{(2)}_{ij} &= \frac{1}{2}\epsilon_{ijklm}\partial^k\Lambda^{(1)lm}.
\end{aligned} \tag{5.14}$$

These residual symmetries will be instrumental to exhibit the modes actually emerging from this unfamiliar sector. Indeed, even in the flat-space limit, where the metric functions A , B , C

and the parameter h are all vanishing, the recovery of the expected modes that we have listed at the beginning of this section is not evident. There is actually a subtlety here, when comparing with the case of circle compactification, whose internal zero modes, which would be independent of r in the present notation, cannot be gauged away. That would require gauge parameters linear in r , which are not allowed in order to maintain periodicity, consistently with the global translational symmetry on the circle. In our case the internal r -space is an interval, and the requirement of periodicity is replaced by proper boundary conditions. Therefore, the parameters on the right-hand side of eqs. (5.14) are arbitrary, which justifies our choice. We shall see this explicitly in the following sections, where we shall also fix diffeomorphism invariance on a case-by-case basis. As we have already stressed, however, other modes appear generically at the ends of the interval.

5.3 PERTURBING THE EINSTEIN EQUATIONS

When the complete Einstein equations (5.2) are linearized around the background, their left-hand side becomes

$$R_{MN} = R_{MN}^{(0)} + \delta R_{MN} , \quad (5.15)$$

where

$$-2\delta R_{NR} = \square_{10} h_{NR} + \nabla_N \nabla_R h_S^S - \nabla^P (\nabla_N h_{PR} + \nabla_R h_{PN}) , \quad (5.16)$$

where the derivatives and the d'Alembertian are covariant with respect to the background. The components of the first-order correction to the energy-momentum tensor can be obtained in a similar fashion, and these steps lead to the linearized Einstein equations

$$\begin{aligned} & \square_{10} h_{NR} + \nabla_N \nabla_R h_S^S - \nabla^P (\nabla_N h_{PR} + \nabla_R h_{PN}) \\ &= -\frac{1}{12} \left(\delta \mathcal{H}_{5(N} \cdot \mathcal{H}_{5R)}^{(0)} - 4 \mathcal{H}_{5NK}^{(0)} \cdot \mathcal{H}_{5RL}^{(0)} h^{KL} \right) . \end{aligned} \quad (5.17)$$

The spacetime components of eqs. (5.17) are

$$\begin{aligned}
\alpha\beta & : (e^{-2A} \square + e^{-2C} \Delta) h_{\alpha\beta} - e^{-2B} (\partial_r - 2A') \partial_{(\alpha} h_{\beta)r} \\
& + \eta_{\alpha\beta} A' e^{2(A-B)} [e^{-2A} (\partial_r - 2A') h^\mu{}_\mu - e^{-2B} (\partial_r - 2B') h_{rr} + e^{-2C} (\partial_r - 2C') h^i{}_i] \\
& - 2\eta_{\alpha\beta} A' e^{2(A-B)} [e^{-2A} \partial^\mu h_{\mu r} + e^{-2C} \partial^i h_{ir}] \\
& + e^{-2B} [(\partial_r - 4A') \partial_r + 4(A')^2] h_{\alpha\beta} \\
& + \partial_\alpha \partial_\beta (e^{-2A} h^\mu{}_\mu + e^{-2B} h^r{}_r + e^{-2C} h^i{}_i) - e^{-2A} \partial^\mu \partial_{(\alpha} h_{\beta)\mu} - e^{-2C} \partial^i \partial_{(\alpha} h_{\beta)i} \\
& = \frac{\hbar}{2\rho} \left\{ 4 e^{2(A-B)} \partial_r b \eta_{\alpha\beta} - \frac{\hbar}{\rho} e^{-10C} (\eta_{\alpha\beta} h_{\rho}{}^\rho - h_{\alpha\beta}) \right\} , \tag{5.18}
\end{aligned}$$

while the αr components are

$$\begin{aligned}
\alpha r & : (e^{-2A} \square + e^{-2C} \Delta) h_{\alpha r} - e^{-2A} (\partial_r - 2A') \partial^\rho h_{\alpha\rho} \\
& + (A' - B') e^{-2B} \partial_\alpha h_{rr} - e^{-2C} (\partial_r - 2A') \partial^i h_{i\alpha} \\
& + e^{-2A} (\partial_r - 2A') \partial_\alpha h^\mu{}_\mu + e^{-2C} (\partial_r - A' - C') \partial_\alpha h^i{}_i \\
& - e^{-2A} \partial_\alpha \partial^\rho h_{\rho r} - e^{-2C} \partial_\alpha \partial^i h_{ri} = 0 , \tag{5.19}
\end{aligned}$$

and the αi components are

$$\begin{aligned}
\alpha i & : e^{-2A} \square h_{\alpha i} + e^{-2C} \Delta h_{\alpha i} + e^{-2B} [(\partial_r - A' - C')^2 - (A' - C')^2] h_{\alpha i} \\
& - e^{-2B} (\partial_r - 2A') \partial_\alpha h_{ir} - e^{-2B} (\partial_r - 2C') \partial_i h_{\alpha r} \\
& + \partial_\alpha \partial_i (e^{-2A} h^\mu{}_\mu + e^{-2B} h^r{}_r + e^{-2C} h^k{}_k) \\
& - e^{-2A} \partial^\rho (\partial_\alpha h_{\rho i} + \partial_i h_{\rho\alpha}) - e^{-2C} \partial^j (\partial_\alpha h_{ij} + \partial_i h_{\alpha j}) \\
& = -\frac{\hbar e^{-8C}}{2\rho} \left[4 (\partial_\alpha b_i - \partial_n b^{(2)}_{\alpha i}{}^n) - \frac{\hbar}{\rho} e^{-2C} h_{\alpha i} \right] . \tag{5.20}
\end{aligned}$$

Moreover, the rr component is

$$\begin{aligned}
rr & : [e^{-2A} \square - e^{-2B} B' (\partial_r - 2B') + e^{-2C} \Delta] h_{rr} \\
& - 2e^{-2A} (\partial_r - B') \partial^\mu h_{\mu r} - 2e^{-2C} (\partial_r - B') \partial^i h_{ri} \\
& + e^{-2A} (\partial_r - B') (\partial_r - 2A') h^\mu{}_\mu + e^{-2C} (\partial_r - B') (\partial_r - 2C') h^i{}_i \\
& = \frac{\hbar}{2\rho} \left[4 \partial_r b - \frac{\hbar}{\rho} e^{6A} h_{\rho}{}^\rho \right] , \tag{5.21}
\end{aligned}$$

while the ri components are

$$\begin{aligned}
ri & : (e^{-2A} \square + e^{-2C} \Delta) h_{ir} - e^{-2C} (\partial_r - 2C') \partial^k h_{ki} \\
& + \partial_i \left\{ e^{-2A} [(\partial_r - A' - C') h^\alpha{}_\alpha - \partial^\alpha h_{\alpha r}] + e^{-2B} (C' - B') h_{rr} \right. \\
& + \left. e^{-2C} [(\partial_r - 2C') h^k{}_k - \partial^k h_{kr}] \right\} - e^{-2A} (\partial_r - 2C') \partial^\alpha h_{\alpha i} \\
& = \frac{2h}{\rho} (\partial_i b - \partial_\mu b^\mu{}_i) .
\end{aligned} \tag{5.22}$$

Finally, the internal ij components are

$$\begin{aligned}
ij & : (e^{-2A} \square + e^{-2C} \Delta) h_{ij} - e^{-2B} (\partial_r - 2C') \partial_{(i} h_{j)r} - 2\delta_{ij} C'' e^{2(C-2B)} h_{rr} \\
& + \delta_{ij} C' e^{2(C-B)} [e^{-2C} (\partial_r - 2C') h^k{}_k - e^{-2B} (\partial_r - 2B') h_{rr} + e^{-2A} (\partial_r - 2A') h^\mu{}_\mu] \\
& - 2\delta_{ij} C' e^{2(C-B)} [e^{-2C} \partial^k h_{kr} + e^{-2A} \partial^\mu h_{\mu r}] + e^{-2B} [(\partial_r - 4C') \partial_r + 4(C')^2] h_{ij} \\
& + \partial_i \partial_j (e^{-2C} h^k{}_k + e^{-2B} h_{rr} + e^{-2A} h^\mu{}_\mu) - e^{-2C} \partial^k \partial_{(i} h_{j)k} - e^{-2A} \partial^\mu \partial_{(i} h_{j)\mu} \\
& = -\frac{h}{2\rho} \left[4\delta_{ij} e^{-8C} \partial_p b^p - \frac{h}{\rho} e^{-10C} (\delta_{ij} h^k{}_k - h_{ij}) \right] .
\end{aligned} \tag{5.23}$$

Summarizing, the equations of motion for the coupled Einstein–five form system are eqs. (5.13), together with eqs. (5.18)–(5.23). We can now analyze their modes, starting from some sectors where the contributions from gravity and the five-form are decoupled, whose dynamics is thus simpler. These are fields in the antisymmetric of $SO(5)$, which originate solely from the four–form gauge field, spin-two modes and scalar modes in the symmetric traceless $SO(5)$ representation, which originate solely from the gravity sector. All other modes are mixed, which makes their analysis more involved and will be treated in Sections 9 – 12.

6 TENSOR MODES DECOUPLED FROM GRAVITY PERTURBATIONS

According to eqs. (5.13), this sector involves the two fields $b^{(2)}{}_\mu{}^{lm}$ and $b_{\mu\nu}{}^{lm}$, which are both valued, for $\mathbf{k} = 0$, in the antisymmetric of $SO(5)$, and no gravity contributions. We begin our analysis from the modes with $\mathbf{k} = 0$, which are somewhat simpler.

6.1 $\mathbf{k} = 0$ TENSOR MODES

For the modes with $\mathbf{k} = 0$, eqs. (5.13) reduce to

$$\begin{aligned}
\partial_{[\mu} b^{(2)}{}_{\nu]}{}^{lm} & = -\frac{e^{-4A-4C}}{2} \epsilon_{\mu\nu\rho\sigma} \partial_r b^{\rho\sigma lm} , \\
\partial_r b^{(2)}{}_\mu{}^{lm} & = e^{2A+6C} \frac{1}{2} \epsilon^{\alpha\beta\gamma}{}_\mu \partial_\alpha b_{\beta\gamma}{}^{lm} ,
\end{aligned} \tag{6.1}$$

and it is now clearly convenient to let

$$\beta_{\mu\nu}{}^{lm} = \frac{1}{2} \epsilon_{\mu\nu\rho\sigma} b^{\rho\sigma lm} , \quad (6.2)$$

so that the equations simplify, and become

$$\partial_{[\mu} b^{(2)}{}_{\nu]}{}^{lm} = - e^{-4A-4C} \partial_r \beta_{\mu\nu}{}^{lm} , \quad \partial_r b^{(2)}{}_{\mu}{}^{lm} = e^{2A+6C} \partial^\alpha \beta_{\alpha\mu}{}^{lm} . \quad (6.3)$$

These equations link quantities that are invariant under residual gauge transformations, with parameters independent of r :

$$\delta \beta_{\mu\nu ij} = \epsilon_{\mu\nu\rho\sigma} \partial^\rho \Lambda^\sigma{}_{ij} , \quad \delta b^{(2)}{}_{\mu ij} = \partial_\mu \Lambda^{(2)}{}_{ij} . \quad (6.4)$$

One can now separate the radial dependence introducing a factor $f(r)$ for $\beta_{\mu\nu ij}$ and a factor $f^{(2)}(r)$ for $b^{(2)}{}_{\mu ij}$, according to

$$\beta_{\mu\nu ij}(x, r) = f(r) \beta_{\mu\nu ij}(x) , \quad b^{(2)}{}_{\mu ij}(x, r) = f^{(2)}(r) b^{(2)}{}_{\mu ij}(x) . \quad (6.5)$$

This leads to the system

$$f' = a_1 e^{4A+4C} f^{(2)} , \quad f^{(2)'} = a_2 e^{2A+6C} f , \quad (6.6)$$

where a_1 and a_2 are two real constants, and the resulting space–time modes satisfy

$$\begin{aligned} \partial_{[\mu} b^{(2)}{}_{\nu]}{}^{lm} &= - a_1 \beta_{\mu\nu}{}^{lm} , \\ a_2 b^{(2)}{}_{\mu}{}^{lm} &= \partial^\alpha \beta_{\alpha\mu}{}^{lm} . \end{aligned} \quad (6.7)$$

From these equations, if $a_1 a_2 \neq 0$ one obtains a second–order Proca equation

$$\square b^{(2)}{}_{\nu}{}^{lm} - \partial_\nu \partial^\rho b^{(2)}{}_{\rho}{}^{lm} + a_1 a_2 b^{(2)}{}_{\nu}{}^{lm} = 0 , \quad (6.8)$$

with a squared mass

$$m^2 = - a_1 a_2 , \quad (6.9)$$

and β is completely determined in terms of $b^{(2)}$.

On the other hand, if $a_1 = a_2 = 0$, f and $f^{(2)}$ are independent of r , and then all non–trivial curvature components arising from the two potentials $\beta_{\mu\nu ij}$ and $b^{(2)}{}_{\mu ij}$,

$$\begin{aligned} H_{\mu\nu\rho ij} &= - \epsilon_{\mu\nu\rho\sigma} \partial_\lambda \beta^{\lambda\sigma}{}_{ij} , & H_{\mu\nu r ij} &= \partial_r b_{\mu\nu ij} , \\ H_{\mu\nu ijk} &= \frac{1}{2} \epsilon_{ijklm} \partial_{[\mu} b^{(2)}{}_{\nu]}{}^{lm} , & H_{\mu r ijk} &= - \frac{1}{2} \epsilon_{ijklm} \partial_r b_\mu^{(2)lm} , \end{aligned} \quad (6.10)$$

vanish, on account of eqs. (6.1), so that this type of solution is pure gauge.

The actual values of m^2 are determined by eqs. (6.6), and as in other sectors it is convenient to recast the system into a manifestly Hermitian form and then attain self-adjointness by a proper choice of boundary conditions. To this end, let us define the two functions g^+ and g^- via

$$f(r) = g^-(r) e^{\frac{A-C}{2}}, \quad f^{(2)}(r) = g^+(r) e^{-\frac{A-C}{2}}, \quad (6.11)$$

while also introducing the variable z of eq. (3.9). These steps lead to

$$\mathcal{A}g^- = a_1 g^+, \quad \mathcal{A}^\dagger g^+ = -a_2 g^-, \quad (6.12)$$

where

$$\mathcal{A} = \partial_z + \frac{A_z - C_z}{2}, \quad \mathcal{A}^\dagger = -\partial_z + \frac{A_z - C_z}{2}. \quad (6.13)$$

Combining the two first-order equations and making use of eq. (6.9) leads to either of the two manifestly Hermitian Schrödinger-like equations

$$\mathcal{A}^\dagger \mathcal{A}g^- = m^2 g^-, \quad \mathcal{A} \mathcal{A}^\dagger g^+ = m^2 g^+, \quad (6.14)$$

which include the potentials

$$V^\mp = \frac{1}{4} (A_z - C_z)^2 \mp \frac{1}{2} \partial_z (A_z - C_z), \quad (6.15)$$

or, in detail,

$$\begin{aligned} V^-(r) &= \frac{e^{\sqrt{\frac{5}{2}} \frac{r}{\rho}}}{320 z_0^2 \sinh^3\left(\frac{r}{\rho}\right)} \left[10\sqrt{10} \sinh\left(\frac{2r}{\rho}\right) - 19 \cosh\left(\frac{2r}{\rho}\right) - 81 \right], \\ V^+(r) &= \frac{e^{\sqrt{\frac{5}{2}} \frac{r}{\rho}}}{320 z_0^2 \sinh^3\left(\frac{r}{\rho}\right)} \left[-14\sqrt{10} \sinh\left(\frac{2r}{\rho}\right) + 41 \cosh\left(\frac{2r}{\rho}\right) + 99 \right]. \end{aligned} \quad (6.16)$$

Their limiting behaviors at the two ends are once more of the form (1.15), with $(\mu, \tilde{\mu}) = (\frac{1}{3}, 1.09)$ for g^- and $(\mu, \tilde{\mu}) = (\frac{2}{3}, 0.09)$ for g^+ . However, only a subset of the solutions of the two Schrödinger-like equations solves the original first-order system (6.12), as we now explain.

Let us first note that the solution of $\mathcal{A}g^- = 0$ is not normalizable. Consequently, a_1 cannot vanish, and it is thus convenient to absorb it in g^+ , turning the system (6.12) into

$$\mathcal{A}g^- = g^+, \quad \mathcal{A}^\dagger g^+ = m^2 g^-. \quad (6.17)$$

The second equation yields, for $m = 0$, a zero mode for g^+ , which solves

$$\mathcal{A}^\dagger g^+ = 0 \quad (6.18)$$

and reads

$$g^+ = g_0 e^{\frac{1}{2}(A-C)}. \quad (6.19)$$

This corresponds to a constant $f^{(2)}$ and behaves as $z^{-\frac{1}{6}}$ close to the origin. However, one must also solve the first equation in (6.17), and a normalizable solution reads

$$g^- = -e^{\frac{C-A}{2}} g_0 \int_z^{z_m} dz' e^{A(z')-C(z')} \sim e^{B-\frac{A+C}{2}} = e^{\frac{7A+9C}{2}}. \quad (6.20)$$

Identifying the upper end of the integral with z_m is crucial in order to obtain a normalizable mode. In fact, the integral in eq. (6.20) can be simply computed, and the result is

$$g^- = -\frac{\sqrt{10}\rho}{2} g_0 \left[h \sinh\left(\frac{r}{\rho}\right) \right]^{\frac{1}{4}} e^{-\frac{9}{4\sqrt{10}}\frac{r}{\rho}}, \quad (6.21)$$

which behaves as $r^{\frac{1}{4}} \sim z^{\frac{1}{6}}$ at the origin. These zero modes describe ten massless vectors, as dictated by eqs. (6.7), and have a constant internal profile $f^{(2)}$.

Consequently

$$\int_0^{z_m} dz (g^-)^2 \sim \int_0^\infty dr e^{3B-2A-C} \quad (6.22)$$

is clearly convergent, since the integrand vanishes as r at the origin and as $e^{-\frac{r}{\rho} \frac{10-7\sqrt{10}}{10}}$ at the other end. All in all, one can work with the Schrödinger equation

$$\mathcal{A}^\dagger \mathcal{A} g^- = m^2 g^-, \quad (6.23)$$

determining g^+ via $g^+ = \mathcal{A} g^-$. The proper normalization integral is also determined by g^- , according to

$$\int dz \left[(g^+)^2 + (g^-)^2 \right] = (1 + m^2) \int dz (g^-)^2. \quad (6.24)$$

The main subtlety, in this case, is that the proper zero mode is not the solution of $\mathcal{A} g^- = 0$, but the other independent massless solution of the second-order equation (6.23), which is given in eq. (6.21).

We can now identify the stable self-adjoint boundary conditions for this sector referring to g^- , which corresponds to case 2 in Section 2. The self-adjoint boundary conditions are thus determined by the behavior at the origin,

$$g^- \sim C_1 \left(\frac{z}{z_m} \right)^{\frac{5}{6}} + C_2 \left(\frac{z}{z_m} \right)^{\frac{1}{6}}, \quad (6.25)$$

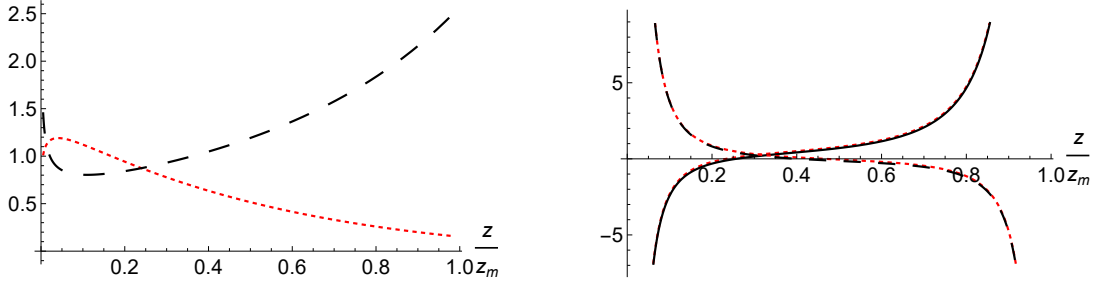


Figure 12: The left panel shows the normalized zero-mode wavefunctions of eqs. (6.20) (black, dashed) and (6.19) (red, dotted). The right panel compares the corresponding potentials V^- and V^+ of eq. (6.16) (black, long-dashed and black, solid) with their approximations (2.29) with $(\mu, \tilde{\mu}) = (\frac{1}{3}, 1.09)$ and $(\mu, \tilde{\mu}) = (\frac{2}{3}, 0.09)$ (red, dash-dotted and red, dashed), both in units of $\frac{1}{z_0^2}$. z_m and z_0 are defined in eqs. (3.10) and (3.11).

and can be parametrized by the ratio $\frac{C_2}{C_1}$, and for the zero mode (6.21)

$$\frac{C_2}{C_1} \simeq -0.7 . \quad (6.26)$$

As in previous cases, we now approximate V^- of eq. (6.16) with a hypergeometric potential (2.29) with $(\mu, \tilde{\mu}) = (\frac{1}{3}, 1.09)$ and a suitable shift ΔV , which we determine demanding that the boundary condition (6.26) correspond to a massless solution for the shifted potential. In this fashion one finds

$$\Delta V \simeq - (0.15)^2 \frac{\pi^2}{z_m^2} , \quad (6.27)$$

and the resulting hypergeometric eigenvalue equation becomes

$$\frac{C_2}{C_1} = - \left(\frac{\pi}{2}\right)^{-\frac{2}{3}} \frac{\Gamma\left(\frac{5}{3}\right) \Gamma\left(0.88 + \sqrt{m^2 + 0.15^2}\right) \Gamma\left(0.88 - \sqrt{m^2 + 0.15^2}\right)}{\Gamma\left(1.21 + \sqrt{m^2 + 0.15^2}\right) \Gamma\left(1.21 - \sqrt{m^2 + 0.15^2}\right)} . \quad (6.28)$$

The solutions are illustrated in fig. 13, and comprise an infinite number of massive modes and at most a single tachyonic mode. These results are qualitatively similar to what we displayed in fig. 1, and the instability region corresponds in this case to the range

$$-0.7 < \frac{C_2}{C_1} < 0 . \quad (6.29)$$

Note that the tachyon mass grows indefinitely, in absolute value, as the ratio $\frac{C_2}{C_1}$ approaches zero from negative values.

We can now examine how the choice of self-adjoint boundary conditions affects the flow of the energy-momentum tensor across the boundary. In this sector, the relevant component of the energy-momentum tensor behaves as

$$\sqrt{-g} T^r{}_\mu \sim g^+ g^- , \quad (6.30)$$

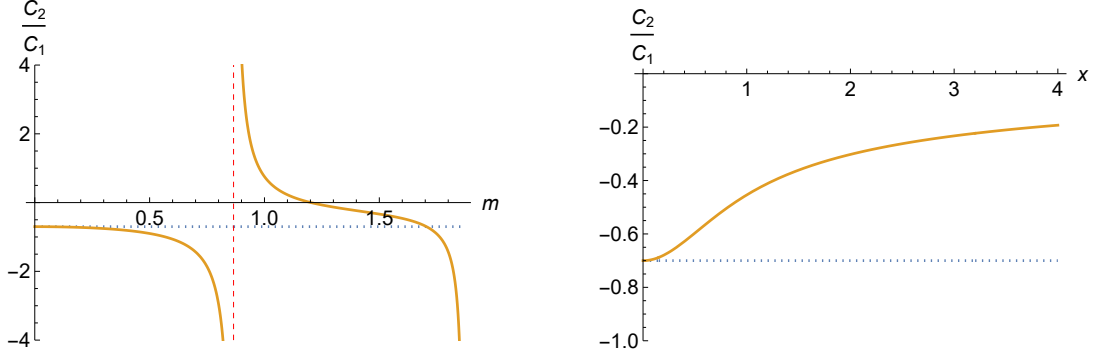


Figure 13: The left panel illustrates the stable eigenvalues of the potential V^- of (6.16) for $\mu = \frac{1}{3}$, $\tilde{\mu} = 1.09$, while the red dashed line corresponds to the value $\frac{C_2}{C_1} = -0.7$ that leads to a massless mode. The right panel illustrates the presence of a tachyonic mode, with $m^2 = -x^2$, for the same values of μ and $\tilde{\mu}$ and $-0.7 < \frac{C_2}{C_1} < 0$.

so that the no-flow conditions (1.16) are violated, at the origin, whenever $C_2 \neq 0$, since $g^+ g^- \sim C_2^2$ at $z = 0$, and in particular by the boundary condition (6.26) allowing the zero mode.

Summarizing, within the stable region $\frac{C_2}{C_1} \geq 0$ or $\frac{C_2}{C_1} \leq -0.7$ there are three classes of boundary conditions: there is a unique choice leading to a massless spectrum for ten vectors in the anti-symmetric of $SO(5)$ corresponding to eq. (6.26), while all other choices lead to purely massive spectra. Among them, a special choice, obtained as $\frac{C_2}{C_1}$ approaches zero from above, respects the no-flow condition.

6.2 $\mathbf{k} \neq 0$ TENSOR MODES

We can now discuss the modes with a non-vanishing internal momentum \mathbf{k} . The starting point is now the system in eqs. (5.13), and including (complex) Fourier modes $e^{i\mathbf{k}\cdot\mathbf{y}}$ in the internal torus leads to the first-order equations

$$\begin{aligned}
\partial_{[\mu} b^{(2)}{}_{\nu]}{}^{lm} + \frac{i}{2} \epsilon^{pqrlm} k_p b_{\mu\nu qr} &= -\frac{e^{-4A-4C}}{2} \epsilon_{\mu\nu\rho\sigma} \partial_r b^{\rho\sigma lm}, \\
-\partial_r b^{(2)}{}_{\mu}{}^{lm} &= -e^{2A+6C} \frac{1}{2} \epsilon^{\alpha\beta\gamma}{}_{\mu} \partial_{\alpha} b_{\beta\gamma}{}^{lm}, \\
k_n b^{(2)}{}_{\mu}{}^{mn} &= 0,
\end{aligned} \tag{6.31}$$

where we omit the \mathbf{k} suffix for brevity. Taking the divergence with respect to the internal coordinates gives

$$k_m \partial_r b^{\rho\sigma lm} = 0, \quad k_m \partial_{[\alpha} b_{\beta\gamma]}{}^{lm} = 0. \tag{6.32}$$

Using the residual gauge symmetries of eqs. (5.14), one can demand that $k_m b^{\rho\sigma lm} = 0$, because the first equation grants that is independent of r , while all preceding gauge choices only involved

the r -dependent portions of the gauge parameters. As a result, one can work with fields that are transverse in the internal space.

Now the momentum \mathbf{k} picks a direction in the internal space, so that for $\mathbf{k} \neq 0$ the two fields in eqs. (6.31) are in the antisymmetric \mathfrak{g} of the residual internal $SO(4)$ that is transverse to it. One can thus decompose them further into portions that are self-dual and antiself-dual with respect to this $SO(4)$ group, which we denote by $b^{(\epsilon)}$ and $b^{(2,\epsilon)}$, with $\epsilon = \pm 1$, such that

$$b^{(\epsilon)\rho\sigma lm} = \frac{\epsilon}{2} \epsilon^{lmpqs} \frac{k_s}{|\mathbf{k}|} b^{(\epsilon)\rho\sigma}_{pq}, \quad b^{(2,\epsilon)\rho lm} = \frac{\epsilon}{2} \epsilon^{lmpqs} \frac{k_s}{|\mathbf{k}|} b^{(2,\epsilon)\rho}_{pq}. \quad (6.33)$$

As a result, for example, $b^{(\epsilon)\rho\sigma}$ is $SO(4)$ -valued along directions transverse to \mathbf{k} , and the system becomes

$$\begin{aligned} \partial_{[\mu} b^{(2,\epsilon)}_{\nu]}{}^{lm} + i |\mathbf{k}| \epsilon b^{(\epsilon)}_{\mu\nu}{}^{lm} &= -\frac{e^{-4A-4C}}{2} \epsilon_{\mu\nu\rho\sigma} \partial_r b^{(\epsilon)\rho\sigma lm}, \\ -\partial_r b^{(2,\epsilon)}_{\mu}{}^{lm} &= -e^{2A+6C} \frac{1}{2} \epsilon^{\alpha\beta\gamma}{}_{\mu} \partial_{\alpha} b^{(\epsilon)}_{\beta\gamma}{}^{lm}. \end{aligned} \quad (6.34)$$

One can now separate variables, letting

$$b^{(2,\epsilon)}_{\nu}{}^{lm}(x, r) = f_2^{\epsilon}(r) b^{(2,\epsilon)}_{\nu}{}^{lm}(x), \quad b^{(\epsilon)}_{\mu\nu}{}^{lm}(x, r) = f^{(\epsilon)}(r) b^{(\epsilon)}_{\mu\nu}{}^{lm}(x), \quad (6.35)$$

and the first of eqs. (6.34) implies that this is only possible if $b^{(\epsilon)}_{\mu\nu}{}^{lm}$ is also self-dual or antiself-dual in spacetime, so that

$$b^{(\epsilon,\zeta)}_{\mu\nu}{}^{lm} = i \frac{\zeta}{2} \epsilon_{\mu\nu\rho\sigma} b^{(\epsilon,\zeta)\rho\sigma lm}, \quad (6.36)$$

with $\zeta = \pm 1$. As a result, f and f_2 satisfy

$$\begin{aligned} i\zeta e^{-4(A+C)} \frac{df^{(\epsilon,\zeta)}}{dr} - i |\mathbf{k}| \epsilon f^{(\epsilon,\zeta)} &= a_1 f_2^{(\epsilon,\zeta)}, \\ \frac{df_2^{(\epsilon,\zeta)}}{dr} &= i\zeta a_2 e^{2A+6C} f^{(\epsilon,\zeta)}, \end{aligned} \quad (6.37)$$

where a_1 and a_2 are two constants, not necessarily real anymore since we are dealing with Fourier modes, while the spacetime equations become

$$\begin{aligned} \partial_{[\mu} b^{(2,\epsilon)}_{\nu]}{}^{lm} &= a_1 b^{(\epsilon,\zeta)}_{\mu\nu}{}^{lm}, \\ a_2 b^{(2,\epsilon)}_{\nu}{}^{lm} &= -\partial^{\alpha} b^{(\epsilon,\zeta)}_{\alpha\mu}{}^{lm}. \end{aligned} \quad (6.38)$$

If $a_1 \neq 0$, the first implies that the field strength of $b_{\mu}^{(2,\epsilon)lm}$ must also satisfy eq. (6.36), and combining them yields, as before, a second-order Proca equation for $b^{(2)}_{\mu}{}^{lm}$,

$$\square b^{(2,\epsilon)}_{\mu}{}^{lm} - \partial_{\mu} \partial^{\nu} b^{(2,\epsilon)}_{\nu}{}^{lm} - m^2 b^{(2,\epsilon)}_{\mu}{}^{lm} = 0, \quad (6.39)$$

with

$$m^2 = -a_1 a_2 , \quad (6.40)$$

where a_1 and a_2 are the constants entering eqs. (6.37).

In order to recast the system in a manifestly Hermitian form, we turn once more to the z variable of eq. (3.9) and redefine the two functions f and f_2 according to

$$f^{(\epsilon,\zeta)} = g^- e^{\frac{A-C}{2} + \chi} , \quad f_2^{(\epsilon,\zeta)} = g^+ e^{\frac{C-A}{2} + \chi} , \quad (6.41)$$

where

$$\partial_z \chi = \frac{|\mathbf{k}|}{2} \epsilon \zeta e^{A-C} , \quad (6.42)$$

and for brevity we leave the two signs ϵ and ζ implicit in g^\pm . The end result is

$$\mathcal{A} g^- = -i \zeta a_1 g^+ , \quad \mathcal{A}^\dagger g^+ = -i \zeta a_2 g^- \quad (6.43)$$

where now

$$\mathcal{A} = \partial_z + \frac{A_z - C_z}{2} - \partial_z \chi , \quad \mathcal{A}^\dagger = -\partial_z + \frac{A_z - C_z}{2} - \partial_z \chi , \quad (6.44)$$

which modify the combinations in eqs. (6.13). The solution to $\mathcal{A} g^- = 0$ is

$$g^- = c_1 e^{\frac{C-A}{2} + \chi} , \quad (6.45)$$

and, as for $\mathbf{k} = 0$, is not normalizable. As a result, a_1 must be different from zero and can again be absorbed in g^+ . The system (6.43) can thus be replaced with

$$\mathcal{A} g^- = g^+ , \quad \mathcal{A}^\dagger \mathcal{A} g^- = m^2 g^- , \quad (6.46)$$

where the Schrödinger-like equation is now

$$\left[-\partial_z^2 + V^- + \frac{|\mathbf{k}|^2}{4} e^{2(A-C)} \right] g^- = m^2 g^- , \quad (6.47)$$

with V^- the first potential in eq. (6.16), and the additional $|\mathbf{k}|^2$ term is subdominant, at both ends, with respect to V^- . Therefore the leading singularities remain the same as for $\mathbf{k} = 0$, and the allowed self-adjoint boundary conditions are still determined by the ratio $\frac{C_2}{C_1}$. Since one is adding to the potential of the preceding section a positive contribution, all modes corresponding to stable boundary conditions for $\mathbf{k} = 0$ are simply lifted in mass by the internal momentum. Moreover, the tachyonic modes, which have a continuous spectrum of masses determined by the

boundary conditions, can be lifted to zero mass. In fact, for all values of \mathbf{k} there are massless modes, which are obtained solving

$$\mathcal{A}^\dagger g^+ = 0, \quad \mathcal{A} g^- = g^+, \quad (6.48)$$

whose internal wavefunctions are

$$g^+ = c_2 e^{\frac{A-C}{2} - \chi}, \quad g^- \sim e^{\frac{C-A}{2} + \chi} \int_{z_m}^z dz' e^{A(z') - C(z') - 2\chi(z')}. \quad (6.49)$$

Here χ can be determined exactly as a function of r solving eq. (6.42), and reads

$$\chi = -\sqrt{10} \epsilon \zeta \rho |\mathbf{k}| e^{-\frac{r}{2\rho\sqrt{10}}}. \quad (6.50)$$

It approaches a constant at both ends of the interval, but nonetheless it changes the value of the ratio $\frac{C_2}{C_1}$ by \mathbf{k} -dependent terms. Note that the emergence of additional massless modes occurs in all sectors, when starting from tachyonic boundary conditions. The peculiar feature of this sector is that, even for $\mathbf{k} \neq 0$, the r -profile of these modes can be still deduced from the first-order equation (6.46).

Summarizing, for all values of $\frac{C_2}{C_1}$ in the range (6.29) there is a boundary condition lifting a $\mathbf{k} = 0$ tachyon to a massless mode carrying an internal momentum. However, for all boundary conditions that yield only stable modes for $\mathbf{k} = 0$ the complete spectrum for $\mathbf{k} \neq 0$ is also stable.

7 SPIN-2 MODES FROM $h_{\mu\nu}$

We can now turn to modes involving perturbations of the metric field. The simplest case is obtained considering a traceless and divergence-free $h_{\mu\nu}$, whose massless modes can describe long-range gravity in lower dimensions. This spin-2 portion cannot mix with anything else, and therefore one can set to zero all other perturbations when addressing it. The dynamical $\alpha\beta$ Einstein equation (5.18) then reduces to

$$(e^{-2A} \square - e^{-2C} \mathbf{k}^2) h_{\alpha\beta} + e^{-2B} [(\partial_r - 4A') \partial_r + 4(A')^2] h_{\alpha\beta} - \frac{h^2}{2\rho^2} e^{-10C} h_{\alpha\beta} = 0, \quad (7.1)$$

while the other equations are identically satisfied. As usual, the d'Alembertian operator defines m^2 , so that the preceding result is equivalent to

$$\left[(\partial_r - 2A')^2 + (m^2 e^{-2A} - \mathbf{k}^2 e^{-2C}) e^{2B} \right] h_{\alpha\beta} = 0, \quad (7.2)$$

where we used some properties of the background, and in particular eqs. (A.15). It is now convenient to introduce once more the variable z of eq. (3.9), and redefining the field according to

$$h_{\alpha\beta} = e^{-\frac{1}{2}B + \frac{5}{2}A} \tilde{h}_{\alpha\beta} , \quad (7.3)$$

leads finally to the Schrödinger-like equation

$$\left[\partial_z^2 + m^2 - \mathbf{k}^2 e^{2(A-C)} - \frac{1}{4}(B_z - A_z)^2 - \frac{1}{2}(B_{zz} - A_{zz}) \right] \tilde{h}_{\alpha\beta} = 0 . \quad (7.4)$$

This equation is identical to the one obtained for the dilaton–axion system in (3.22), and leads to the same spectra for the self-adjoint boundary conditions discussed there. The same considerations apply, and in particular there are boundary conditions granting spectra with $m^2 \geq 0$, as in fig. 5. For $\mathbf{k} = 0$ there is the zero mode (3.25), which translates in this case into the graviton wavefunction

$$h_{\alpha\beta}(r) = e^{2A} \tilde{h}^{(0)}_{\alpha\beta} , \quad (7.5)$$

which satisfies the boundary condition

$$\partial_r \left(r^{\frac{1}{2}} h_{\mu\nu} \right) \sim 0 . \quad (7.6)$$

The finite normalization integral for this ground-state wavefunction,

$$\int_0^\infty dr e^{2B-6A} h_{\alpha\beta} h^{\alpha\beta} \sim \int_0^\infty dr e^{2(B-A)} , \quad (7.7)$$

also determines a finite value of the four-dimensional Planck mass, as discussed in [19]. This zero mode is crucial, since it grants the existence of a long-range four-dimensional effective gravity. It corresponds to the same self-adjoint boundary conditions identified in Section 3. As for the dilaton, for any given boundary condition the spectrum for $\mathbf{k} \neq 0$ is lifted upwards in mass, and therefore all stable choices remain stable also in the presence of an internal momentum.

8 SCALAR MODES FROM h_{ij}

Metric perturbations arising from h_{ij} are also simple to analyze. These are symmetric traceless $SO(5)$ two-tensors for $\mathbf{k} = 0$, which are also transverse in the internal space if $\mathbf{k} \neq 0$ and cannot mix with other modes. All Einstein equations are then identically satisfied, aside from the ij equation (5.23), which reduces to

$$\begin{aligned} (ij) & : (e^{-2A} \square + e^{-2C} \Delta) h_{ij} + e^{-2B} [(\partial_r - 4C') \partial_r + 4(C')^2] h_{ij} \\ & = -\frac{h^2}{2\rho^2} e^{-10C} h_{ij} . \end{aligned} \quad (8.1)$$

In terms of Fourier modes and of the z variable, this becomes

$$\left(m^2 - e^{2(A-C)} \mathbf{k}^2\right) h_{ij} + \left(\partial_z + 3(A_z + C_z)\right) \left(\partial_z - 2C_z\right) h_{ij} = 0, \quad (8.2)$$

after using some identities for the background collected in Appendix A. One can now turn this equation into a manifestly Hermitian form, letting

$$h_{ij} = \tilde{h}_{ij} e^{-\frac{3A+C}{2}}, \quad (8.3)$$

and the result is identical to eq. (7.4) or eq. (3.22). Therefore, the arguments of the preceding section apply almost verbatim, the only difference being that the spacetime profile of the massless mode, which is now valued in the 14 of $SO(5)$, is in this case

$$h_{ij} \sim e^{B-A}. \quad (8.4)$$

As a result $h_{ij} \sim r^{\frac{1}{2}}$ as $r \rightarrow 0$, or equivalently as $z^{\frac{1}{6}}$ as $z \rightarrow 0$, s. Moreover, this wavefunction behaves as $(z_m - z)^{-\frac{2}{\sqrt{10}}}$ as $z \rightarrow z_m$.

9 SINGLET VECTOR MODES

We can now turn to the four-dimensional vector modes that are invariant under the effective internal symmetry group ($SO(5)$ or $SO(4)$), as we have seen, depending on the values of \mathbf{k} .

These vector modes originate partly from the tensor, with

$$b_{\mu i} = \frac{1}{\Sigma} \partial_i V_{1\mu}, \quad (9.1)$$

and partly from gravity, with the relevant fluctuations parametrized as

$$h_{\mu\nu} = \frac{1}{\Sigma} \partial_{(\mu} V_{2\nu)}, \quad h_{\mu r} = V_{3\mu}, \quad h_{\mu i} = \frac{1}{\Sigma} \partial_i V_{4\mu}, \quad (9.2)$$

where Σ is a scale that grants the different fields the standard dimension. Moreover, the four vector fields V_1 , V_2 , V_3 and V_4 are all assumed to be divergence-free,

$$\partial^\mu V_{a\mu} = 0 \quad (a = 1, \dots, 4), \quad (9.3)$$

in order not to include scalar components in them. As a result, the tensor equations (5.13) become

$$\begin{aligned} \partial^{[l} b_\mu^{m]} &= 0, & \frac{\hbar}{2\rho} h_\mu^m - e^{-6A} \partial_r b_\mu^m &= 0, \\ \partial_\mu b^{\mu m} &= 0, & h^\mu{}_\mu &= 0, \end{aligned} \quad (9.4)$$

and the only non-trivial one is the second, which leads to

$$\partial^m \left[\frac{h}{2\rho} V_{4\mu} - e^{-6A} \partial_r V_{1\mu} \right] = 0, \quad (9.5)$$

while the others are identically satisfied. Now $V_{2\mu}$ can be gauged away, and the Einstein equations (5.18) – (5.20) reduce to

$$\begin{aligned} (\alpha\beta) &: \partial_{(\alpha} \left[e^{-2B} (\partial_r - 2A') V_{3\beta)} + \frac{\mathbf{k}^2}{\Sigma} e^{-2C} V_{4\beta)} \right] = 0, \\ (\alpha r) &: (e^{-2A} m^2 - e^{-2C} \mathbf{k}^2) V_{3\alpha} + \frac{\mathbf{k}^2}{\Sigma} e^{-2C} (\partial_r - 2A') V_{4\alpha} = 0, \\ (\alpha i) &: \partial_i \left\{ \frac{e^{-2A}}{\Sigma} m^2 V_{4\alpha} - e^{-2B} (\partial_r - 2C') V_{3\alpha} \right. \\ &\quad \left. + \frac{1}{\Sigma} e^{-2B} \left[(\partial_r - A' - C')^2 - (A' - C')^2 \right] V_{4\alpha} - \frac{e^{-10C}}{2\rho^2 \Sigma} h^2 V_{4\alpha} \right\} = 0, \end{aligned} \quad (9.6)$$

while the rest, the (rr) , (ri) and (ij) equations, are all identically satisfied. One can also remove the overall ∂_α from the first group of equations, while the (αi) equation, together with the $V_{1\mu}$ and $V_{4\mu}$ fields, is only present for nonzero momenta.

9.1 $\mathbf{k} = 0$ MODES

For $\mathbf{k} = 0$ only the first two of eqs. (9.6) are left, with only V_3 , and give

$$\begin{aligned} (\alpha\beta) &: (\partial_r - 2A') V_{3\beta} = 0, \\ (\alpha r) &: m^2 V_{3\alpha} = 0. \end{aligned} \quad (9.7)$$

Therefore, there is in principle a massless vector with a wavefunction in the radial direction

$$V_{3\mu} = h_{\mu r} = e^{2A} V^{(0)}{}_{3\mu}(x). \quad (9.8)$$

This, however, is not a normalizable mode, since the norm inherited from the Einstein–Hilbert action,

$$\int_0^\infty dr \sqrt{-g} \partial_\rho h_{\mu r} \partial_\sigma h_{\nu r} \eta^{\mu\nu} \eta^{\rho\sigma} e^{-2(2A+B)} = - \int_0^\infty dr V^{(0)}{}_{3\mu} \square V^{(0)}{}_{3\nu} \eta^{\mu\nu}, \quad (9.9)$$

diverges. In conclusion, this sector describes no modes altogether.

9.2 $\mathbf{k} \neq 0$ MODES

For $\mathbf{k} \neq 0$, the system becomes

$$\begin{aligned}
(\alpha\beta) &: e^{-2B} (\partial_r - 2A') V_{3\beta} + \frac{\mathbf{k}^2}{\Sigma} e^{-2C} V_{4\beta} = 0, \\
(\alpha r) &: (e^{-2A} m^2 - e^{-2C} \mathbf{k}^2) V_{3\alpha} + \frac{\mathbf{k}^2}{\Sigma} e^{-2C} (\partial_r - 2A') V_{4\alpha} = 0, \\
(\alpha i) &: \frac{e^{-2A}}{\Sigma} m^2 V_{4\alpha} - e^{-2B} (\partial_r - 2C') V_{3\alpha} \\
&+ \frac{1}{\Sigma} e^{-2B} [(\partial_r - A' - C')^2 - (A' - C')^2] V_{4\alpha} - \frac{e^{-10C}}{2\rho^2 \Sigma} h^2 V_{4\alpha} = 0. \quad (9.10)
\end{aligned}$$

The first of these equations determines V_4 in terms of V_3 , and this relation can be used in the second, which becomes

$$e^{2(A-B)} (\partial_r - 2A' - 2B' + 2C') (\partial_r - 2A') V_{3\alpha} + (m^2 - \mathbf{k}^2 e^{2(A-C)}) V_{3\alpha} = 0, \quad (9.11)$$

while the third equation follows from the first two. Notice that the scale Σ does not enter this eigenvalue equation, which determines the mass spectrum.

In terms of z -derivatives, making use of eq. (3.9), eq. (9.11) becomes

$$(\partial_z - 3A_z - B_z + 2C_z) (\partial_z - 2A_z) V_{3\alpha} + (m^2 - \mathbf{k}^2 e^{2(A-C)}) V_{3\alpha} = 0, \quad (9.12)$$

and letting

$$\omega = \frac{5A_z + 3C_z}{2}, \quad V_{3\alpha} = e^{\frac{9A_z + 3C_z}{2}} \tilde{V}_\alpha(x) f(z), \quad (9.13)$$

leads to the manifestly Hermitian equation

$$(\partial_z - \omega) (\partial_z + \omega) f + (m^2 - \mathbf{k}^2 e^{2(A-C)}) f = 0. \quad (9.14)$$

We have thus reached once more a familiar form

$$[\mathcal{A}^\dagger \mathcal{A} + \mathbf{k}^2 e^{2(A-C)}] f = m^2 f, \quad (9.15)$$

where now

$$\mathcal{A} = \partial_z + \omega, \quad \mathcal{A}^\dagger = -\partial_z + \omega, \quad (9.16)$$

so that the Schrödinger potential is

$$V = \frac{e^{\sqrt{\frac{5}{2}} \frac{r}{\rho}}}{320 z_0^2 \sinh^3\left(\frac{r}{\rho}\right)} \left[10\sqrt{10} \sinh\left(\frac{2r}{\rho}\right) + 29 \cosh\left(\frac{2r}{\rho}\right) - 129 \right]. \quad (9.17)$$

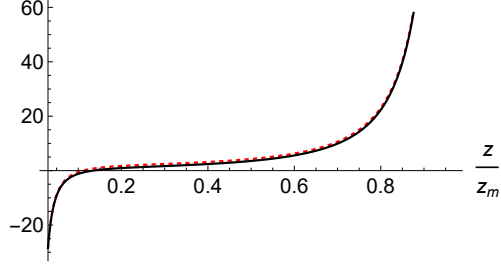


Figure 14: The $\mathbf{k} = 0$ portion of the Schrödinger potential for f in eq. (9.17) (black, solid) and its approximation (2.29) (red, dashed) with $(\mu, \tilde{\mu}) = (\frac{1}{3}, 2.18)$, in units of $\frac{1}{z_0^2}$. z_m and z_0 are defined in eqs. (3.10) and (3.11).

The limiting behavior of the potential at the two ends is as in eq. (1.15), with $\mu = \frac{1}{3}$ and $\tilde{\mu} = \frac{1}{15} (4\sqrt{10} + 20) \simeq 2.18$. Since $\tilde{\mu} > 1$, the only limiting behavior allowed at the right end is

$$f \sim \left(1 - \frac{z}{z_m}\right)^{\frac{55 + 8\sqrt{10}}{30}}, \quad (9.18)$$

while there are different options at the left end, with

$$f \sim C_1 \left(\frac{z}{z_m}\right)^{\frac{5}{6}} + C_2 \left(\frac{z}{z_m}\right)^{\frac{1}{6}}, \quad (9.19)$$

and the self-adjoint boundary conditions are determined by the ratio $\frac{C_2}{C_1}$. Note that the solution of $\mathcal{A}f = 0$ that we found in the previous section is not normalizable, due to its behavior as $r \rightarrow \infty$, but there is another independent massless solution of the Schrödinger equation (9.15) with $\mathbf{k} = 0$. It can be determined by the Wronskian method, and is given by

$$f = e^{\frac{11A+13C}{2}}. \quad (9.20)$$

It is normalizable and is characterized by

$$\frac{C_2}{C_1} \simeq -0.47. \quad (9.21)$$

Note that this zero mode is not a solution of eqs. (9.10) for $\mathbf{k} = 0$, but nonetheless it can be used to determine the shift for the hypergeometric approximation to the \mathbf{k} -independent portion of the potential,

$$\Delta V \simeq -\frac{\pi^2}{z_m^2} (0.39)^2. \quad (9.22)$$

The resulting eigenvalue equation reads

$$\frac{C_2}{C_1} = -\left(\frac{\pi}{2}\right)^{-\frac{2}{3}} \frac{\Gamma\left(\frac{4}{3}\right) \Gamma\left(1.42 + \sqrt{m^2 + (0.39)^2}\right) \Gamma\left(1.42 - \sqrt{m^2 + (0.39)^2}\right)}{\Gamma\left(\frac{2}{3}\right) \Gamma\left(1.76 + \sqrt{m^2 + (0.39)^2}\right) \Gamma\left(1.76 - \sqrt{m^2 + (0.39)^2}\right)}, \quad (9.23)$$

so that the corresponding instability region for the $\mathbf{k} = 0$ portion of the potential is

$$-0.47 < \frac{C_2}{C_1} < 0. \quad (9.24)$$

In conclusion, if $\frac{C_2}{C_1}$ lies outside this range, only massive modes emerge from this sector, when one takes into account the complete \mathbf{k} -dependent potential in eq. (9.15). However, fine-tuning the ratio as a function of the toroidal radius it is possible to lift a tachyonic mode of the \mathbf{k} -independent potential to zero mass, whenever it is present.

10 NON-SINGLET VECTOR MODES

These modes also originate partly from the self-dual tensor and partly from gravity, and can be exhibited letting

$$\begin{aligned} b_{\mu}^{(2)ij} &= \frac{1}{\Sigma} \partial^{[i} W_{1\mu}^{j]} , & \frac{1}{2} \epsilon^{\alpha\beta\mu\nu} b_{\mu\nu}{}^{ij} &= \frac{1}{\Sigma^2} \partial^{[i} \partial^{[\alpha} W_{2\beta]j]} + \frac{1}{2\Sigma^2} \epsilon^{\alpha\beta\mu\nu} \partial_{[\mu} \partial^{[i} \widetilde{W}_{2\beta]j]} , \\ b_{\mu}{}^i &= W_{3\mu}{}^i , & h_{\mu}{}^i &= W_{4\mu}{}^i , \end{aligned} \quad (10.1)$$

where Σ is again a scale that grants the different fields standard dimensions. All other perturbations are set to zero. Moreover, in order to leave aside scalar and singlet vector modes, the W fields thus defined are chosen to be *divergence-free* both in spacetime and in the internal space, where the second condition is only relevant for $\mathbf{k} \neq 0$. In this fashion, the tensor equations reduce to

$$\begin{aligned} \partial^{[i} \partial_{[\mu} W_{1\nu]}^{j]} &= -\frac{e^{-4A-4C}}{\Sigma} \partial_r \partial^{[i} \left(\partial_{[\mu} W_{2\nu]}^{j]} + \frac{1}{2} \epsilon_{\mu\nu}{}^{\alpha\beta} \partial_{[\alpha} \widetilde{W}_{2\beta]}^{j]} \right) , \\ \frac{1}{\Sigma} \partial_r \partial^{[i} W_{1\mu}^{j]} &= e^{2A+6C} \left(\partial^{[i} W_{3\mu}^{j]} + \frac{m^2}{\Sigma^2} \partial^{[i} W_{2\mu}^{j]} \right) , \\ -\frac{\mathbf{k}^2}{\Sigma} W_{1\mu}{}^i &= e^{-2C} \left[\frac{h}{2\rho} W_{4\mu}{}^i - e^{-6A} \partial_r W_{3\mu}{}^i \right] . \end{aligned} \quad (10.2)$$

Moreover, only the αi Einstein equation (5.20) is left, and reads

$$\begin{aligned} \alpha i &: e^{-2A} m^2 W_{4\alpha i} - e^{-2C} \mathbf{k}^2 W_{4\alpha i} + e^{-2B} \left[(\partial_r - A' - C')^2 - (A' - C')^2 \right] W_{4\alpha i} \\ &= e^{-8C} \left[\frac{2\mathbf{k}^2 h}{\rho \Sigma} W_{1\alpha i} + \frac{h^2}{2\rho^2} e^{-2C} W_{4\alpha i} \right] , \end{aligned} \quad (10.3)$$

after taking into account that the fields are divergence-free, and after using, as in previous cases, the conditions $\square = m^2$ and $\Delta = -\mathbf{k}^2$.

10.1 $\mathbf{k} = 0$ MODES

We can now solve these equations, starting from the toroidal zero modes. In this case W_1 , W_2 and \widetilde{W}_2 are absent, while W_3 is linked to W_4 according to

$$\partial_r W_{3\mu}{}^i = \frac{\hbar}{2\rho} e^{6A} W_{4\mu}{}^i . \quad (10.4)$$

This leaves in principle an r -independent contribution to $W_{3\mu}^i$, which does not affect the tensor field strength of Appendix B and therefore can be gauged away. Only W_4 is thus left as an independent field in this sector. It is divergence-free, as we have stated, and satisfies

$$e^{-2A} m^2 W_{4\alpha i} + e^{-2B} \left[(\partial_r - A' - C')^2 - (A' - C')^2 \right] W_{4\alpha i} = \frac{\hbar^2}{2\rho^2} e^{-10C} W_{4\alpha i} , \quad (10.5)$$

or, using the results for the background metric in Appendix A,

$$m^2 W_{4\alpha i} + e^{2(A-B)} (\partial_r - 2C') (\partial_r - 2A') W_{4\alpha i} = 0 . \quad (10.6)$$

Turning to the z variable of eq. (3.9) and performing the redefinition

$$W_{4\alpha i} = e^{-\frac{A+3C}{2}} Z_{\alpha i}(x) f(z) \quad (10.7)$$

leads finally to the manifestly Hermitian Schrödinger-like equation for f ,

$$(-\partial_z + \beta) (\partial_z + \beta) f = m^2 f , \quad (10.8)$$

with

$$\beta = -\frac{1}{2} (5A_z + 3C_z) . \quad (10.9)$$

The Schrödinger potential is now

$$V = \frac{e^{\sqrt{\frac{5}{2}} \frac{z}{\rho}}}{320 z_0^2 \sinh^3 \left(\frac{r}{\rho} \right)} \left[2\sqrt{10} \sinh \left(\frac{2r}{\rho} \right) + 9 \cosh \left(\frac{2r}{\rho} \right) + 131 \right] , \quad (10.10)$$

and is displayed as a function of z in fig. 15. Note that the Schrödinger-like equation is once more of the form

$$\mathcal{A} \mathcal{A}^\dagger f = m^2 f , \quad (10.11)$$

with

$$\mathcal{A} = -\partial_z + \beta , \quad \mathcal{A}^\dagger = -\partial_z + \beta . \quad (10.12)$$

Close to $z = 0$ the potential is as in eq. (1.15), with $\mu = \frac{2}{3}$, while $\tilde{\mu} = \frac{1}{15} (4\sqrt{10} + 5) \simeq 1.18$.

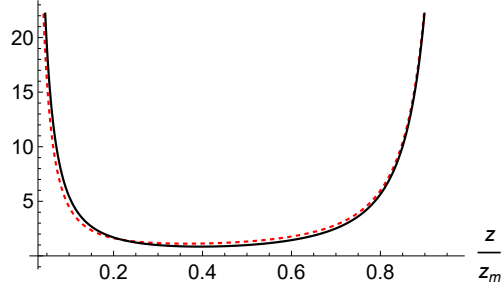


Figure 15: The potential V of eq. (10.10) (black, solid) with its approximation (2.29) (red, dashed) with $(\mu, \tilde{\mu}) = (\frac{2}{3}, 1.18)$, in units of $\frac{1}{z_0^2}$. z_m and z_0 are defined in eqs. (3.10) and (3.11).

The allowed wavefunctions thus behave as

$$f \sim \left(1 - \frac{z}{z_m}\right)^{1.68} \quad (10.13)$$

near the right end of the interval, while there are different options at the left end that are compatible with the leading behavior of the potential, with

$$f \sim C_1 \left(\frac{z}{z_m}\right)^{\frac{7}{6}} + C_2 \left(\frac{z}{z_m}\right)^{-\frac{1}{6}}, \quad (10.14)$$

and self-adjoint boundary conditions are characterized by fixed values of the ratio between these two coefficients.

There is a normalizable ground-state wavefunction,

$$f(r) = f_0 e^{\frac{5A+3C}{2}}, \quad (10.15)$$

with f_0 a constant, which solves $\mathcal{A}^\dagger f = 0$ and corresponds to the special choice of boundary conditions

$$\frac{C_2}{C_1} \simeq -2.42. \quad (10.16)$$

This result translates into the spacetime wavefunction

$$W_{4\alpha i}(x, r) = f_0 Z_{\alpha i}(x) e^{2A}. \quad (10.17)$$

Comparing with the hypergeometric potential (2.29) determines the corresponding shift,

$$\Delta V \simeq -\frac{\pi^2}{z_m^2} (0.71)^2, \quad (10.18)$$

so that the eigenvalue equation for this sector reads

$$\frac{C_2}{C_1} = -\left(\frac{\pi}{2}\right)^{-\frac{4}{3}} \frac{\Gamma\left(\frac{4}{3}\right) \Gamma\left(0.76 + \sqrt{m^2 + (0.71)^2}\right) \Gamma\left(0.76 - \sqrt{m^2 + (0.71)^2}\right)}{\Gamma\left(\frac{1}{3}\right) \Gamma\left(1.42 + \sqrt{m^2 + (0.71)^2}\right) \Gamma\left(1.42 - \sqrt{m^2 + (0.71)^2}\right)}. \quad (10.19)$$

A tachyonic instability is present, in this sector, within the range

$$- 2.42 < \frac{C_2}{C_1} < 0 . \quad (10.20)$$

The limiting form of W_4 in eq. (10.17), which diverges proportionally to $r^{-\frac{1}{2}}$ as $r \rightarrow 0$, violates the no-flow conditions of [22]. This can be seen relatively simply starting from the Kaluza-Klein toroidal reduction to five dimensions, so that the gravity field components of interest, $h_{\mu i}$, behave as Abelian vector fields. The further reduction on the interval can then be analyzed referring to their Maxwell energy momentum tensor, and this leads simply to the preceding conclusion.

10.2 $\mathbf{k} \neq 0$ MODES

For nonzero internal momenta, one must consider the full system of eqs. (10.2) and (10.3), but the transversality conditions that the fields satisfy allow one to remove the overall ∂_i . We can now describe how one can build from them a manifestly Hermitian system of second-order equations for these modes.

10.2.1 THE SCHRÖDINGER-LIKE SYSTEM

Taking the exterior derivative of the first equation and making use of the transversality conditions implies that \widetilde{W}_2 vanishes identically for $m^2 \neq 0$. On the other hand, for $m^2 = 0$ it can be regarded as a mere redefinition of W_2 , which does not enter the other equations. In the following we shall thus remove \widetilde{W}_2 altogether, and as a result one can also remove one spacetime derivative from the first of eqs. (10.2), so that the system reduces further to

$$\begin{aligned} W_{1\mu}{}^i &= - \frac{e^{-4A-4C}}{\Sigma} \partial_r W_{2\mu}{}^i , \\ \frac{1}{\Sigma} \partial_r W_{1\mu}{}^i &= e^{2A+6C} \left(W_{3\mu}{}^i + \frac{m^2}{\Sigma^2} W_{2\mu}{}^i \right) , \\ - \frac{\mathbf{k}^2}{\Sigma} W_{1\mu}{}^i &= e^{-2C} \left[\frac{\hbar}{2\rho} W_{4\mu}{}^i - e^{-6A} \partial_r W_{3\mu}{}^i \right] . \end{aligned} \quad (10.21)$$

Note that the second-order equation (10.3) relates W_1 to W_4 , so that it is natural to deduce from this system another second-order equation linking these two fields. In order to do this, one can start from the second of eqs. (10.21), which implies

$$\partial_r W_{3\mu}{}^i = \frac{1}{\Sigma} e^{-2A-6C} (\partial_r - 2A' - 6C') \partial_r W_{1\mu}{}^i - \frac{m^2}{\Sigma^2} \partial_r W_{2\mu}{}^i . \quad (10.22)$$

Combining it with the first gives

$$\partial_r W_{3\mu}{}^i = \frac{1}{\Sigma} e^{-2A-6C} (\partial_r - 2A' - 6C') \partial_r W_{1\mu}{}^i + e^{4A+4C} \frac{m^2}{\Sigma} W_{1\mu}{}^i, \quad (10.23)$$

and substituting these results into the last of eqs. (10.21) gives

$$\begin{aligned} -\frac{\mathbf{k}^2}{\Sigma} W_{1\mu}{}^i &= \frac{h}{2\rho} e^{-2C} W_{4\mu}{}^i - \frac{e^{-8(A+C)}}{\Sigma} (\partial_r - 2A' - 6C') \partial_r W_{1\mu}{}^i \\ &- \frac{e^{2(C-A)}}{\Sigma} m^2 W_{1\mu}{}^i. \end{aligned} \quad (10.24)$$

This is the second equation we were after, to be considered in combination with eq. (10.3). One can now separate variables, letting

$$W_{a\mu}{}^i(x, z) = w_\mu{}^i(x) W_a(z), \quad (a = 1, 2) \quad (10.25)$$

which leads to the matrix form

$$\mathcal{M}Y = m^2 Y, \quad (10.26)$$

where Y is a column vector containing the two fields W_1 and W_4 ,

$$Y = \begin{pmatrix} W_1 \\ W_4 \end{pmatrix}, \quad (10.27)$$

and

$$\mathcal{M} = \begin{pmatrix} \mathcal{K}^2 - e^{2(A-B)} (\partial_r - 2A' - 6C') \partial_r & \frac{h\Sigma}{2\rho} e^{2A-4C} \\ \frac{2h\mathcal{K}^2}{\rho\Sigma} e^{-6C} & \mathcal{K}^2 - e^{2(A-B)} (\partial_r - 2C') (\partial_r - 2A') \end{pmatrix}, \quad (10.28)$$

with

$$\mathcal{K} = |\mathbf{k}| e^{A-C}. \quad (10.29)$$

The mass spectrum is determined by this system, and therefore it is convenient to try to reduce it to a manifestly Hermitian Schrödinger-like form. To this end, we turn once more to the z variable of eq. (3.9), so that M becomes

$$\mathcal{M} = \begin{pmatrix} \mathcal{K}^2 - (\partial_z + A_z - C_z) \partial_z & \frac{h\Sigma}{2\rho} e^{2A-4C} \\ \frac{2h\mathcal{K}^2}{\Sigma\rho} e^{-6C} & \mathcal{K}^2 - (\partial_z + 3A_z + 3C_z) (\partial_z - 2A_z) \end{pmatrix}. \quad (10.30)$$

This operator is still not manifestly Hermitian, but after redefining the fields according to

$$Y = \Lambda Z, \quad (10.31)$$

with

$$\Lambda = \begin{pmatrix} \sqrt{\frac{\Sigma}{2|\mathbf{k}|}} e^{\frac{C-A}{2}} & 0 \\ 0 & \sqrt{\frac{2|\mathbf{k}|}{\Sigma}} e^{-\frac{A+3C}{2}} \end{pmatrix}, \quad Z = \begin{pmatrix} Z_1 \\ Z_2 \end{pmatrix}, \quad (10.32)$$

the system finally takes the desired form,

$$\widetilde{\mathcal{M}} Z = m^2 Z . \quad (10.33)$$

Now the matrix is

$$\widetilde{\mathcal{M}} = \begin{pmatrix} \mathcal{K}^2 + (-\partial_z + \alpha_z)(\partial_z + \alpha_z) & \frac{|\mathbf{k}|h}{\rho} e^{2(A-3C)} \\ \frac{|\mathbf{k}|h}{\rho} e^{2(A-3C)} & \mathcal{K}^2 + (-\partial_z + \beta_z)(\partial_z + \beta_z) \end{pmatrix}, \quad (10.34)$$

where

$$\alpha_z = \frac{C_z - A_z}{2}, \quad \beta_z = -\frac{5A_z + 3C_z}{2}, \quad (10.35)$$

and is manifestly Hermitian and independent of Σ . The scalar product

$$\int dz \left(|Z_1|^2 + |Z_2|^2 \right) = \frac{\Sigma}{2|\mathbf{k}|} \int dz \left[\left(\frac{2|\mathbf{k}|}{\Sigma} \right)^2 e^{A-C} |W_1|^2 + e^{A+3C} |W_4|^2 \right] \quad (10.36)$$

can also be deduced from these results, and the contribution within square brackets is precisely what the effective action would yield. Note that, although $\widetilde{\mathcal{M}}$ is well defined in the $\mathbf{k} \rightarrow 0$ limit, the scalar product is singular when expressed in terms of the original variables. The behavior of $\widetilde{\mathcal{M}}$ in this limit and its implications for the boundary conditions are examined in detail in Appendix D.

10.2.2 BOUNDARY CONDITIONS AND STABILITY ANALYSIS

We can now address the possible emergence of instabilities for nonzero values of \mathbf{k} . This very problem jeopardizes [13] the non-supersymmetric $AdS \times S$ vacua of [9, 10], but here there is an important novelty, since the toroidal radius R is a free parameter, insofar as it is large enough with respect to the Planck scale to make the present low-energy setup reliable.

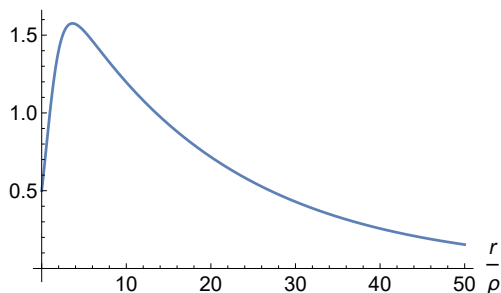


Figure 16: The bounded function u of eq. (10.39), in units of $\frac{|\mathbf{k}|\rho}{z_0^2}$

To begin with, let us note that letting

$$Q = \begin{pmatrix} \partial_z + \alpha_z & \mathcal{K} \\ \mathcal{K} & \partial_z + \beta_z \end{pmatrix}, \quad (10.37)$$

where \mathcal{K} was defined in eq. (10.29), $\widetilde{\mathcal{M}}$ can be cast in the form

$$\widetilde{\mathcal{M}} = Q^\dagger Q - u \sigma_1, \quad (10.38)$$

with σ_1 the familiar Pauli matrix and

$$u = - |\mathbf{k}| \left(4 A_z e^{A-C} + \frac{\hbar}{\rho} e^{2(A-3C)} \right) = \frac{|\mathbf{k}| \rho}{2 z_0^2} \frac{e^{\frac{3r}{\rho \sqrt{10}}}}{\cosh^2 \left(\frac{r}{2\rho} \right)}, \quad (10.39)$$

where z_0 is the scale first defined in eq. (1.4).

Note that u is a positive and bounded function of r , which is displayed in fig. 16, but nonetheless the presence of the Pauli matrix σ_1 in eq. (10.38) yields negative contributions to the m^2 eigenvalues. As a result, $\widetilde{\mathcal{M}}$ is *not* a manifestly positive operator, but for large values of \mathbf{k} the contribution of u is subdominant with respect to the \mathcal{K}^2 terms in $Q^\dagger Q$. The internal momentum \mathbf{k} is quantized in units of $\frac{1}{R}$, with R the radius of the internal torus, and enters all these expressions via the dimensionless combination

$$\xi = \mathbf{k} \rho \sim \frac{|\mathbf{k} z_m|}{(3 H z_m)^{\frac{1}{3}}}. \quad (10.40)$$

Therefore, there is a minimum nonzero value for ξ in this sector, corresponding to the minimal non-vanishing internal momenta. It can be expressed in several equivalent ways, as

$$\xi_0 = \left(\frac{z_m^2}{3 H R^3} \right)^{\frac{1}{3}} \simeq \frac{\rho}{R} \simeq 2 \pi \left(\frac{\ell}{\Phi^{\frac{1}{4}}} \right)^{\frac{4}{5}}, \quad (10.41)$$

where the flux Φ and the length ℓ of the interval were defined in the Introduction. For ξ_0 larger than a critical value ξ_c , and thus for $\frac{R}{\rho}$ below a corresponding critical value, no unstable modes can be present, since as we have stressed the terms depending on \mathcal{K} eventually dominate. However, special choices of boundary conditions may remove the tachyons altogether, and in order to address this question and to obtain an estimate for ξ_c one needs to characterize how m^2 depends on the boundary conditions, while also taking into account the contributions depending on the internal momentum \mathbf{k} .

Our next goal is to characterize the independent self-adjoint boundary conditions at the two ends of the interval that grant the positivity of $Q^\dagger Q$. Let us begin by considering the behavior at the origin, which is more intricate. At the $z = 0$ end, the eigenvalue equation (10.33) reduces to

$$Q_0^\dagger Q_0 Z = 0, \quad (10.42)$$

where Q_0 , the dominant term in Q near $z = 0$, is given by

$$Q_0 = \partial_z + \frac{1}{6z} + \xi \left(\frac{z_m}{z} \right)^{\frac{1}{3}} \sigma_1 . \quad (10.43)$$

The contributions involving u and m^2 are negligible with respect to these singular terms, which include some \mathbf{k} -dependent contributions at this end. As a result, the analysis can be split into a pair of steps. One first solves

$$Q_0^\dagger \Psi = 0 , \quad (10.44)$$

obtaining

$$\Psi = \left(\frac{z}{z_m} \right)^{\frac{1}{6}} \left\{ \cosh \left[\frac{3\xi}{2} \left(\frac{z}{z_m} \right)^{\frac{2}{3}} \right] + \sigma_1 \sinh \left[\frac{3\xi}{2} \left(\frac{z}{z_m} \right)^{\frac{2}{3}} \right] \right\} \Psi_0 , \quad (10.45)$$

with Ψ_0 a constant vector, and the complete solution of $Q_0^\dagger Q_0 Z = 0$ can then be obtained solving the inhomogeneous equation

$$Q_0 Z = \Psi . \quad (10.46)$$

It reads

$$\begin{aligned} Z &= \left(\frac{z_m}{z} \right)^{\frac{1}{6}} \left\{ \cosh \left[\frac{3\xi}{2} \left(\frac{z}{z_m} \right)^{\frac{2}{3}} \right] - \sigma_1 \sinh \left[\frac{3\xi}{2} \left(\frac{z}{z_m} \right)^{\frac{2}{3}} \right] \right\} \\ &\times \left\{ \chi_0 + \int_{z_m}^z dy y^{\frac{1}{3}} \left[\cosh \left(3\xi y^{\frac{2}{3}} \right) + \sigma_1 \sinh \left(3\xi y^{\frac{2}{3}} \right) \right] \Psi_0 \right\} , \end{aligned} \quad (10.47)$$

where χ_0 is another constant vector⁴. We now let

$$\chi_0 = \begin{pmatrix} C_{12} \\ C_{22} \end{pmatrix} , \quad \Psi_0 = \frac{4}{3} \begin{pmatrix} C_{11} \\ C_{21} \end{pmatrix} , \quad (10.48)$$

and the limiting behavior of the preceding expression close to $z = 0$ then yields

$$\begin{aligned} Z_1 &\sim C_{11} \left(\frac{z}{z_m} \right)^{\frac{7}{6}} + C_{12} \left(\frac{z}{z_m} \right)^{-\frac{1}{6}} + \frac{\xi}{2} \left[C_{21} \left(\frac{z}{z_m} \right)^{\frac{11}{6}} - 3 C_{22} \left(\frac{z}{z_m} \right)^{\frac{1}{2}} \right] , \\ Z_2 &\sim C_{21} \left(\frac{z}{z_m} \right)^{\frac{7}{6}} + C_{22} \left(\frac{z}{z_m} \right)^{-\frac{1}{6}} + \frac{\xi}{2} \left[C_{11} \left(\frac{z}{z_m} \right)^{\frac{11}{6}} - 3 C_{12} \left(\frac{z}{z_m} \right)^{\frac{1}{2}} \right] . \end{aligned} \quad (10.49)$$

This limiting behavior will be important in the following, since it characterizes generic wavefunctions Z such that $\widetilde{\mathcal{M}}Z$ is also in L^2 , insofar as the left end of the interval is concerned. Note that the structure of eqs. (10.49) is fully determined by the ξ -independent terms, which

⁴In this section, for simplicity, we are not rescaling the C_{ij} by the μ_i , as in Section 10.2, since $\mu_1 = \mu_2$, and therefore this would only introduce an overall factor in the following equations.

rest on the indicial exponents for the limiting diagonal system discussed in Appendix D. Yet, the additional terms that we have identified are instrumental to guarantee that the \mathbf{k} -dependent terms contained in $\widetilde{\mathcal{M}}$ do not give rise to divergent contributions from the $z = 0$ end.

As discussed in Section 2, the boundary terms that ought to vanish in order to grant self-adjointness are of the form

$$\left[\widetilde{Z}^\dagger \partial_z Z - \left(\partial_z \widetilde{Z}^\dagger \right) Z \right]_{z=0}^{z=z_m} , \quad (10.50)$$

with Z and \widetilde{Z} a pair of two-component vectors whose asymptotic behavior at the origin is as in eq. (10.49), with coefficients C and \widetilde{C} . We shall focus on the natural choice of conditions given independently at the two ends. At the origin the coefficients must thus satisfy

$$\widetilde{C}_{12}^* C_{11} - \widetilde{C}_{11}^* C_{12} + \widetilde{C}_{22}^* C_{21} - \widetilde{C}_{21}^* C_{22} = 0 , \quad (10.51)$$

which is independent of ξ , as expected.

The linear relations granting that eq. (10.51) holds were discussed in Section 2 for systems involving n -component vectors. However, in the present $n = 2$ case there is an alternative, more convenient formulation that we can now describe. Let us therefore start by considering the two-component vectors

$$\underline{X}_1 = \begin{pmatrix} C_{11} \\ C_{12} \end{pmatrix} , \quad \underline{X}_2 = \begin{pmatrix} C_{22} \\ C_{21} \end{pmatrix} , \quad (10.52)$$

and their counterparts $\widetilde{\underline{X}}_{1,2}$, while also recasting eq. (10.51) as the invariance condition for a quadratic form resting on σ_2 :

$$\widetilde{\underline{X}}_1^\dagger \sigma_2 \underline{X}_1 = \widetilde{\underline{X}}_2^\dagger \sigma_2 \underline{X}_2 . \quad (10.53)$$

The self-adjoint boundary conditions given independently at $z = 0$ rest on a $U(1,1)$ matrix U , such that

$$U^\dagger \sigma_2 U = \sigma_2 , \quad (10.54)$$

which links the two vectors $\underline{X}_{1,2}$ according to

$$\underline{X}_2 = U \underline{X}_1 . \quad (10.55)$$

The U matrix is conveniently parametrized as

$$U(\rho, \theta_1, \theta_2, \beta) = e^{i\beta} [\cosh \rho (\cos \theta_1 \underline{1} - i \sigma_2 \sin \theta_1) + \sinh \rho (\sigma_3 \cos \theta_2 + \sigma_1 \sin \theta_2)] , \quad (10.56)$$

and the self-adjoint boundary conditions at $z = 0$ thus depend, in general, on four real numbers.

Moreover, an integration by parts leads to

$$\int_0^{z_m} dz Z^\dagger Q^\dagger Q Z = \int_0^{z_m} dz |Q Z|^2 - \left[Z^\dagger Q Z \right]_{z=0}^{z=z_m}, \quad (10.57)$$

where the first term on the *r.h.s.* is manifestly positive. Consequently, the contribution from the $z = 0$ end is not negative if the limiting contributions from $Z^\dagger Q Z$ at both ends are positive. In particular, at $z = 0$ one is led to

$$\text{Re} [C_{12}^* C_{11} + C_{22}^* C_{21}] \geq 0, \quad (10.58)$$

where the self-adjointness condition was taken into account. Making use of eq. (10.55), this positivity condition at $z = 0$ is equivalent to demanding the positivity of the symmetric matrix

$$\mathcal{S} = \sigma_1 + U^\dagger \sigma_1 U, \quad (10.59)$$

as shown in [14]. In terms of the global parametrization (2.8), the restrictions thus enforced on the parameters read

$$\sin(\theta_1 + \theta_2) \geq 0, \quad \tanh^2 \rho \cos^2 \theta_2 - \cos^2 \theta_1 \leq 0. \quad (10.60)$$

Identical conditions emerged, in a similar context, in Section 3.2.5 of [14].

Our next task is to identify the possible independent self-adjoint boundary conditions at $z = z_m$. These depend on the values $(\tilde{\mu}_1, \tilde{\mu}_2) = (0.09, 1.1)$ that were given after eq. (D.2). This analysis is simpler, since the \mathbf{k} -dependent terms vanish in the limit, and consequently the dominant terms in $\tilde{\mathcal{M}}$ are captured by the diagonal matrix

$$Q_\infty^\dagger Q_\infty, \quad (10.61)$$

with

$$Q_\infty = \begin{pmatrix} \partial_z + \frac{\frac{1}{2} + \tilde{\mu}_1}{z_m - z} & 0 \\ 0 & \partial_z + \frac{\frac{1}{2} + \tilde{\mu}_2}{z_m - z} \end{pmatrix}. \quad (10.62)$$

The allowed limiting behaviors are

$$Z_1 \sim C_{13} \left(\frac{z_m - z}{z_m} \right)^{\frac{1}{2} + \tilde{\mu}_1} + C_{14} \left(\frac{z_m - z}{z_m} \right)^{\frac{1}{2} - \tilde{\mu}_1}, \quad Z_2 \sim C_{23} \left(\frac{z_m - z}{z_m} \right)^{\frac{1}{2} + \tilde{\mu}_2}, \quad (10.63)$$

since $\tilde{\mu}_2 > 1$, and therefore only one of the two possible options for Z_2 leads to normalizable solutions. The contribution from the upper end to the boundary term in eq. (10.50) yields the condition

$$\tilde{C}_{14}^* C_{13} - \tilde{C}_{13}^* C_{14} = 0, \quad (10.64)$$

and consequently the ratio between C_{13} and C_{14} must be a real number, and we let

$$\cot\left(\frac{\tilde{\alpha}}{2}\right) = \frac{C_{13}}{C_{14}}. \quad (10.65)$$

Turning now to the positivity condition, let us note that there is a difference with respect to the other end, since Q_∞ annihilates the least singular contribution to Z_1 , while Q_0 was suppressing the most singular one. As a result, the boundary contribution from z_m to eq. (10.57) is now dominated by

$$-\frac{1 - \tilde{\mu}_1}{z_m} |C_{14}|^2 \left(1 - \frac{z}{z_m}\right)^{-2\tilde{\mu}_1}, \quad (10.66)$$

which is singular and negative. Although this term can be canceled by the bulk contribution in eq. (10.57), positivity is clearly guaranteed if $C_{14} = 0$, or $\tilde{\alpha} = 0$, and we shall abide to this choice in the following.

We can now explore whether, for the self-adjoint boundary conditions granting positivity of $Q^\dagger Q$, which in this case are characterized by $\tilde{\alpha} = 0$ and by the restrictions on the $U(1,1)$ parameters in eq. (10.60), instabilities can arise when the \mathbf{k} -dependent terms in $\widetilde{\mathcal{M}}$ are fully taken into account. Finding this out exactly is difficult, but one can rely on the variational principle, according to which the ground-state energy of the Schrödinger system is given by

$$m_0^2(U, \tilde{\alpha}) = \text{Inf}_{\Psi \in \mathcal{S}} \left[\frac{\langle \Psi | \widetilde{\mathcal{M}} | \Psi \rangle}{\langle \Psi | \Psi \rangle} \right], \quad (10.67)$$

where the *infimum* is over the set \mathcal{S} of all normalizable wavefunctions Ψ for which $\widetilde{\mathcal{M}}\Psi$ is also normalizable, and which satisfy the boundary conditions (10.55) and (10.65). In practice, working within a subset $\mathcal{S}_0 \subset \mathcal{S}$ determined by a finite number of parameters and minimizing over them can yield results that approximate closely from above the actual value of m_0^2 :

$$m^2(\mathcal{S}_0) = \text{Inf}_{\Psi \in \mathcal{S}_0} \left[\frac{\langle \Psi | \widetilde{\mathcal{M}} | \Psi \rangle}{\langle \Psi | \Psi \rangle} \right] \geq m_0^2. \quad (10.68)$$

Negative values of $m^2(\mathcal{S}_0)$ arising from these estimates thus signal the presence of tachyonic instabilities.

Some details on our variational tests are collected in Appendix E, and their indications can be summarized as follows:

- self-adjoint boundary conditions exist for which *no tachyons are present for all values of ξ_0* . An example of this type, with $(\rho, \theta_1, \theta_2, \beta) = (2, -\frac{\pi}{2}, \frac{\pi}{2}, 0)$, is presented in the left panel of fig. 17;

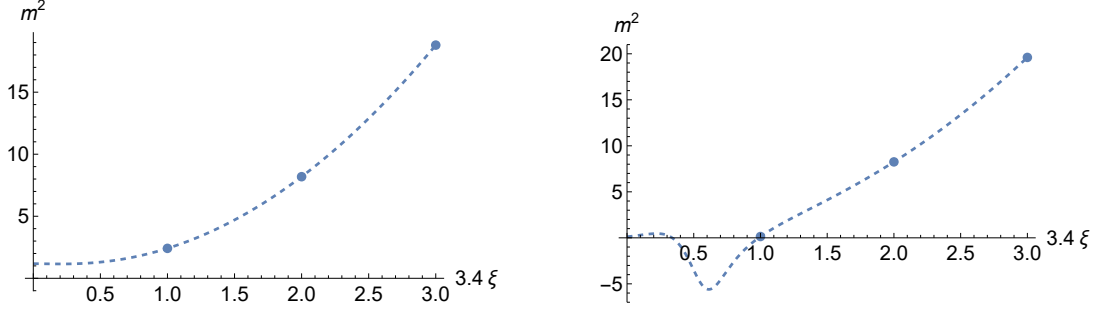


Figure 17: m^2 as a function of ξ , with $(\rho, \theta_1, \theta_2, \beta) = (2, -\frac{\pi}{2}, \frac{\pi}{2}, 0)$ (left panel) and with $(\rho, \theta_1, \theta_2, \beta) = (0, 0, 0, 0)$ (right panel). The dots are examples of possible allowed values for ξ , if the quantization of \mathbf{k} is taken into account.

- other boundary conditions lead to the absence of tachyons provided ξ_0 is larger than a critical value ξ_c . An example of this type, with $(\rho, \theta_1, \theta_2, \beta) = (0, 0, 0, 0)$ determines $\xi_c \simeq 3.4$, and is presented in the right panel of fig. 17.

In conclusion, no tachyonic modes are present in this sector with proper choices of boundary conditions. The parameter space characterizing them depends on the background through the combination ξ_0 of eq. (10.41), and its measure grows as $\xi_0 \sim \frac{L}{R}$ increases.

11 NON-SINGLET SCALAR MODES

We can now turn to scalar perturbations, and we begin by considering the modes that for $\mathbf{k} = 0$ are valued in the fundamental representation of $SO(5)$. These originate from the field profiles

$$\begin{aligned}
 b^i &= \phi_1^i, & b_\mu^i &= \frac{1}{\Sigma} \partial_\mu \phi_2^i, & b_\mu^{(2)ij} &= \frac{1}{\Sigma^2} \partial_\mu \partial^{[i} \phi_3^{j]}, \\
 h^{ij} &= \frac{1}{\Sigma} \partial^{(i} \phi_4^{j)}, & h_\mu^i &= \frac{1}{\Sigma} \partial_\mu \phi_5^i, & h_r^i &= \phi_6^i,
 \end{aligned}
 \tag{11.1}$$

which involve the independent scalar fields ϕ_a^i , with $a = 1, \dots, 6$. A convenient choice of gauge fixing, using the ξ^i of eqs. (5.9), is in this case

$$\phi_5^i = 0,
 \tag{11.2}$$

and, as for the preceding sectors, we begin our analysis from the modes with $\mathbf{k} = 0$.

11.1 $\mathbf{k} = 0$ MODES

In this case the fields ϕ_3 and ϕ_4 disappear, and in the gauge of eq. (11.2) the tensor equations (5.13) reduce to

$$\begin{aligned}\phi_1^i &= -\frac{1}{\Sigma} e^{-2C-6A} \partial_r \phi_2^i, \\ \partial_r \phi_1^i &= e^{-2C} \left[\frac{h}{2\rho} \phi_6^i + \frac{m^2}{\Sigma} e^{10C} \phi_2^i \right].\end{aligned}\quad (11.3)$$

In addition, the αi and αr Einstein equations (5.20) and (5.22) reduce to

$$\begin{aligned}e^{-2B} (\partial_r - 2A') \phi_6^i &= \frac{2h}{\rho} e^{-8C} \phi_1^i, \\ m^2 \Sigma e^{-2A} \phi_6^i &= -m^2 \frac{2h}{\rho} \phi_2^i.\end{aligned}\quad (11.4)$$

When $m \neq 0$, making use of this last equation, one can express ϕ_6 in terms of ϕ_2 , and then the first of eqs. (11.4) becomes identical to the first of eqs. (11.3), while the second becomes

$$e^{-2B+8C} (\partial_r - 2B' + 8C') (\partial_r - 2A') \phi_6^i = e^{-2C} \left[\frac{h^2}{\rho^2} \phi_6^i - m^2 e^{10C-2A} \phi_6^i \right].\quad (11.5)$$

Note, however, that the end result also applies if $m = 0$, as can be seen retracing the preceding steps.

Working in terms of the variable z of eq. (3.9) and performing the field redefinition and the separation of variables

$$\phi_6^i(x, z) = e^{\frac{7A-3C}{2}} \chi_6^i(x) f(z),\quad (11.6)$$

leads to the manifestly Hermitian Schrodinger-like equation

$$\left(\partial_z + \frac{3}{2}(C_z - A_z) \right) \left(\partial_z - \frac{3}{2}(C_z - A_z) \right) f(z) = -m^2 \chi_6^i + \frac{h^2}{\rho^2} e^{2A-10C} f(z).\quad (11.7)$$

The corresponding potential

$$V(r) = \frac{e^{\sqrt{\frac{5}{2}} \frac{r}{\rho}}}{320 z_0^2 \sinh^3 \left(\frac{r}{\rho} \right)} \left[18\sqrt{10} \sinh \left(\frac{2r}{\rho} \right) + 9 \cosh \left(\frac{2r}{\rho} \right) + 131 \right]\quad (11.8)$$

is displayed in fig. 18.

Using eqs. (A.19), eq. (11.7) can be surprisingly recast in the form

$$\mathcal{A}^\dagger \mathcal{A} f(z) = m^2 f(z),\quad (11.9)$$

where

$$\mathcal{A} = \partial_z - \frac{9}{2} A_z - \frac{7}{2} C_z, \quad \mathcal{A}^\dagger = -\partial_z - \frac{9}{2} A_z - \frac{7}{2} C_z,\quad (11.10)$$

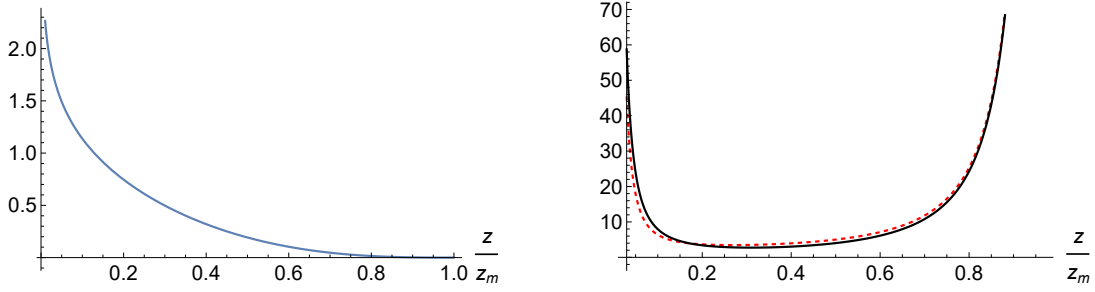


Figure 18: The left panel shows the normalized zero-mode wavefunctions of eqs. (11.6). The right panel compares the corresponding potential V of eq. (11.8) (black, solid) with its approximation (2.29) (red, dashed) with $(\mu, \tilde{\mu}) = (\frac{2}{3}, 2.27)$, in units of $\frac{1}{z_0^2}$. z_m and z_0 are defined in eqs. (3.10) and (3.11).

using the identities involving A_z and C_z collected in Appendix A.

Close to $z = 0$ the potential is as in eq. (1.15), with $\mu = \frac{2}{3}$, while $\tilde{\mu} = \frac{1}{5}(2\sqrt{10} + 5) \simeq 2.27$. Consequently, a single limiting behavior is allowed at z_m , with $f(z) \sim (z_m - z)^{2.77}$, but close to $z = 0$ there is more freedom, and in general

$$f(z) \sim C_1 \left(\frac{z}{z_m}\right)^{\frac{7}{6}} + C_2 \left(\frac{z}{z_m}\right)^{-\frac{1}{6}} \quad (11.11)$$

so that self-adjoint boundary conditions exist for arbitrary fixed ratios $\frac{C_2}{C_1}$. A particular choice solves $\mathcal{A}f(z) = 0$,

$$f(z) = C e^{\frac{9A+7C}{2}}. \quad (11.12)$$

This wavefunction is normalizable, as the reader can simply verify, and corresponds to the choice

$$\frac{C_2}{C_1} = -6.2, \quad (11.13)$$

and thus to the profile

$$\phi_6^i(x, z) = e^{8A+2C} \chi_6^i(x) \quad (11.14)$$

for h_r^i .

As in other sectors, one can approximate the potential by the hypergeometric form of eq. (2.29), up to a shift that can be determined demanding that the resulting massless mode correspond to the ratio between C_2 and C_1 in eq. (11.13). In this case one finds

$$\Delta V = -\frac{\pi^2}{z_m^2} (1.23)^2, \quad (11.15)$$

so that the instability region for this sector is

$$-6.2 < \frac{C_2}{C_1} < 0. \quad (11.16)$$

11.2 $\mathbf{k} \neq 0$ MODES

Let us now turn to modes with a nonzero internal momentum \mathbf{k} . As in previous cases, the scalars are valued in the fundamental representation of the $SO(4)$ transverse to \mathbf{k} , and the fields satisfy the conditions

$$k_i \phi_a^i = 0, \quad a = 1, \dots, 6. \quad (11.17)$$

The longitudinal excitations will contribute to the singlet scalar spectrum.

11.2.1 THE SCHRÖDINGER-LIKE SYSTEM

In the gauge of eq. (11.2), the tensor equations become

$$\begin{aligned} \partial_r \phi_3^j &= e^{2A+6C} \Sigma \phi_2^j, \\ \phi_1^i - \frac{\mathbf{k}^2}{\Sigma^2} \phi_3^i &= -\frac{1}{\Sigma} e^{-6A-2C} \partial_r \phi_2^i, \\ \partial_r \phi_1^i &= e^{-2C} \left[\frac{h}{2\rho} \phi_6^i + \frac{m^2}{\Sigma} e^{10C} \phi_2^i \right]. \end{aligned} \quad (11.18)$$

The αi Einstein equation (5.20) reduces to

$$e^{-2B} (\partial_r - 2A') \phi_6^i - e^{-2C} \frac{\mathbf{k}^2}{\Sigma} \phi_4^i = e^{-8C} \frac{2h}{\rho} \left(\phi_1^i - \frac{\mathbf{k}^2}{\Sigma^2} \phi_3^i \right), \quad (11.19)$$

while the ri and ij Einstein equations (5.22) and (5.23) reduce to

$$\begin{aligned} (e^{-2A} m^2 - e^{-2C} \mathbf{k}^2) \phi_6^i + \frac{1}{\Sigma} e^{-2C} (\partial_r - 2C') \mathbf{k}^2 \phi_4^i &= -\frac{2m^2 h}{\rho \Sigma} \phi_2^i, \\ m^2 e^{-2A} \phi_4^i - \Sigma e^{-2B} (\partial_r - 2C') \phi_6^i + e^{-2B} [(\partial_r - 4C') \partial_r + 4(C')^2] \phi_4^i &= -\frac{h^2}{2\rho^2} e^{-10C} \phi_4^i, \end{aligned} \quad (11.20)$$

which can also be cast in the form

$$\begin{aligned} \mathbf{k}^2 e^{-2C} [\Sigma \phi_6^i - (\partial_r - 2C') \phi_4^i] &= \frac{2m^2 h}{\rho} \left[\phi_2^i + \frac{\rho \Sigma}{2h} e^{-2A} \phi_6^i \right], \\ m^2 \phi_4^i - \Sigma e^{2(A-B)} (\partial_r - 2C') [\Sigma \phi_6^i - (\partial_r - 2C') \phi_4^i] &= 0. \end{aligned} \quad (11.21)$$

This is a complicated-looking system for five different fields, which comprises one second-order equation and five first-order ones. Note that there is still a local symmetry that allows one to shift ϕ_1^i and ϕ_3^i by r -independent amounts in such a way that $\left(\phi_1^i - \frac{\mathbf{k}^2}{\Sigma^2} \phi_3^i \right)$ is unaffected. Up to this gauge symmetry, the system determines uniquely ϕ_1^i , ϕ_3^i and ϕ_4^i in terms of ϕ_2^i and ϕ_6^i .

We can now obtain a system of second-order equations for ϕ_2^i and ϕ_6^i . To this end, one can use the second of eqs. (11.18) in eq. (11.19), obtaining

$$e^{-2B} \Sigma (\partial_r - 2A') \phi_6^i - e^{-2C} \mathbf{k}^2 \phi_4^i = -\frac{2h}{\rho} e^{-6A-10C} \partial_r \phi_2^i. \quad (11.22)$$

Next, one can combine the derivative of the second of eqs. (11.18) with the first and the third, obtaining the first equation we were after

$$e^{-6A-2C} (\partial_r - 6A' - 2C') \partial_r \phi_2^i = -\frac{\Sigma h}{2\rho} e^{-2C} \phi_6^i - (m^2 e^{8C} - \mathbf{k}^2 e^{2A+6C}) \phi_2^i. \quad (11.23)$$

In order to obtain the second, one can differentiate eq. (11.22), and adding it to the first of eqs. (11.20) gives

$$\begin{aligned} & e^{-2B} (\partial_r - 2B') (\partial_r - 2A') \phi_6^i + (e^{-2A} m^2 - e^{-2C} \mathbf{k}^2) \phi_6^i \\ &= -\frac{2h}{\Sigma\rho} [e^{-6A-10C} (\partial_r - 6A' - 10C') \partial_r + m^2] \phi_2^i. \end{aligned} \quad (11.24)$$

One can also combine eqs. (11.23) and (11.24) in order to eliminate the second derivative of ϕ_2 from the second equation, and the system can be presented in the more convenient form

$$\begin{aligned} & - \left[e^{2(A-B)} (\partial_r - 6A' - 2C') \partial_r - \mathbf{k}^2 e^{2(A-C)} \right] \phi_2^i - \frac{\Sigma h}{2\rho} e^{-10C} \phi_6^i = m^2 \phi_2^i, \\ & - \left[e^{2(A-B)} (\partial_r - 2B') (\partial_r - 2A') - \mathbf{k}^2 e^{2(A-C)} - \frac{h^2}{\rho^2} e^{2A-10C} \right] \phi_6^i \\ & + \frac{2h}{\Sigma\rho} (8C' e^{-4A-10C} \partial_r - \mathbf{k}^2 e^{4A-2C}) \phi_2^i = m^2 \phi_6^i. \end{aligned} \quad (11.25)$$

Now, as a first step toward attaining a manifestly Hermitian form, we turn to the independent variable z of eq. (3.9), and the system becomes

$$\begin{aligned} & - \left[(\partial_z - 3A_z + 3C_z) \partial_z - \mathbf{k}^2 e^{2(A-C)} \right] \phi_2^i - \frac{\Sigma h}{2\rho} e^{-10C} \phi_6^i = m^2 \phi_2^i, \\ & - \left[(\partial_z - 5(A_z + C_z)) (\partial_z - 2A_z) - e^{2(A-C)} \mathbf{k}^2 - \frac{h^2}{\rho^2} e^{2A-10C} \right] \phi_6^i \\ & + \frac{2h}{\Sigma\rho} e^{2A} (8C_z \partial_z - \mathbf{k}^2 e^{2(A-C)}) \phi_2^i = m^2 \phi_6^i. \end{aligned}$$

Separating variables letting

$$\phi_a^i(x, z) = \phi^i(x) f_a(z) \quad (a = 2, 6), \quad (11.26)$$

in matrix notation the system becomes

$$\mathcal{M} \Psi = m^2 \Psi, \quad \text{with} \quad \Psi = \begin{pmatrix} f_2 \\ f_6 \end{pmatrix} \quad (11.27)$$

and

$$\mathcal{M} = \begin{pmatrix} -[(\partial_z - 3A_z + 3C_z) \partial_z - \mathcal{K}^2] & -\frac{\Sigma h}{2\rho} e^{-10C} \\ \frac{2h}{\Sigma\rho} e^{2A} [8C_z \partial_z - \mathcal{K}^2] & -[(\partial_z - 5(A_z + C_z)) (\partial_z - 2A_z) - \mathcal{K}^2 - 16\mathcal{W}_5^2] \end{pmatrix}. \quad (11.28)$$

The two quantities \mathcal{K}^2 and \mathcal{W}_5 that enter this expression were defined in eqs. (10.29) and (A.20), and a number of related properties can be found in Appendix A. Note that the differential operator \mathcal{M} is, once more, not in a manifestly Hermitian form. This form can be reached, as in Section 10.2, by a convenient change of basis, which is now slightly more involved.

In general, letting

$$\Psi = \Lambda \tilde{\Psi} , \quad (11.29)$$

with Λ an invertible matrix, one obtains for $\tilde{\Psi}$ the new system

$$\tilde{\mathcal{M}} \tilde{\Psi} = m^2 \tilde{\Psi} , \quad (11.30)$$

with

$$\tilde{\mathcal{M}} = \Lambda^{-1} \mathcal{M} \Lambda . \quad (11.31)$$

In this sector the matrix Λ and its inverse are not diagonal, and read

$$\Lambda = \begin{pmatrix} e^{\xi_1} & 0 \\ -e^{\xi_3} & e^{\xi_2} \end{pmatrix} , \quad \Lambda^{-1} = \begin{pmatrix} e^{-\xi_1} & 0 \\ e^{\xi_3 - \xi_1 - \xi_2} & e^{-\xi_2} \end{pmatrix} , \quad (11.32)$$

where

$$e^{\xi_1} = e^{\frac{3}{2}(A-C)} \sqrt{\frac{\Sigma}{2|\mathbf{k}|}} , \quad e^{\xi_2} = e^{\frac{1}{2}(7A+5C)} \sqrt{\frac{2|\mathbf{k}|}{\Sigma}} , \quad e^{\xi_3} = e^{\frac{1}{2}(7A-3C)} \frac{h}{\rho \Sigma} \sqrt{\frac{2\Sigma}{|\mathbf{k}|}} . \quad (11.33)$$

These redefinitions lead to the manifestly Hermitian operator

$$\tilde{\mathcal{M}} = \begin{pmatrix} (-\partial_z + \alpha_z)(\partial_z + \alpha_z) + \mathcal{K}^2 + 16\mathcal{W}_5^2 & -4\mathcal{W}_5\mathcal{K} \\ -4\mathcal{W}_5\mathcal{K} & (-\partial_z + \beta_z)(\partial_z + \beta_z) + \mathcal{K}^2 \end{pmatrix} , \quad (11.34)$$

where

$$\alpha_z = \frac{3}{2}(A_z - C_z) , \quad \beta_z = -\frac{1}{2}(3A_z + 5C_z) , \quad (11.35)$$

and the scalar product, after separating variables, takes the form

$$\begin{aligned} & \int dz \left[\left| \tilde{\Psi}_1 \right|^2 + \left| \tilde{\Psi}_2 \right|^2 \right] \\ &= \frac{\Sigma}{2|\mathbf{k}|} \int dz \left[\left(\frac{2|\mathbf{k}|}{\Sigma} \right)^2 e^{3(C-A)} |f_2|^2 + e^{-(3A+5C)} \left| f_2 + e^{-2A} \frac{\rho \Sigma}{2h} f_6 \right|^2 \right] . \end{aligned} \quad (11.36)$$

The correspondence with the scalar product implied by the Schrödinger system (11.9) of the previous section can be exhibited dividing this expression, which becomes singular for vanishing \mathbf{k} , by an overall factor proportional to $|\mathbf{k}|$, and focusing on the first term.

Actually, using the result in Section 11.1, $\widetilde{\mathcal{M}}$ can be recast in a form that is very similar to eq. (10.34),

$$\widetilde{\mathcal{M}} = \begin{pmatrix} (-\partial_z + \widetilde{\alpha}_z)(\partial_z + \widetilde{\alpha}_z) + \mathcal{K}^2 & -\frac{|\mathbf{k}|h}{\rho} e^{2(A-3C)} \\ -\frac{|\mathbf{k}|h}{\rho} e^{2(A-3C)} & (-\partial_z + \beta_z)(\partial_z + \beta_z) + \mathcal{K}^2 \end{pmatrix}, \quad (11.37)$$

where

$$\widetilde{\alpha}_z = -\frac{9}{2}A_z - \frac{7}{2}C_z, \quad \beta_z = -\frac{1}{2}(3A_z + 5C_z), \quad (11.38)$$

and the sign of the off-diagonal terms is not significant, since it could be flipped conjugating by σ_3 , or equivalently redefining one of the two wavefunctions by an overall sign.

11.2.2 BOUNDARY CONDITIONS AND STABILITY ANALYSIS

As before, self-adjoint boundary conditions are determined by the leading behavior of the wavefunctions at the two ends, and thus by the indices μ_i and $\tilde{\mu}_1$ that first emerged in eq. (1.15). In this case $\mu_1 = \frac{2}{3}$ and $\mu_2 = \frac{1}{3}$, so that close to the origin, proceeding as in Section 10.2, one can identify the limiting behavior ⁵

$$\begin{aligned} \widetilde{\Psi}_1 &\sim \frac{C_{11}}{\sqrt{2}} \left(\frac{z}{z_m}\right)^{\frac{7}{6}} + \frac{C_{12}}{\sqrt{2}} \left(\frac{z}{z_m}\right)^{-\frac{1}{6}} + 2\xi \left[-\frac{3}{5} C_{21} \left(\frac{z}{z_m}\right)^{\frac{3}{2}} + C_{22} \left(\frac{z}{z_m}\right)^{\frac{5}{6}} \right] \\ &+ \frac{3}{4\sqrt{2}} \xi^2 \left[\frac{19}{40} C_{11} \left(\frac{z}{z_m}\right)^{\frac{5}{2}} - 3 C_{12} \left(\frac{z}{z_m}\right)^{\frac{7}{6}} \log \left(\frac{z}{z_m}\right) \right], \\ \widetilde{\Psi}_2 &\sim C_{21} \left(\frac{z}{z_m}\right)^{\frac{5}{6}} + C_{22} \left(\frac{z}{z_m}\right)^{\frac{1}{6}} + \sqrt{2}\xi \left[-\frac{1}{5} C_{11} \left(\frac{z}{z_m}\right)^{\frac{11}{6}} + 3 C_{12} \left(\frac{z}{z_m}\right)^{\frac{1}{2}} \right] \\ &+ \frac{1}{8} \xi^2 \left[\frac{27}{5} C_{21} \left(\frac{z}{z_m}\right)^{\frac{13}{6}} - C_{22} \left(\frac{z}{z_m}\right)^{\frac{3}{2}} \right], \end{aligned} \quad (11.39)$$

where

$$\xi = \frac{|\mathbf{k} z_m|}{(3H z_m)^{\frac{1}{3}}} \quad (11.40)$$

is the dimensionless quantity that already emerged in eq. (10.40). These expressions are more complicated than those obtained in Section 10.2, but the additional terms proportional to \mathbf{k}^2 are needed to grant that $\widetilde{\mathcal{M}}\widetilde{\Psi}$ be in L^2 .

The behavior at the other end of the interval is simpler, since $\widetilde{\mathcal{M}}$ is dominated by the diagonal matrix

$$\widetilde{\mathcal{M}} = \begin{pmatrix} \left(-\partial_z + \frac{\frac{1}{2} + \tilde{\mu}_1}{z_m - z}\right) \left(\partial_z + \frac{\frac{1}{2} + \tilde{\mu}_1}{z_m - z}\right) & 0 \\ 0 & \left(-\partial_z + \frac{\frac{1}{2}}{z_m - z}\right) \left(\partial_z + \frac{\frac{1}{2}}{z_m - z}\right) \end{pmatrix}, \quad (11.41)$$

⁵For simplicity, all these C_{ij} coefficients were redefined by an overall factor $\sqrt{3}$ with respect to Section 2.

with the two indices $\tilde{\mu}_1 \simeq 2.27$ and $\tilde{\mu}_2 = 0$. Consequently, the limiting behavior of the wavefunctions close to z_m is captured by

$$\tilde{\Psi}_1 \sim \left(1 - \frac{z}{z_m}\right)^{2.77}, \quad \tilde{\Psi}_2 \sim \left(1 - \frac{z}{z_m}\right)^{\frac{1}{2}} \left[C_{23} \log\left(1 - \frac{z}{z_m}\right) + C_{24} \right], \quad (11.42)$$

since the other possible exponent for $\tilde{\Psi}_1$ would be incompatible with the L^2 condition.

As in Section 10.2, the limiting behaviors at the origin that grant self-adjointness are parametrized by a $U(1,1)$ matrix such that

$$\begin{pmatrix} C_{22} \\ C_{21} \end{pmatrix} = U \begin{pmatrix} C_{11} \\ C_{12} \end{pmatrix}, \quad (11.43)$$

while the allowed choices at the other end are parametrized by

$$\cot\left(\frac{\tilde{\alpha}}{2}\right) = \frac{C_{23}}{C_{24}}. \quad (11.44)$$

At the upper end positivity is guaranteed if $C_{23} = 0$, while at the lower end one is led again to eq. (10.58), and thus positivity is surely guaranteed if the conditions in eq. (10.60) hold. We shall focus on these options in the following.

Before ending the section, let us note that in this sector $\tilde{\mathcal{M}}$ admits the decomposition

$$\tilde{\mathcal{M}} = \hat{Q}^\dagger \hat{Q} + \Delta, \quad (11.45)$$

where

$$\hat{Q} = \begin{pmatrix} \partial_z + \alpha_z & 0 \\ 0 & \partial_z + \beta_z \end{pmatrix} \quad (11.46)$$

and

$$\Delta = \begin{pmatrix} \mathcal{K}^2 + 16 \mathcal{W}_5^2 & -4 \mathcal{W}_5 \mathcal{K} \\ -4 \mathcal{W}_5 \mathcal{K} & \mathcal{K}^2 \end{pmatrix}, \quad (11.47)$$

is a manifestly positive-definite matrix, since its trace and determinant are both positive, while $\hat{Q}^\dagger \hat{Q}$ can be positive definite with self-adjoint boundary conditions determined by α_z and β_z . However, Δ contains contributions proportional to $\frac{1}{z^2}$, and therefore the self-adjoint boundary conditions for $\tilde{\mathcal{M}}$ are different in general, so that eq. (11.45) does not suffice to imply its positivity.

With general self-adjoint boundary conditions appropriate to $\tilde{\mathcal{M}}$, our variational tests summarized in Appendix E provide evidence that stability is generally granted, in this sector, by values of ξ_0 of eq. (10.41) beyond a few units, while special choices of boundary conditions lead to spectra that are fully stable without any conditions on ξ_0 .

12 SINGLET SCALAR MODES

We can now conclude our analysis with a discussion of the most intricate sector of the spectrum, which concerns scalar singlets. These originate from a number of different tensor and metric perturbations, which can be parametrized as follows:

$$\begin{aligned}
b &= \phi_1, & b^i &= \frac{1}{\Sigma} \partial^i \phi_2, & b_\mu^i &= \frac{1}{\Sigma^2} \partial_\mu \partial^i \phi_3, \\
h_{\mu\nu} &= \eta_{\mu\nu} \phi_4 + \frac{1}{\Sigma^2} \partial_\mu \partial_\nu \phi_5, & h_{\mu r} &= \frac{1}{\Sigma} \partial_\mu \phi_6, & h_{\mu i} &= \frac{1}{\Sigma^2} \partial_\mu \partial_i \phi_7, \\
h_{rr} &= \phi_8, & h_{ri} &= \frac{1}{\Sigma} \partial_i \phi_9, & h_{ij} &= \delta_{ij} \phi_{10} + \frac{1}{\Sigma^2} \partial_i \partial_j \phi_{11}.
\end{aligned} \tag{12.1}$$

Since the background values of the dilaton–axion pair are constant, their perturbations decouple from these other scalar modes. For this reason we could treat them separately in Section 3, and the same happened in Section 4 for the perturbations arising from the two-forms B_{MN}^i , so that here we can set all of them to zero. One can also fix diffeomorphism invariance, using the three parameters ξ_μ , ξ_r and ξ_i , making the convenient gauge choice

$$\phi_5 = \phi_6 = \phi_7 = 0, \tag{12.2}$$

but these steps leave nonetheless, in general, eight fields within this sector. They also introduce boundary fields, as in other sectors. For brevity we shall not discuss them, although they can change the massless spectrum, since they cannot give rise to instabilities. Moreover, here we confine our attention to the $\mathbf{k} = 0$ modes, where some simplifications occur, leaving the general case, which involves a number of novel features, to a future publication [28].

For $\mathbf{k} = 0$, only the four fields ϕ_1, ϕ_4, ϕ_8 and ϕ_{10} are left. The tensor equations reduce to

$$\frac{h}{4\rho} (-4e^{-2A} \phi_4 - e^{-2B} \phi_8 + 5e^{-2C} \phi_{10}) + e^{-8A} \partial_r \phi_1 = 0, \tag{12.3}$$

and determine ϕ_1 in terms of the different metric perturbations, while the $\alpha\beta$ Einstein equation involves two different structures, associated to $\partial_\alpha \partial_\beta$ and $\eta_{\alpha\beta}$, and the corresponding terms are to vanish separately. This gives for the modes belonging to this sector the two additional equations

$$\alpha\beta_1 : 2e^{-2A} \phi_4 + e^{-2B} \phi_8 + 5e^{-2C} \phi_{10} = 0, \tag{12.4}$$

$$\begin{aligned}
\alpha\beta_2 : & e^{-2A} m^2 \phi_4 + A' e^{2(A-B)} [4e^{-2A} (\partial_r - 2A') \phi_4 \\
& - e^{-2B} (\partial_r - 2B') \phi_8 + 5e^{-2C} (\partial_r - 2C') \phi_{10}] \\
& + e^{-2B} [(\partial_r - 4A') \partial_r + 4(A')^2] \phi_4 = 2 \frac{h}{\rho} e^{2(A-B)} \partial_r \phi_1 - \frac{3}{2} \frac{h^2}{\rho^2} e^{-10C} \phi_4.
\end{aligned} \tag{12.5}$$

The remaining Einstein equations become

$$\begin{aligned}
\alpha r &: 3e^{-2A} (\partial_r - 2A') \phi_4 + (A' - B') e^{-2B} \phi_8 + 5e^{-2C} (\partial_r - A' - C') \phi_{10} = 0, \\
rr &: e^{-2A} m^2 \phi_8 - B' \partial_r (e^{-2B} \phi_8) \\
&+ 4e^{-2A} (\partial_r - B') (\partial_r - 2A') \phi_4 + 5e^{-2C} (\partial_r - B') (\partial_r - 2C') \phi_{10} \\
&= 2 \frac{h}{\rho} \partial_r \phi_1 - 2 \frac{h^2}{\rho^2} e^{6A} \phi_4, \\
ij &: e^{-2A} m^2 \phi_{10} + 4C' e^{2(C-A-B)} (\partial_r - 2A') \phi_4 - e^{2(C-2B)} [2C'' + C' (\partial_r - 2B')] \phi_8 \\
&+ e^{-2B} [\partial_r^2 + C' \partial_r - 6(C')^2] \phi_{10} = 2 \frac{h^2}{\rho^2} e^{-10C} \phi_{10}. \tag{12.6}
\end{aligned}$$

One can now eliminate ϕ_8 using eq. (12.4), and then eq. (12.3) reduces to

$$\partial_r \phi_1 = \frac{h}{2\rho} (e^{6A} \phi_4 - 5e^{8A-2C} \phi_{10}), \tag{12.7}$$

and determines ϕ_1 up to an r -independent contribution that is pure gauge, so that only ϕ_4 and ϕ_{10} are left. After the convenient redefinitions

$$e^{-2A} \phi_4 = \chi_4, \quad e^{-2B} \phi_8 = \chi_8, \quad e^{-2C} \phi_{10} = \chi_{10}, \tag{12.8}$$

the $\alpha\beta_1$ Einstein equation (12.4) reduces to the simple algebraic constraint

$$2\chi_4 + \chi_8 + 5\chi_{10} = 0, \tag{12.9}$$

and eliminating χ_8 now leads to a system of four equations for the two fields χ_4 and χ_{10}

$$\begin{aligned}
\alpha\beta_2 &: m^2 \chi_4 + e^{2(A-B)} \left[10A' \partial_r + \frac{5h^2}{\rho^2} e^{8A} \right] \chi_{10} \\
&+ e^{2(A-B)} \left[\partial_r^2 + 6A' \partial_r + \frac{h^2}{\rho^2} e^{8A} \right] \chi_4 = 0, \\
rr &: -m^2 (2\chi_4 + 5\chi_{10}) + e^{2(A-B)} \left[(4\partial_r + 8A' - 2B') \partial_r + \frac{h^2}{\rho^2} e^{8A} \right] \chi_4 \\
&+ e^{2(A-B)} \left[5(\partial_r + 2C') \partial_r + \frac{5h^2}{\rho^2} e^{8A} \right] \chi_{10} = 0, \\
ij &: m^2 \chi_{10} + e^{2(A-B)} \left[6C' \partial_r - \frac{h^2}{\rho^2} e^{8A} \right] \chi_4 \\
&+ e^{2(A-B)} \left[\partial_r^2 + 10C' \partial_r - \frac{5h^2}{\rho^2} e^{8A} \right] \chi_{10} = 0, \\
\alpha r &: (3\partial_r + 6A' + 10C') \chi_4 + 5(\partial_r + 2A' + 6C') \chi_{10} = 0. \tag{12.10}
\end{aligned}$$

In terms of the z variable of eq. (3.9), this system takes the more compact form

$$\begin{aligned}
10 (A_z \partial_z + 8 \mathcal{W}_5^2) \chi_{10} + [(\partial_z + 9A_z + 5C_z) \partial_z + m^2 + 16 \mathcal{W}_5^2] \chi_4 &= 0, \\
2 [(2\partial_z + 6A_z + 5C_z) \partial_z - m^2 + 8 \mathcal{W}_5^2] \chi_4 + 5 [(\partial_z + 3A_z + 7C_z) \partial_z - m^2 + 16 \mathcal{W}_5^2] \chi_{10} &= 0, \\
2 (3C_z \partial_z - 8 \mathcal{W}_5^2) \chi_4 + [(\partial_z + 3A_z + 15C_z) \partial_z + m^2 - 80 \mathcal{W}_5^2] \chi_{10} &= 0, \\
(\partial_z + 2A_z) (3 \chi_4 + 5 \chi_{10}) + 10 C_z (\chi_4 + 3 \chi_{10}) &= 0.
\end{aligned} \tag{12.11}$$

However, the rr equation is a linear combination of the $\alpha\beta$ and ij ones, once the αr equation is used. Moreover, the three second-order equations can be combined into another first-order one. This is in fact the rr Einstein equation, which we often refer to as ‘‘Hamiltonian constraint’’,

$$\begin{aligned}
- m^2 (3\chi_4 + 5\chi_{10}) + e^{2(A-B)} \left[-20(A' + C') \partial_r + \frac{5h^2}{\rho^2} e^{8A} \right] \chi_{10} \\
+ e^{2(A-B)} \left[-4(3A' + 5C') \partial_r + \frac{h^2}{\rho^2} e^{8A} \right] \chi_4 = 0,
\end{aligned} \tag{12.12}$$

or, in terms of the z variable,

$$m^2 (3\chi_4 + 5\chi_{10}) + 20 [(A_z + C_z) \partial_z - 4 \mathcal{W}_5^2] \chi_{10} + 4 [(3A_z + 5C_z) \partial_z - 4 \mathcal{W}_5^2] \chi_4 = 0. \tag{12.13}$$

In this fashion, one ends up with two first-order equations linking χ_4 and χ_{10} , and all second-order equations follow from them. Therefore, the system only contains one independent scalar degree of freedom, from which all other wavefunctions can be deduced.

In flat space, with the internal T^5 and an S_1 along the r -direction, these equations would allow *two* r -independent wavefunctions for $m = 0$, and actually a pair of four-dimensional massless scalars $\chi_4(x)$ and $\chi_{10}(x)$. The constant parts of χ_8 and χ_{10} would be associated to independent deformations of the radius of the S_1 and the overall size of the internal torus. In our case the length ℓ of the r -interval is fixed by the background, and indeed a single independent constant part is left by the preceding conditions, since the first three of eqs. (12.10) demand that r -independent quantities satisfy

$$\chi_4 + 5 \chi_{10} = 0. \tag{12.14}$$

Equivalently, using eq. (12.9), constant shifts of B and C , which are captured by χ_8 and χ_{10} , are surprisingly not independent, but

$$\chi_8 = 5 \chi_{10}. \tag{12.15}$$

The reason behind this result is explained in detail in [19]: the equal radii R of the internal torus can be scaled out, so that the background only depends on two parameters, the conserved flux Φ

and the length ℓ of the r -interval, whose perturbation is described by χ_8 . As a result, the size of the internal torus is effectively determined by the combination $(\Phi \ell)^{\frac{1}{5}}$, as can be seen in eqs. (1.8). Note, however, that there is no massless field in four dimensions associated to this deformation, which is just a constant shift.

In flat space, for $m^2 \neq 0$ eqs. (12.10) or, equivalently, eq. (12.12), demand that

$$\chi \equiv 3\chi_4 + 5\chi_{10} = 0 . \quad (12.16)$$

This is a familiar result in Kaluza–Klein theory: massive scalar excitations are eaten by corresponding massive vectors. In our background, however, it is actually convenient to obtain a second–order equation for this very field,

$$\chi \equiv 3\chi_4 + 5\chi_{10} , \quad (12.17)$$

which will be singular in the flat limit. To this end, we also let

$$\psi = \chi_4 + 3\chi_{10} , \quad (12.18)$$

and then the αr Einstein equation becomes

$$(\partial_r + 2A') \chi + 10 C' \psi = 0 , \quad (12.19)$$

and determines ψ algebraically, while eq. (12.12) takes the form

$$\begin{aligned} 0 = & -m^2 \chi - 2 e^{2(A-B)} \left[(2A' + 5C') \partial_r + \frac{h^2}{4\rho^2} e^{8A} \right] \chi \\ & + 10 e^{2(A-B)} \left[C' \partial_r + \frac{h^2}{4\rho^2} e^{8A} \right] \psi . \end{aligned} \quad (12.20)$$

In terms of the z -variable of eq. (3.9), these equations become

$$\begin{aligned} (\partial_z + 2A_z) \chi + 10 C_z \psi &= 0 , \\ m^2 \chi + 2 [(2A_z + 5C_z) \partial_z + 4\mathcal{W}_5^2] \chi - 10 [C_z \partial_z + 4\mathcal{W}_5^2] \psi &= 0 , \end{aligned} \quad (12.21)$$

where \mathcal{W}_5 was defined in eq. (A.20). The two equations (12.21) can now be combined into a second–order one,

$$\begin{aligned} \partial_z (\partial_z + 2A_z) \chi + \left(\frac{4\mathcal{W}_5^2}{C_z} - \frac{C_{zz}}{C_z} \right) (\partial_z + 2A_z) \chi + m^2 \chi \\ + 2 [(2A_z + 5C_z) \partial_z + 4\mathcal{W}_5^2] \chi = 0 , \end{aligned} \quad (12.22)$$

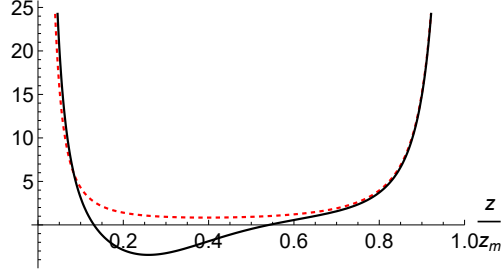


Figure 19: The potential V of eq. (12.28) (black, solid) with its approximation (2.29) (red,dashed) with $(\mu, \tilde{\mu}) = (\frac{2}{3}, 1)$, in units of $\frac{1}{z_0^2}$. z_m and z_0 are defined in eqs. (3.10) and (3.11).

that, using the results collected in Appendix A, can be cast in the form

$$m^2 \chi + \partial_z^2 \chi + \left[3(3A_z + 5C_z) + \frac{8\mathcal{W}_5^2}{C_z} \right] \partial_z \chi + 16\mathcal{W}_5^2 \left(1 + \frac{A_z}{C_z} \right) \chi = 0, \quad (12.23)$$

The redefinition

$$\chi = Y C_z e^{-\frac{1}{2}(3A+5C)}, \quad (12.24)$$

leads finally to the Schrödinger-like equation

$$m^2 Y = -\frac{d^2 Y}{dz^2} + V Y, \quad (12.25)$$

and letting

$$\alpha = \frac{4\mathcal{W}_5^2}{C_z} + \frac{3}{2}(3A_z + 5C_z), \quad (12.26)$$

the potential takes the form

$$V = -16\mathcal{W}_5^2 \left(1 + \frac{A_z}{C_z} \right) + \alpha^2 + \frac{d\alpha}{dz}, \quad (12.27)$$

or in detail

$$V = \frac{5e^{\sqrt{\frac{5}{2}}r}}{256 z_0^2 \sinh^5\left(\frac{r}{\rho}\right) \left[\sqrt{10} - 5 \coth\left(\frac{r}{\rho}\right) \right]^2} \left[-84\sqrt{10} \sinh\left(\frac{4r}{\rho}\right) + 128\sqrt{10} \sinh\left(\frac{2r}{\rho}\right) \right. \\ \left. - 928 \cosh\left(\frac{2r}{\rho}\right) + 267 \cosh\left(\frac{4r}{\rho}\right) + 1221 \right]. \quad (12.28)$$

Consequently, near the two ends V behaves as in eq. (1.15), with $\mu = \frac{2}{3}$ and $\tilde{\mu} = 1$. As a result, the allowed wavefunctions have the limiting behaviors

$$Y \sim C_1 \left(\frac{z}{z_m} \right)^{\frac{7}{6}} + C_2 \left(\frac{z_m}{z} \right)^{\frac{1}{6}} \quad \text{and} \quad Y \sim \left(1 - \frac{z}{z_m} \right)^{\frac{3}{2}}, \quad (12.29)$$

and self-adjoint boundary conditions are determined by the ratio $x = \frac{C_2}{C_1}$. In fact, eq. (12.25) can be cast in the formally positive form

$$m^2 Y = \mathcal{A}^\dagger \mathcal{A} Y + \mathcal{V} Y, \quad (12.30)$$

where now

$$\mathcal{A} = \frac{d}{dz} - \alpha, \quad \mathcal{A}^\dagger = -\frac{d}{dz} - \alpha, \quad (12.31)$$

and

$$\mathcal{V} = -16 \mathcal{W}_5^2 \left(1 + \frac{A_z}{C_z}\right) = \frac{16 \mathcal{W}_5^2}{\frac{\sqrt{10}}{2} \coth\left(\frac{r}{\rho}\right) - 1} > 0. \quad (12.32)$$

The $\mathcal{A}^\dagger \mathcal{A}$ portion of the potential has a zero mode,

$$Y \sim e^{\int \alpha dz}, \quad (12.33)$$

which is normalizable and behaves as

$$Y \sim \left(\frac{z}{z_m}\right)^{\frac{7}{6}} \quad (12.34)$$

close to the left end of the interval, where $\alpha \sim \frac{7}{6z}$. For this zero mode the absence of the $z^{-\frac{1}{6}}$ contribution indicates that

$$\frac{C_2}{C_1} = 0. \quad (12.35)$$

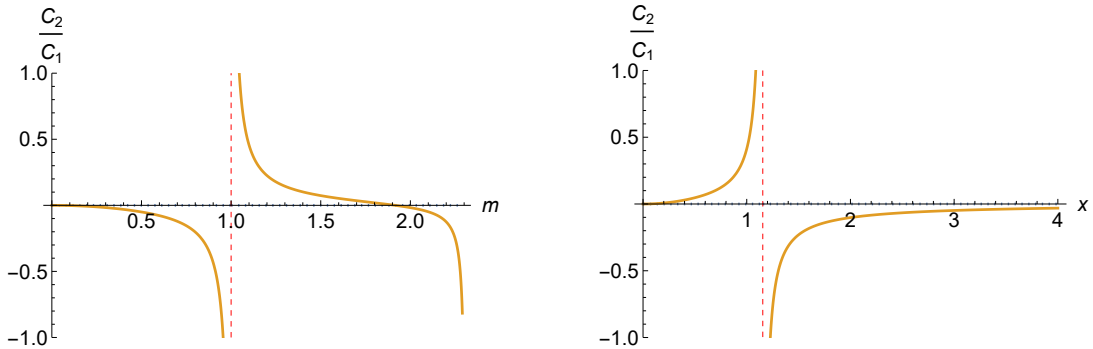


Figure 20: The left panel illustrates how the stable eigenvalues of the shifted hypergeometric potential $V_{1,-1}$ of eq. (2.39) with $\mu = \frac{2}{3}$, $\tilde{\mu} = 1$ depend on the boundary conditions. The right panel illustrates the corresponding tachyonic eigenvalues, with $m^2 = -x^2$, for the same values of μ and $\tilde{\mu}$.

The $\mathcal{A}^\dagger \mathcal{A}$ portion of the potential can be approximated by the shifted hypergeometric potential of eq. (2.39) with $\epsilon_1 = 1$ and $\epsilon_2 = -1$, whose zero mode in eq. (2.43) has the same boundary

condition (12.35). The corresponding shift,

$$\Delta V = - \left(\frac{4}{3} \right)^2 \frac{\pi^2}{z_m^2}, \quad (12.36)$$

can be read from eq. (2.39). By the general argument of [14], the \mathcal{AA}^\dagger potential has a stable spectrum if $C_2 = 0$, and a closer look at the eigenvalue equation shows that every other boundary condition gives rise to an unstable mode (see fig. 20). Therefore, in this sector there is at least one stable boundary condition for the full potential in eq. (12.30), where the would be massless mode becomes slightly massive, due to the positive contribution \mathcal{V} . As a result, a small range of stable boundary conditions exists for the complete potential, where stability holds for $\frac{C_2}{C_1} \geq 0$.

13 CONCLUSIONS AND OPEN ISSUES

In this paper we have explored in detail the bosonic modes that can emerge in a family of four-dimensional IIB Randall–Sundrum-like [32] non-supersymmetric vacua, and the resulting indications for vacuum stability. These backgrounds are supported by a flux of the self-dual five-form field strength that is homogeneous in spacetime and in an internal five-torus, and depend on a parameter ρ that determines the size of an internal interval and the corresponding scale of supersymmetry breaking⁶. The vacua thus obtained have a constant dilaton profile, and thus overcome the strong string-coupling problem that typically plagues broken supersymmetry, but the interval introduces some complications related to the choices of boundary conditions at its ends. The α' corrections can be bounded, away from the singularities [19] at the ends of the interval, within wide portions of the internal space. All these reasons, together with the well-known stability problems of string vacua in the absence of supersymmetry, motivated us to undertake the detailed analysis presented in the preceding sections, combining a number of different techniques.

Our analysis relied, all along, on the most general self-adjoint boundary conditions that are in principle available for the different fields, and thus, implicitly, on second-order actions for the internal profiles. For example, for a free complex scalar field ϕ in D dimensions the second-order action

$$\mathcal{S}_2 = \int d^D x \bar{\phi} \square \phi, \quad (13.1)$$

⁶The presence of an interval with singularities at its ends establishes a connection between this work and the ongoing activity devoted to “dynamical cobordism” [33]. The link will be made more precise in [28], where we shall compute tensions and charges at the ends of the interval.

allows the most general self-adjoint boundary conditions, while only a subset of them eliminate the boundary terms that emerge when varying the standard first-order action

$$\mathcal{S}_2 = - \int d^D x \partial^\mu \bar{\phi} \partial_\mu \phi . \quad (13.2)$$

In this fashion, we also ran across a peculiar property of gauge fields in the presence of an internal interval: additional modes localized on the boundary can emerge, in general, unless one confines the attention to gauge transformations that vanish there. We could thus classify the stable boundary conditions for the different sectors of the spectrum, and we could also tackle, in rather general terms, the possible instabilities of their Kaluza–Klein excitations. These represent an essentially insurmountable problem [13] for the non-supersymmetric AdS vacua of the ten-dimensional strings of [5, 6, 7], since the length scales of the internal sphere and of the AdS spacetimes are correlated by the Einstein equations. In our setting, which includes an internal torus, or more generally with a Ricci-flat internal manifold, there are boundary conditions compatible with a stable spectrum, although the available choices can depend on the background when mixings involving Kaluza–Klein modes occur. For the Kaluza–Klein excitations, the boundary conditions that yield massless modes with $\mathbf{k} = 0$ can bring along a finite number of tachyons, as we saw in Sections 10.2 and 11.2). However, this pathology can be eluded if the parameter ρ in eqs. (1.1) lies one or two orders of magnitude above the radius R of the internal torus. Equivalently, this condition sets on the scale of supersymmetry breaking

$$\mu_S = \frac{1}{\ell h^{\frac{1}{4}}} , \quad (13.3)$$

which we identified in [19], the upper bound

$$\mu_S (\Phi h)^{\frac{1}{4}} < \mathcal{O}(10^{-2}) . \quad (13.4)$$

Alternatively, one can select boundary conditions granting the absence of tachyons for all values of \mathbf{k} , but these typically eliminate the massless modes with $\mathbf{k} = 0$.

While the preceding results are clearly encouraging, our analysis is still incomplete, since we left out the Kaluza–Klein excitations of singlet scalars. These appear resilient to our approach, since they lead to a three-component Schrödinger system where the potential cannot be put in a symmetric form with the techniques used in the other cases. We are thus leaving to a future work a proper identification of the norm of these perturbations, and of its correspondence with the convenient Henneaux–Teitelboim action [21], together with a final statement on the stability region determined by this sector.

4D hel. $\times SO(5)$	4D $m = 0$ Content	10D origin	Equation
(0, 1)	1 dilaton	ϕ	(3.25)
(0, 1)	1 axion	a	(3.25)
($\pm 1, 0$)	1 real vector, 1 real scalar	$B_{\mu\nu}^{1,2}, B_{\mu r}^{1,2}$	(4.110)
2 ($\pm 1, 5$)	10 real vectors	$B_{\mu i}^{1,2}, B_{r i}^{1,2}$	(4.118)
2 (0, 15)	30 real scalars	$B_{ij}^{1,2}$	(4.134)
($\pm 1, 10$)	10 real vectors	$B_{\mu\nu ij}$	(6.19)
($\pm 2, 1$)	1 graviton	$h_{\mu\nu}$	(7.5)
(0, 14)	14 real scalars	h_{ij}	(8.4)
($\pm 1, 5$)	5 real vectors	$h_{\mu i}, B_{\mu\nu\rho i}$	(10.17)
(0, 5)	5 real scalars	$h_{ri}, B_{\mu\nu\rho i}, B_{ijkl}$	(11.14)
(0, 1)	1 real scalar \star	$b, b^i, b_{\mu}^i, h_{\mu\nu}, h_{rr}$	

Table 2: The maximum numbers of four-dimensional real massless bosonic modes that can arise from the bulk, for generic values of R , within the stability window of eq. (13.4). The scalar singlet in the last line, accompanied by the (\star) symbol, could be fine-tuned to zero mass. However, we do not have an analytic form for its wavefunction, which originates from the second-order equation (12.25). There are at most 26 vectors and 53 scalars, for a total of 107 massless bosonic degrees of freedom after including the graviton.

The first two columns in Table 2 collect the maximum numbers of massless modes found explicitly in the previous sections. In four dimensions, these correspond to a graviton, 26 real vectors and 53 real scalars, which are a large fraction of the modes that would emerge, from the type-IIB theory, after a toroidal compactification to four dimensions. These numbers are purely indicative, since we are focusing on the quadratic terms, and interactions and/or quantum corrections could lift in mass many of these modes. In addition, their number could be reduced by choices of boundary conditions dictated by symmetry requirements. For example, some of these modes lead to the flow [22], across the boundary, of charges that would be conserved in its absence. This was the case for the ten vector modes of section 6 arising from the four-form gauge field, and for the five vector modes from $h_{\mu i}$ of Section 11.1 arising from the metric field, and self-adjoint boundary conditions eliminating the flow can make all these modes massive. Table 3 collects the additional massless modes that could be present on the boundary.

Summarizing, the bosonic spectrum of the vacua of eqs. (1.1) confronted us with a number of technical difficulties, revealing some novelties and bringing along some surprises. The main novelty was the indication that *stable vacua may be attained in non-supersymmetric compactifications to four-dimensional Minkowski space*. The main surprises were the emergence of additional

4D hel. $\times SO(5)$	4D $m = 0$ Content	corresponding gauge parameters
$(\pm 1, 0)$	2 real vectors	$\Lambda_\mu^{1,2}$
$(0, 5)$	10 real scalars	$\Lambda_i^{1,2}$
$(0, 5)$	5 real scalars	$\Lambda_{\mu\nu i}$
$(\pm 1, 10)$	10 real vectors	$\Lambda_{\mu ij}$
$(0, 10)$	10 real scalars	Λ_{ijk}
$(\pm 1, 0)$	1 real vector	ξ_μ
$(\pm 0, 5)$	5 real scalars	ξ_i

Table 3: The maximum numbers of four-dimensional real massless bosonic modes that can arise from the boundary of the internal interval. There are in principle 56 degrees of freedom of this type, if one concentrates them on one of the two boundaries. The resulting vector equations are gauge invariant, in view of the discussion presented in [28].

moduli related to boundary conditions and of corresponding boundary modes, and two technical findings. In Section 4.3.2 massless modes of the type-IIB three-forms led to dynamical equations with three derivatives, and in Section 6.2 massless modes emerged, for all internal momenta, from the first-order equations of tensor modes. This last result is not pathological, since these modes were excitations of tachyonic ground states with different \mathbf{k} -dependent boundary conditions.

Identifying the effective four-dimensional theory resulting from this type of compactifications would be clearly an interesting further step, for which the present work can provide some indications. Local supersymmetry is a key requirement, and boundary terms will be needed to grant it, as we saw for bosonic gauge symmetries. The T^5 reduction to five dimensions of the type-IIB theory, which would yield the corresponding maximal supergravity, could provide some useful guidance [34]. Finally, the widespread activity devoted, over the years, to supersymmetric flux compactifications (for reviews, see [35]) rests on different geometrical setups and has typically addressed supersymmetric vacua. Generalizing the geometric approach to non-supersymmetric settings should elicit detailed links with the present work, and is likely to lead to further progress.

ACKNOWLEDGMENTS

We are grateful to C. Bachas, G. Dall’Agata, E. Dudas and A. Tomasiello for stimulating discussions. AS was supported in part by Scuola Normale, by INFN (IS GSS-Pi) and by the MIUR-PRIN contract 2017CC72MK_003. JM is grateful to Scuola Normale Superiore for the kind hospitality

while this work was in progress. AS is grateful to Université de Paris Cité and DESY–Hamburg for the kind hospitality, and to the Alexander von Humboldt foundation for the kind and generous support, while this work was in progress. Finally, we are both very grateful to Dr. M. Nardelli, who kindly helped us to retrieve some mathematical literature.

Appendix A CONVENTIONS AND PROPERTIES OF THE BACKGROUND

In this Appendix we collect some useful properties of the background described in Section 1. Our main conventions are the following. Capital Latin labels like M denote curved ten-dimensional indices, and Greek or Latin labels like (μ, r, i) denote their spacetime or internal portions. Moreover, when we need to distinguish the curved radial index r from the remaining nine-dimensional ones, we denote them collectively by m , while primed labels like a' denote the flat internal indices (r, a) and others like i' will denote the corresponding curved ones. We use a “mostly-plus” signature, defining the Riemann curvature tensor via ⁷

$$[\nabla_M, \nabla_N]V_P = R_{MNP}{}^Q V_Q, \quad (\text{A.1})$$

so that

$$R_{MNP}{}^Q = \partial_N \Gamma^Q{}_{MP} - \partial_M \Gamma^Q{}_{NP} + \Gamma^Q{}_{NR} \Gamma^R{}_{MP} - \Gamma^Q{}_{MR} \Gamma^R{}_{NP}. \quad (\text{A.2})$$

We also define the Ricci tensor as

$$R_{MP} = R_{MNP}{}^N. \quad (\text{A.3})$$

For backgrounds of the type

$$ds^2 = e^{2A(r)} dx^2 + e^{2B(r)} dr^2 + e^{2C(r)} dy^2, \quad (\text{A.4})$$

where the x^μ -coordinates, with $\mu = 0, \dots, 3$, refer to the four-dimensional spacetime, while the y^i -coordinates, with $i = 1, \dots, 5$ refer to the internal torus, the Christoffel symbols are

$$\begin{aligned} \Gamma^\mu{}_{\nu r} &= A' \delta^\mu{}_\nu, \quad \Gamma^i{}_{jr} = C' \delta^i{}_j, \\ \Gamma^r{}_{rr} &= B', \quad \Gamma^r{}_{\mu\nu} = -\eta_{\mu\nu} A' e^{2(A-B)}, \quad \Gamma^r{}_{ij} = -\delta_{ij} C' e^{2(C-B)}. \end{aligned} \quad (\text{A.5})$$

The components of the Ricci tensor read

$$\begin{aligned} R^{(0)}{}_{\mu\nu} &= -\eta_{\mu\nu} e^{2A} \left[3(A')^2 e^{-2B} + 5A' C' e^{-2B} + (A' e^{A-B})' e^{-A-B} \right] \\ &= -\eta_{\mu\nu} e^{2(A-B)} \left[A' (4A' + 5C' - B') + A'' \right], \\ R^{(0)}{}_{rr} &= -\left[4(A' e^{A-B})' e^{B-A} + 5(C' e^{C-B})' e^{B-C} \right] \\ &= -\left[4A'(A' - B') + 5C'(C' - B') + 4A'' + 5C'' \right], \\ R^{(0)}{}_{ij} &= -\delta_{ij} e^{2C} \left[4(C')^2 e^{-2B} + 4A' C' e^{-2B} + (C' e^{C-B})' e^{-B-C} \right] \\ &= -\delta_{ij} e^{2(C-B)} \left[C' (4A' + 5C' - B') + C'' \right], \end{aligned} \quad (\text{A.6})$$

⁷These conventions are as in [17] and [18].

and in the “harmonic” gauge, where

$$B = 4A + 5C, \quad (\text{A.7})$$

they reduce to

$$\begin{aligned} R^{(0)}_{\mu\nu} &= -\eta_{\mu\nu} e^{2(A-B)} A'', \\ R^{(0)}_{rr} &= -\left[4(A'e^{A-B})'e^{B-A} + 5(C'e^{C-B})'e^{B-C}\right] \\ &= [4A'(3A' + 5C') + 20C'(A' + C') - 4A'' - 5C''] , \\ R^{(0)}_{ij} &= -\delta_{ij} e^{2(C-B)} C'' . \end{aligned} \quad (\text{A.8})$$

Consequently the scalar curvature takes the form

$$R^{(0)} = e^{-2B} [-8A'' - 10C'' + 4A'(3A' + 5C') + 20C'(A' + C')] , \quad (\text{A.9})$$

and the components of the Einstein tensor read

$$\begin{aligned} G^{(0)}_{\mu\nu} &= \eta_{\mu\nu} e^{2(A-B)} [3A'' + 5C'' - 2(3(A')^2 + 10A'C' + 5(C')^2)] , \\ G^{(0)}_{rr} &= 2[3(A')^2 + 10A'C' + 5(C')^2] , \\ G^{(0)}_{ij} &= \delta_{ij} e^{2(C-B)} [4(A'' + C'') - 2(3(A')^2 + 10A'C' + 5(C')^2)] . \end{aligned} \quad (\text{A.10})$$

For the vacua of interest the Einstein equations

$$G^{(0)}_{MN} = \frac{1}{4!} \left(\mathcal{H}_5^{(0)2} \right)_{MN} = \frac{1}{24} g^{(0)PP'} g^{(0)QQ'} g^{(0)RR'} g^{(0)SS'} \mathcal{H}_5^{(0)MPQRS} \mathcal{H}_5^{(0)NP'Q'R'S'} \quad (\text{A.11})$$

reduce to

$$\begin{aligned} G^{(0)}_{\mu\nu} &= R^{(0)}_{\mu\nu} = -\frac{h^2}{4\rho^2} e^{2A-10C} \eta_{\mu\nu} , \quad G^{(0)}_{rr} = R^{(0)}_{rr} = -\frac{h^2}{4\rho^2} e^{2B-10C} , \\ G^{(0)}_{ij} &= R^{(0)}_{ij} = \frac{h^2}{4\rho^2} e^{-8C} \delta_{ij} . \end{aligned} \quad (\text{A.12})$$

In particular, the rr equation is the “Hamiltonian constraint”

$$3(A')^2 + 10A'C' + 5(C')^2 = -\frac{h^2}{8\rho^2} e^{8A} = -\frac{H^2}{2} e^{8A} , \quad (\text{A.13})$$

and making use of it turns the Einstein tensor into

$$\begin{aligned} \sqrt{-g} G^{(0)}_{\mu\nu} &= g_{\mu\nu} [3A'' + 5C'' + H^2 e^{8A}] , \quad \sqrt{-g} G^{(0)}_{rr} = -g_{rr} H^2 e^{8A} , \\ \sqrt{-g} G^{(0)}_{ij} &= g_{ij} [4(A'' + C'') + H^2 e^{8A}] . \end{aligned} \quad (\text{A.14})$$

Note that the Einstein equations (A.12) imply the useful relations

$$A'' = -C'' = \frac{h^2}{4\rho^2} e^{8A}. \quad (\text{A.15})$$

Eqs. (1.1) solve the background equations, up to the contact terms localized on the boundaries discussed in [28].

There are some useful identities for the tensor background of eqs. (1.1). The simplest ones are

$$\begin{aligned} \left(\mathcal{H}_5^{(0)}\right)_{\mu\nu}^2 &= -6 \frac{h^2}{\rho^2} e^{2A-10C} \eta_{\mu\nu}, & \left(\mathcal{H}_5^{(0)}\right)_{rr}^2 &= -6 \frac{h^2}{\rho^2} e^{8A}, \\ \left(\mathcal{H}_5^{(0)}\right)_{ij}^2 &= 6 \frac{h^2}{\rho^2} e^{-8C} \delta_{ij}, \end{aligned} \quad (\text{A.16})$$

but for studying perturbations one also needs to compute the components of

$$\left(\mathcal{H}_5^{(0)}\right)_{MN,PQ}^2 = g^{(0)R_1S_1} g^{(0)R_2S_2} g^{(0)R_3S_3} \mathcal{H}_5^{(0)}{}_{MNR_1R_2R_3} \mathcal{H}_5^{(0)}{}_{PQS_1S_2S_3} \quad (\text{A.17})$$

which are determined by symmetry and by the comparison with the preceding expressions, and read

$$\begin{aligned} \left(\mathcal{H}_5^{(0)}\right)_{\mu\rho,\nu\sigma}^2 &= -\frac{3}{2} \frac{h^2}{\rho^2} e^{4A-10C} (\eta_{\mu\nu} \eta_{\rho\sigma} - \eta_{\mu\sigma} \eta_{\nu\rho}), \\ \left(\mathcal{H}_5^{(0)}\right)_{\mu r,\nu r}^2 &= -\frac{3}{2} \frac{h^2}{\rho^2} e^{10A} \eta_{\mu\nu}, & \left(\mathcal{H}_5^{(0)}\right)_{\mu i,\nu j}^2 &= 0, \\ \left(\mathcal{H}_5^{(0)}\right)_{ik,jl}^2 &= \frac{3}{2} \frac{h^2}{\rho^2} e^{-6C} (\delta_{ij} \delta_{kl} - \delta_{il} \delta_{jk}), & \left(\mathcal{H}_5^{(0)}\right)_{ir,jr}^2 &= 0. \end{aligned} \quad (\text{A.18})$$

In terms of the z variable of eq. (3.9), the equations for the background become

$$\begin{aligned} 3(A_z)^2 + 10A_z C_z + 5(C_z)^2 &= -2\mathcal{W}_5^2, \\ A_{zz} &= 4\mathcal{W}_5^2 - (3A_z + 5C_z)A_z, \\ C_{zz} &= -4\mathcal{W}_5^2 - (3A_z + 5C_z)C_z, \end{aligned} \quad (\text{A.19})$$

where we have introduced the convenient combinations

$$\mathcal{W}_5 = \frac{h}{4\rho} e^{A-5C}, \quad \mathcal{K} = |\mathbf{k}| e^{A-C}, \quad (\text{A.20})$$

which are used repeatedly in the main body of the paper. Recalling also that

$$h = 2H\rho, \quad z_0 = (2H\rho^3)^{\frac{1}{2}} = \rho h^{\frac{1}{2}}, \quad (\text{A.21})$$

the limiting behavior of several useful quantities close to $z = 0$ is

$$\begin{aligned}\frac{z}{z_0} &= \frac{2}{3} \left(\frac{r}{\rho}\right)^{\frac{3}{2}} - \frac{1}{\sqrt{10}} \left(\frac{r}{\rho}\right)^{\frac{5}{2}} + \frac{19}{168} \left(\frac{r}{\rho}\right)^{\frac{7}{2}} + \mathcal{O}\left[\left(\frac{r}{\rho}\right)^{\frac{9}{2}}\right], \\ \frac{r}{\rho} &= \left(\frac{3z}{2z_0}\right)^{\frac{2}{3}} \left\{ 1 + \frac{1}{\sqrt{10}} \left(\frac{3z}{2z_0}\right)^{\frac{2}{3}} + \frac{47}{420} \left(\frac{3z}{2z_0}\right)^{\frac{4}{3}} + \mathcal{O}\left[\left(\frac{z}{z_0}\right)^2\right] \right\}.\end{aligned}\quad (\text{A.22})$$

Consequently

$$\begin{aligned}e^A &= \frac{1}{h^{\frac{1}{4}}} \left(\frac{2z_0}{3z}\right)^{\frac{1}{6}} \left\{ 1 - \frac{1}{4\sqrt{10}} \left(\frac{3z}{2z_0}\right)^{\frac{2}{3}} - \frac{121}{2240} \left(\frac{3z}{2z_0}\right)^{\frac{4}{3}} + \mathcal{O}\left[\left(\frac{z}{z_0}\right)^{\frac{7}{3}}\right] \right\} \\ e^C &= h^{\frac{1}{4}} \left(\frac{3z}{2z_0}\right)^{\frac{1}{6}} \left\{ 1 - \frac{1}{4\sqrt{10}} \left(\frac{3z}{2z_0}\right)^{\frac{2}{3}} + \frac{23}{2240} \left(\frac{3z}{2z_0}\right)^{\frac{4}{3}} + \mathcal{O}\left[\left(\frac{z}{z_0}\right)^{\frac{7}{3}}\right] \right\}, \\ A_z &= -\frac{1}{6z} - \frac{1}{6\sqrt{10}} \left(\frac{3}{2z_0}\right)^{\frac{2}{3}} z^{-\frac{1}{3}} - \frac{8}{105} \left(\frac{3}{2z_0}\right)^{\frac{4}{3}} z^{\frac{1}{3}} + \mathcal{O}\left[\left(\frac{z}{z_0}\right)\right], \\ C_z &= \frac{1}{6z} - \frac{1}{6\sqrt{10}} \left(\frac{3}{2z_0}\right)^{\frac{2}{3}} z^{-\frac{1}{3}} + \frac{1}{105} \left(\frac{3}{2z_0}\right)^{\frac{4}{3}} z^{\frac{1}{3}} + \mathcal{O}\left[\left(\frac{z}{z_0}\right)\right], \\ \mathcal{W}_5^2 &= \frac{1}{36z^2} + \frac{1}{18\sqrt{10}} \left(\frac{3}{2z_0}\right)^{\frac{2}{3}} z^{-\frac{4}{3}} + \frac{1}{2520} \left(\frac{3}{2z_0}\right)^{\frac{4}{3}} z^{-\frac{2}{3}} + \mathcal{O}\left[\left(\frac{z}{z_0}\right)^0\right].\end{aligned}\quad (\text{A.23})$$

The leading behavior of the metric, \mathcal{K}^2 and the five-form backgrounds is

$$\begin{aligned}ds^2 &\sim \frac{dx^2 + dz^2}{(3|H|z)^{\frac{1}{3}}} + (3|H|z)^{\frac{1}{3}} d\vec{y}^2, \quad \mathcal{K}^2 \sim \frac{|\mathbf{k}|^2}{(3|H|z)^{\frac{2}{3}}}, \\ \mathcal{H}_5 &\sim H \left\{ \frac{dx^0 \wedge \dots \wedge dx^3 \wedge dz}{[3|H|z]^{\frac{5}{3}}} + dy^1 \wedge \dots \wedge dy^5 \right\}.\end{aligned}\quad (\text{A.24})$$

The limiting behavior for large r , and thus for z close to the finite value z_m of eq. (3.10) corresponding to the right end of the interval, for the quantities entering the non-supersymmetric

backgrounds of eqs. (1.1), are

$$\begin{aligned}
\frac{z_m - z}{z_0} &\sim \frac{\sqrt{2}}{3} (\sqrt{10} + 2) e^{-\frac{r}{4\rho}(\sqrt{10}-2)} \left[1 - \frac{4\sqrt{10} - 11}{26} e^{-\frac{2r}{\rho}} \right], \\
e^{-\frac{r}{2\rho}} &\sim \left[\frac{\sqrt{5} - \sqrt{2}}{2} \left(\frac{z_m - z}{z_0} \right) \right]^{\frac{\sqrt{10}+2}{3}} \left\{ 1 + \frac{6 - \sqrt{10}}{26} \left[\frac{\sqrt{5} - \sqrt{2}}{2} \left(\frac{z_m - z}{z_0} \right) \right]^{\frac{4(\sqrt{10}+2)}{3}} \right\}, \\
e^{2A} &\sim \sqrt{\frac{2}{h}} \left[\frac{\sqrt{5} - \sqrt{2}}{2} \left(\frac{z_m - z}{z_0} \right) \right]^{\frac{\sqrt{10}+2}{3}} \left\{ 1 + \frac{19 - \sqrt{10}}{26} \left[\frac{\sqrt{5} - \sqrt{2}}{2} \left(\frac{z_m - z}{z_0} \right) \right]^{\frac{4(\sqrt{10}+2)}{3}} \right\}, \\
e^{2C} &\sim \sqrt{\frac{h}{2}} \left[\frac{\sqrt{5} - \sqrt{2}}{2} \left(\frac{z_m - z}{z_0} \right) \right]^{-\frac{\sqrt{10}}{5}} \left\{ 1 + \frac{-105 + 11\sqrt{10}}{130} \left[\frac{\sqrt{5} - \sqrt{2}}{2} \left(\frac{z_m - z}{z_0} \right) \right]^{\frac{4(\sqrt{10}+2)}{3}} \right\}, \\
A_z &\sim -\frac{1}{6} \frac{\sqrt{10} + 2}{z_m - z}, \quad C_z \sim \frac{1}{\sqrt{10}} \frac{1}{z_m - z}, \\
\mathcal{W}_5 &\sim \frac{\sqrt{2}}{2z_0} \left[\frac{\sqrt{5} - \sqrt{2}}{2} \left(\frac{z_m - z}{z_0} \right) \right]^{\frac{2\sqrt{10}+1}{3}}, \quad \mathcal{K}^2 \sim \frac{2(|\mathbf{k}| \rho)^2}{z_0^2} \left[\frac{\sqrt{5} - \sqrt{2}}{2} \left(\frac{z_m - z}{z_0} \right) \right]^{\frac{2\sqrt{10}+16}{15}}.
\end{aligned} \tag{A.25}$$

Appendix B INTERMEDIATE RESULTS FOR TENSOR PERTURBATIONS

In this Appendix we collect some intermediate results that are needed to obtain the tensor equations of Section 5. As explained there, we parametrize the independent components of the tensor gauge field perturbations δB_{MNPQ} according to eq. (5.4). The corresponding field strengths then take the form

$$\begin{aligned}
\delta H_{\mu\nu\rho\sigma} &= \epsilon_{\mu\nu\rho\sigma} (\partial_r b - \partial_\tau b^\tau), \quad \delta H_{\mu\nu\rho\sigma i} = \epsilon_{\mu\nu\rho\sigma} (\partial_i b - \partial_\tau b^\tau{}_i), \\
\delta H_{\mu\nu\rho i} &= \epsilon_{\mu\nu\rho\sigma} \left(\partial_i b^\sigma - \partial_r b^\sigma{}_i - \frac{1}{2} \epsilon^{\alpha\beta\gamma\sigma} \partial_\alpha b_{\beta\gamma i} \right), \\
\delta H_{\mu\nu\rho ij} &= -\epsilon_{\mu\nu\rho\sigma} \left(\partial_{[i} b^\sigma{}_{j]} + \frac{1}{2} \epsilon^{\alpha\beta\gamma\sigma} \partial_\alpha b_{\beta\gamma ij} \right), \\
\delta H_{\mu\nu r ij} &= \partial_{[\mu} b_{\nu] ij}^{(1)} + \partial_r b_{\mu\nu ij} - \partial_{[i} b_{\mu\nu] j}, \\
\delta H_{\mu\nu ijk} &= \frac{1}{2} \epsilon_{ijklm} \left(\partial_{[\mu} b^{(2)}{}_{\nu]}{}^{lm} + \frac{1}{2} \epsilon^{pqrlm} \partial_p b_{\mu\nu qr} \right), \\
\delta H_{\mu r ijk} &= \frac{1}{2} \epsilon_{ijklm} \left(\partial_\mu b^{lm} - \partial_r b^{(2)}{}_\mu{}^{lm} + \frac{1}{2} \epsilon^{pqslm} \partial_p b^{(1)}{}_{\mu qs} \right), \\
\delta H_{\mu i jkl} &= \epsilon_{ijklm} \left(\partial_\mu b^m - \partial_n b^{(2)}{}_\mu{}^{mn} \right), \quad \delta H_{r i jkl} = \epsilon_{ijklm} (\partial_r b^m - \partial_n b^{mn}), \\
\delta H_{i jklm} &= \epsilon_{ijklm} \partial_p b^p.
\end{aligned} \tag{B.1}$$

Starting from the self-duality conditions

$$H_{M_1 \dots M_5} = \frac{\sqrt{-g}}{5!} \epsilon_{M_1 \dots M_{10}} g^{M_6 N_6} \dots g^{M_{10} N_{10}} H_{N_6 \dots N_{10}} , \quad (\text{B.2})$$

and expanding them to first order in the tensor and gravity perturbations gives

$$\begin{aligned} \delta H_{M_1 \dots M_5} &= \frac{\sqrt{-g^{(0)}}}{5!} \epsilon_{M_1 \dots M_{10}} g^{(0)M_6 N_6} \dots g^{(0)M_{10} N_{10}} \delta H_{N_6 \dots N_{10}} + \frac{1}{2} h^M{}_M H_{M_1 \dots M_5}^{(0)} \\ &- \frac{\sqrt{-g^{(0)}}}{4!} \epsilon_{M_1 \dots M_6}{}^{i_7 \dots i_{10}} h^{M_6 i_6} e^{-8C} H_{i_6 i_7 \dots i_{10}}^{(0)} \\ &- \frac{\sqrt{-g^{(0)}}}{4!} \epsilon_{M_1 \dots M_6}{}^{\mu_7 \dots \mu_{10}} h^{M_6 r} e^{-8A} H_{r \mu_7 \dots \mu_{10}}^{(0)} \\ &- \frac{\sqrt{-g^{(0)}}}{3!} \epsilon_{M_1 \dots M_6}{}^{\mu_7 \dots \mu_{9r}} h^{M_6 \mu_6} e^{-6A-2B} H_{\mu_6 \mu_7 \dots \mu_{9r}}^{(0)} , \end{aligned} \quad (\text{B.3})$$

where the ϵ tensors are flat, so that their indices are raised and lowered with the flat metric, $\epsilon_{0\dots 9} = 1$, and the indices of the metric perturbations h_{MN} are raised with the background metric.

One can now specialize the left-hand side to the independent cases, which leads to the five groups of independent tensor equations

$$\begin{aligned} \delta H_{\mu_1 \dots \mu_4 r} &= \frac{e^{2B-10C}}{5!} \epsilon_{\mu_1 \dots \mu_4}{}^{i_6 \dots i_{10}} \delta H_{i_6 \dots i_{10}} \\ &+ \frac{h e^{8A}}{4\rho} \left(e^{-2A} h^\mu{}_\mu + e^{-2B} h_{rr} - e^{-2C} h^k{}_k \right) \epsilon_{\mu_1 \dots \mu_4} , \\ \delta H_{\mu_1 \mu_2 \mu_3 r i} &= \frac{e^{2B-2A-8C}}{4!} \epsilon_{\mu_1 \dots \mu_3}{}^{\mu_4} \epsilon_i{}^{j_7 \dots j_{10}} \delta H_{\mu_4 j_7 \dots j_{10}} \\ &- \frac{h}{2\rho} e^{2B-2A-10C} \epsilon_{\mu_1 \dots \mu_3}{}^{\mu_4} h_{\mu_4 i} , \\ \delta H_{\mu_1 \mu_2 r i j} &= \frac{e^{4(A+C)}}{2! 3!} \epsilon_{\mu_1 \mu_2}{}^{\mu_3 \mu_4} \epsilon_{ij}{}^{klm} \delta H_{\mu_3 \mu_4 klm} , \\ \delta H_{\mu_1 r i j k} &= \frac{e^{2A+6C}}{2! 3!} \epsilon_{\mu_1}{}^{\mu_2 \mu_3 \mu_4} \epsilon_{ijk}{}^{lm} \delta H_{\mu_2 \mu_3 \mu_4 lm} , \\ \delta H_{r i j k l} &= \frac{e^{8C}}{4!} \epsilon^{\mu_1 \dots \mu_4} \epsilon_{ijkl}{}^m \delta H_{\mu_1 \dots \mu_4 m} + \frac{h}{2\rho} \epsilon_{ijkl}{}^m h_{mr} e^{-2C} , \end{aligned} \quad (\text{B.4})$$

where now all indices are raised and lowered with the flat metric. Making use of eqs. (B.1) leads finally to eqs. (5.5).

With the gauge choice

$$B_{rMNP} = 0 , \quad (\text{B.5})$$

which translates into the conditions

$$b_\mu = 0 , \quad b_{\mu\nu i} = 0 , \quad b_{\mu ij}^{(1)} = 0 , \quad b_{ij} = 0 , \quad (\text{B.6})$$

the field strengths finally reduce to

$$\begin{aligned}
\delta \mathcal{H}_{\mu\nu\rho\sigma} &= \epsilon_{\mu\nu\rho\sigma} \partial_r b , & \delta \mathcal{H}_{\mu\nu\rho\sigma i} &= \epsilon_{\mu\nu\rho\sigma} (\partial_i b - \partial_\tau b^\tau{}_i) , \\
\delta \mathcal{H}_{\mu\nu\rho i} &= -\epsilon_{\mu\nu\rho\sigma} \partial_r b^\sigma{}_i , & \delta \mathcal{H}_{\mu\nu\rho ij} &= -\epsilon_{\mu\nu\rho\sigma} \left(\partial_{[i} b^\sigma{}_{j]} + \frac{1}{2} \epsilon^{\alpha\beta\gamma\sigma} \partial_\alpha b_{\beta\gamma ij} \right) , \\
\delta \mathcal{H}_{\mu\nu r ij} &= \partial_r b_{\mu\nu ij} , & \delta \mathcal{H}_{\mu\nu ij k} &= \frac{1}{2} \epsilon_{ijklm} \left(\partial_{[\mu} b^{(2)}{}_{\nu]}{}^{lm} + \frac{1}{2} \epsilon^{pqrlm} \partial_p b_{\mu\nu qr} \right) , \\
\delta \mathcal{H}_{\mu r ij k} &= -\frac{1}{2} \epsilon_{ijklm} \partial_r b^{(2)}{}_{\mu}{}^{lm} , & \delta \mathcal{H}_{\mu ij k l} &= \epsilon_{ijklm} \left(\partial_\mu b^m - \partial_n b^{(2)}{}_{\mu}{}^{mn} \right) , \\
\delta \mathcal{H}_{r ij k l} &= \epsilon_{ijklm} \partial_r b^m , & \delta \mathcal{H}_{ijklm} &= \epsilon_{ijklm} \partial_p b^p .
\end{aligned} \tag{B.7}$$

Appendix C INTERMEDIATE RESULTS FOR THE EINSTEIN EQUATIONS

In this Appendix we collect some technical results needed to obtain the perturbed Einstein equations discussed in Section 5 starting from

$$R_{MN} = \frac{1}{24} (\mathcal{H}_5^2)_{MN} . \tag{C.1}$$

C.1 INTERMEDIATE RESULTS FOR THE RICCI CURVATURE

The perturbed Christoffel symbols read

$$\delta \Gamma^P{}_{MN} = \frac{1}{2} (\nabla_M h^P{}_N + \nabla_N h^P{}_M - \nabla^P h_{MN}) , \tag{C.2}$$

where the gradient ∇ refers to the background, and from the Palatini identity

$$\delta R_{MNP}{}^Q = \nabla_N \delta \Gamma^Q{}_{MP} - \nabla_M \delta \Gamma^Q{}_{NP} \tag{C.3}$$

one can deduce the perturbed Ricci curvature

$$-2 \delta R_{NR} = \square_{10} h_{NR} + \nabla_N \nabla_R h_S{}^S - \nabla^P (\nabla_N h_{PR} + \nabla_R h_{PN}) . \tag{C.4}$$

Using the results collected in Appendix A, one can compute the divergences of gradients that are needed in eq. (C.4). Their general expression is

$$\nabla^P \nabla_N h_{PR} = g^{PQ} (\partial_Q \nabla_N h_{PR} - \Gamma^S{}_{QN} \nabla_S h_{PR} - \Gamma^S{}_{QP} \nabla_N h_{SR} - \Gamma^S{}_{QR} \nabla_N h_{PS}) , \tag{C.5}$$

where the metric g and the connection Γ refer to the background. Some simplifications occur since the background satisfies the harmonic gauge conditions (A.7), which are equivalent to

$$g^{PQ} \Gamma^S{}_{PQ} = 0 , \tag{C.6}$$

and one is left with

$$\nabla^P \nabla_N h_{PR} = g^{PQ} (\partial_Q \nabla_N h_{PR} - \Gamma^S_{QN} \nabla_S h_{PR} - \Gamma^S_{QR} \nabla_N h_{PS}) . \quad (\text{C.7})$$

C.2 THE PERTURBED ENERGY–MOMENTUM TENSOR

The right–hand side of the perturbed Einstein equations involves the variation of $(\mathcal{H}_5^2)_{MN}$ about the background values, which reads

$$\delta [(\mathcal{H}_5^2)_{MN}] = \delta \mathcal{H}_{5(M} \cdot \mathcal{H}_{5N)}^{(0)} - 4 \mathcal{H}_{5MK}^{(0)} \cdot \mathcal{H}_{5NL}^{(0)} h^{KL} , \quad (\text{C.8})$$

where h_{KL} denotes, as before, the metric perturbation, and where indices are raised and lowered with the background metric. Taking into account the background in eqs. (1.1) and eqs. (1.10), one thus finds

$$\begin{aligned} \delta \mathcal{H}_{5(\mu} \cdot \mathcal{H}_{5\nu)}^{(0)} &= \frac{h}{2\rho} e^{2(A-B)} \delta \mathcal{H}_5^{\rho\sigma\tau}{}_{r(\mu} \epsilon_{\nu)\rho\sigma\tau} , \\ \delta \mathcal{H}_{5(\mu} \cdot \mathcal{H}_{5r)}^{(0)} &= 0 , \\ \delta \mathcal{H}_{5(\mu} \cdot \mathcal{H}_{5i)}^{(0)} &= \frac{h}{\rho} e^{-8C} \epsilon_{ik_1\dots k_4} \delta \mathcal{H}_{5\mu}{}^{k_1\dots k_4} - 6 \frac{h^2}{\rho^2} e^{-10C} h_{\mu i} , \\ \delta \mathcal{H}_{5r} \cdot \mathcal{H}_{5r}^{(0)} &= \frac{h}{2\rho} \delta \mathcal{H}_5^{\mu\rho\sigma\tau}{}_{r} \epsilon_{\mu\rho\sigma\tau} , \\ \delta \mathcal{H}_{5(r} \cdot \mathcal{H}_{5i)}^{(0)} &= 6 \frac{h^2}{\rho^2} e^{-10C} h_{ri} + \frac{h}{\rho} \epsilon_{\beta_1\dots\beta_4} \delta \mathcal{H}_{5i}{}^{\beta_1\dots\beta_4} , \\ \delta \mathcal{H}_{5(i} \cdot \mathcal{H}_{5j)}^{(0)} &= \frac{h}{2\rho} e^{-8C} \delta \mathcal{H}_5^{klmn}{}_{(i} \epsilon_{j)klmn} , \end{aligned} \quad (\text{C.9})$$

where indices are now raised with the flat metrics $\eta^{\mu\nu}$ and δ^{ij} . Finally, $\delta \mathcal{H}_5$ must be expressed in terms of the components of the four–form gauge field listed in eqs. (5.4), which lead to eqs. (B.7) after gauge fixing.

The final form of the perturbed energy–momentum tensor,

$$T^{(1)}_{MN} = \frac{1}{24} \left(\delta \mathcal{H}_{5(M} \cdot \mathcal{H}_{5N)}^{(0)} - 4 \mathcal{H}_{5MK}^{(0)} \cdot \mathcal{H}_{5NL}^{(0)} h^{KL} \right) \quad (\text{C.10})$$

is

$$\begin{aligned}
T^{(1)}_{\mu\nu} &= -\frac{h}{4\rho} e^{2(A-B)} \partial_r b \eta_{\mu\nu} + \frac{h^2}{4\rho^2} [e^{-10C} (\eta_{\mu\nu} h_{\rho}{}^{\rho} - h_{\mu\nu}) + e^{10A-4B} \eta_{\mu\nu} h_{rr}] , \\
T^{(1)}_{\mu r} &= -\frac{h^2}{4\rho^2} e^{8A-2B} h_{\mu r} , \\
T^{(1)}_{\mu i} &= e^{-8C} \left[\frac{h}{\rho} (\partial_{\mu} b_i - \partial_n b^{(2)}{}_{\mu i}{}^n) - \frac{h^2}{4\rho^2} e^{-2C} h_{\mu i} \right] , \\
T^{(1)}_{rr} &= -\frac{h}{\rho} \partial_r b + \frac{h^2}{4\rho^2} e^{6A} h_{\rho}{}^{\rho} , \\
T^{(1)}_{ri} &= \frac{h^2}{4\rho^2} e^{-10C} h_{ri} - \frac{h}{\rho} (\partial_i b - \partial_{\mu} b^{\mu}{}_i) , \\
T^{(1)}_{ij} &= \frac{h}{\rho} \delta_{ij} e^{-8C} \partial_p b^p - \frac{h^2}{4\rho^2} e^{-10C} (\delta_{ij} h_k{}^k - h_{ij}) .
\end{aligned} \tag{C.11}$$

and the equations that we actually write are

$$-2\delta R_{MN} = -2T^{(1)}{}_{MN} . \tag{C.12}$$

Appendix D THE NON-SINGLET VECTOR MODES AS $\mathbf{k} \rightarrow 0$

In this Appendix we discuss the possible self-adjoint boundary conditions for the non-singlet vector modes at the left end of the internal interval, focusing on the \mathbf{k} -independent part of the operator $\widetilde{\mathcal{M}}$ of eq. (10.34), or if you will on its small- \mathbf{k} limit, which is diagonal. The potential in the (1,1) entry,

$$V_1(r) = \frac{1}{320 z_0^2} \frac{e^{\sqrt{\frac{5}{2}} \frac{r}{\rho}}}{\sinh^3\left(\frac{r}{\rho}\right)} \left[-14\sqrt{10} \sinh\left(\frac{2r}{\rho}\right) + 41 \cosh\left(\frac{2r}{\rho}\right) + 99 \right] \tag{D.1}$$

only emerges for $\mathbf{k} \neq 0$, while the potential in the (2,2) entry is the one already discussed in Section 10.1 for $\mathbf{k} = 0$.

One can rely once more on the correspondence with the hypergeometric potentials of eq. (2.29) to identify stability regions in the small- \mathbf{k} limit. To this end, one needs to examine the limiting behavior of $\widetilde{\mathcal{M}}$ as z approaches the two ends of the interval. From eq. (10.35) and from Appendix A, one can see that, as $z \rightarrow 0$,

$$\widetilde{\mathcal{M}} \sim \left(-\partial_z^2 + \frac{7}{36 z^2} \right) \mathbf{1} , \tag{D.2}$$

which is of the form (2.12) with $\mu_1 = \mu_2 = \frac{2}{3}$. In a similar fashion, as $z \rightarrow z_m$, $\widetilde{\mathcal{M}}$ is of the form (2.13), with $\tilde{\mu}_1 = 0.09$ and $\tilde{\mu}_2 = 1.1$. The resulting setting is the first case discussed in

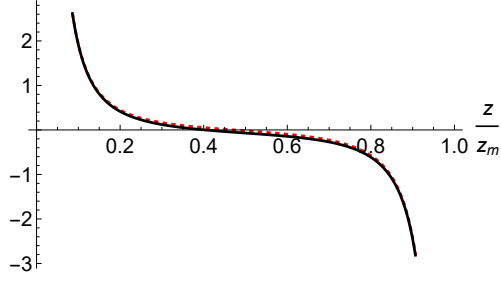


Figure 21: The $\mathbf{k} = 0$ portion of the Schrödinger potential for W_1 in eq. (D.1) (black, solid) and its approximation (2.29) (red, dashed) with $(\mu, \tilde{\mu}) = (\frac{2}{3}, 0.09)$, in units of $\frac{1}{z_0^2}$. z_m and z_0 are defined in eqs. (3.10) and (3.11).

Section 2.4, and the self-adjoint boundary conditions given independently at the two ends thus depend on six real parameters.

The dominant terms in eq. (10.34) identify a two-dimensional vector space of normalizable zero modes spanned by

$$Z^{(1)} = \begin{pmatrix} e^{\frac{A-C}{2}} \\ 0 \end{pmatrix}, \quad Z^{(2)} = \begin{pmatrix} 0 \\ e^{\frac{5A+3C}{2}} \end{pmatrix}. \quad (\text{D.3})$$

For the first zero mode

$$\frac{C_{11}}{C_{12}} = -0.16, \quad \frac{C_{13}}{C_{14}} = 0.2, \quad (\text{D.4})$$

while for the second zero mode

$$\frac{C_{21}}{C_{22}} = -0.41. \quad (\text{D.5})$$

As in the simpler one-component systems that we have analyzed, one can approach the $\mathbf{k} = 0$ portion of $\tilde{\mathcal{M}}$ by a pair of shifted hypergeometric potentials, with shifts

$$\Delta V_1 = \frac{\pi^2}{z_m^2} (0.1)^2, \quad \Delta V_2 = -\frac{\pi^2}{z_m^2} (0.71)^2, \quad (\text{D.6})$$

relying once more on the one-component formalism of Section 2. The two potentials V_1 and V_2 are displayed in figs. 21 and 15, together with their hypergeometric approximations. Letting, in the notation of eq. (2.71)

$$\frac{C_{11}}{C_{12}} = \cot\left(\frac{\alpha_1}{2}\right), \quad \frac{C_{13}}{C_{14}} = \cot\left(\frac{\tilde{\alpha}_1}{2}\right), \quad \frac{C_{22}}{C_{21}} = \tan\left(\frac{\alpha_2}{2}\right). \quad (\text{D.7})$$

one can thus identify the stability regions in the $(\alpha_1, \tilde{\alpha}_1)$ plane displayed in fig. 22, and the results of Section 10.1 translate, for α_2 , into the stability interval

$$-2.42 < \tan\left(\frac{\alpha_2}{2}\right) < 0. \quad (\text{D.8})$$

As we have seen, the matrix $\widetilde{\mathcal{M}}$ in eq. (10.34) becomes diagonal as $\mathbf{k} \rightarrow 0$, and we could thus identify two zero modes. $Z^{(2)}$ is indeed the expected zero mode that we found in Section 10.2, while the presence of $Z^{(1)}$ is somewhat surprising, since it is also normalizable. The point is that the $\mathbf{k} \rightarrow 0$ limit is singular for the original theory, which can be seen from the need to perform the redefinition of eq. (10.32). Consequently, in this limit $Z^{(1)}$ would correspond to a field W_1 of vanishing norm with respect to W_4 , while the original operator in eq. (10.30) is definitely not Hermitian for $\mathbf{k} = 0$.

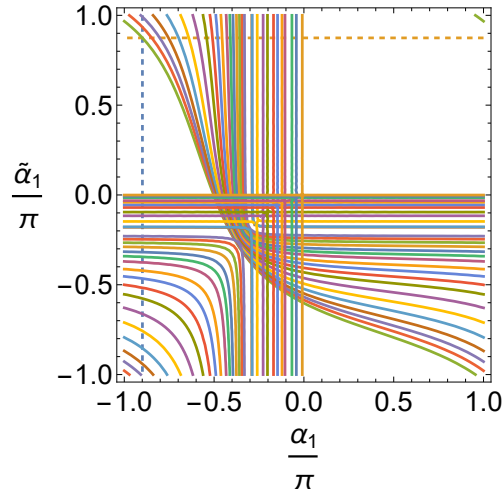


Figure 22: The point $(\alpha_1, \tilde{\alpha}_1) = \pi(-0.9, 0.87)$ identifies the special boundary conditions corresponding to the zero mode $Z^{(1)}$. The shaded regions identify the boundary conditions leading to instabilities for the \mathbf{k} -independent portion of $\widetilde{\mathcal{M}}$.

When the \mathbf{k} -dependent terms in $\widetilde{\mathcal{M}}$ are taken into account, their mean value computed with the vectors in eq. (D.3) diverges. As a result, the dominant terms that we have analyzed are suitable to identify self-adjoint boundary conditions but are not a good starting point for perturbation theory. For this reason our variational tests relied on the \mathbf{k} -dependent corrections described in Section 10.2.

Appendix E SELF-ADJOINT VARIATIONAL TESTS

This Appendix provides some details on the variational estimates of the lowest m^2 eigenvalues described in Sections 10.2 and 11.2.

For our estimates of Section 10.2, we resorted on a pair of test functions $Z_1(z)$ and $Z_2(z)$ that comply to the limiting behavior at the two ends, taking into account the ξ -dependent corrections

that we identified, which grant delicate compensations between singular contributions from kinetic and potential terms:

$$\begin{aligned}
Z_1 &= \left\{ C_{11} \left(\frac{z}{z_m} \right)^{\frac{7}{6}} + C_{12} \left(\frac{z}{z_m} \right)^{-\frac{1}{6}} + \frac{\xi}{2} \left[C_{21} \left(\frac{z}{z_m} \right)^{\frac{11}{6}} - 3 C_{22} \left(\frac{z}{z_m} \right)^{\frac{1}{2}} \right] \right\} \exp \left[-\frac{az^4}{z_m^4 - z^4} \right] \\
&\quad + \gamma_1 \left(\frac{z_m - z}{z_m} \right)^{\frac{1}{2} + \tilde{\mu}_1} \exp \left[-\frac{a(z_m - z)^4}{z_m^4 - (z_m - z)^4} \right], \\
Z_2 &= \left\{ C_{21} \left(\frac{z}{z_m} \right)^{\frac{7}{6}} + C_{22} \left(\frac{z}{z_m} \right)^{-\frac{1}{6}} + \frac{\xi}{2} \left[C_{11} \left(\frac{z}{z_m} \right)^{\frac{11}{6}} - 3 C_{12} \left(\frac{z}{z_m} \right)^{\frac{1}{2}} \right] \right\} \exp \left[-\frac{az^4}{z_m^4 - z^4} \right] \\
&\quad + \gamma_2 \left(\frac{z_m - z}{z_m} \right)^{\frac{1}{2} + \tilde{\mu}_2} \exp \left[-\frac{a(z_m - z)^4}{z_m^4 - (z_m - z)^4} \right] \tag{E.1}
\end{aligned}$$

The exponential factors separate the contributions from the two ends, which is instrumental to grant the needed cancellations. The self-adjoint boundary conditions that we have explored are parametrized, in general, by an $SL(2, R)$ matrix and a phase β , so that

$$\begin{aligned}
C_{22} &= e^{i\beta} [(\cosh \rho \cos \theta_1 + \sinh \rho \cos \theta_2) C_{11} + (-\cosh \rho \sin \theta_1 + \sinh \rho \sin \theta_2) C_{12}] , \\
C_{21} &= e^{i\beta} [(\cosh \rho \sin \theta_1 + \sinh \rho \sin \theta_2) C_{11} + (\cosh \rho \cos \theta_1 - \sinh \rho \cos \theta_2) C_{12}] . \tag{E.2}
\end{aligned}$$

The variational parameters for this case were thus a , γ_1 , γ_2 , C_{11} and C_{12} . For simplicity, we have set $\beta = 0$ in all our tests.

At the right end of the interval the Hamiltonian $\widetilde{\mathcal{M}}$ approaches a diagonal $Q^\dagger Q$ form, which is granted to be positive for the asymptotic behaviors compatible with the L^2 conditions, which are annihilated by Q , so that the contributions associated to $\gamma_{1,2}$ are not expected to lower significantly our estimates for the minimal m^2 eigenvalue. Therefore, we concentrated our efforts on test functions with $\gamma_1 = 0$ and $\gamma_2 = 0$. Furthermore, different choices for a of order one gave similar results. In this fashion, C_{11} and C_{12} were our actual variational parameters, with resulting estimates of the form

$$m^2 = \frac{c^\dagger N c}{c^\dagger D c}, \tag{E.3}$$

where c is a two-component vector collecting them and N and D two real symmetric matrices depending on ξ and on the $SL(2, R)$ parameters, which we built numerically. In this setup, the best estimate is determined by the lowest eigenvalue of $D^{-1}N$.

The main indications that we collected from our numerical tests are the following:

- there are self-adjoint boundary conditions where no tachyons emerge for all values of \mathbf{k} . An

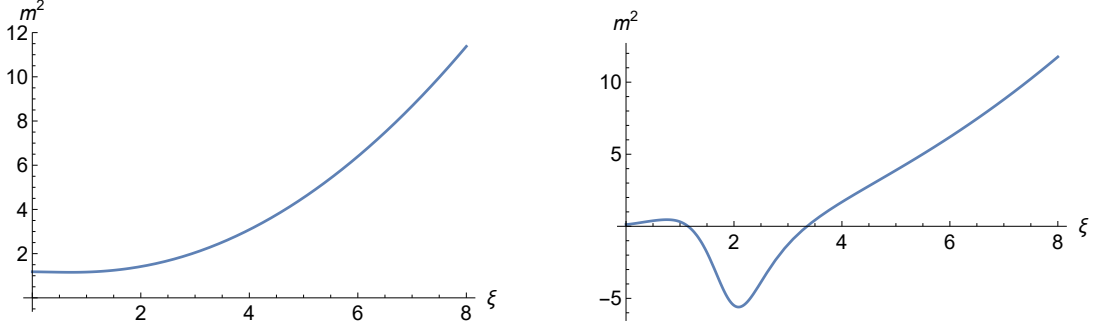


Figure 23: Estimates for the lowest $m^2(\xi)$ (in units of $\frac{1}{z_0^2}$) for non-singlet vector modes obtained for $(\theta_1, \theta_2, \rho) = (-\frac{\pi}{2}, \frac{\pi}{2}, 2)$ (left panel), and for $(\theta_1, \theta_2, \rho) = (0, 0, 0)$ (right panel).

example of this type has $(\rho, \theta_1, \theta_2, \beta) = (2, -\frac{\pi}{2}, \frac{\pi}{2}, 0)$, and a plot of the corresponding m^2 as a function of ξ is shown in the left panel of fig. 23;

- there are other boundary conditions where tachyonic modes are not present only for sufficiently small values of R , as explained in Section 10.2. An example of this type has $(\rho, \theta_1, \theta_2, \beta) = (0, 0, 0, 0)$, and a plot of the corresponding m^2 as a function of ξ is shown in the right panel of fig. 23.

The variational tests for the scalar modes of Section 11.2 proceeded along similar lines, but relied on the slightly more complicated functions

$$\begin{aligned}
\tilde{\Psi}_1 &= \left\{ \frac{C_{11}}{\sqrt{2}} \left(\frac{z}{z_m} \right)^{\frac{7}{6}} + \frac{C_{12}}{\sqrt{2}} \left(\frac{z}{z_m} \right)^{-\frac{1}{6}} + 2\xi \left[-\frac{3}{5} C_{21} \left(\frac{z}{z_m} \right)^{\frac{3}{2}} + C_{22} \left(\frac{z}{z_m} \right)^{\frac{5}{6}} \right] \right. \\
&+ \left. \frac{3}{4\sqrt{2}} \xi^2 \left[\frac{19}{40} C_{11} \left(\frac{z}{z_m} \right)^{\frac{5}{2}} - 3 C_{12} \left(\frac{z}{z_m} \right)^{\frac{7}{6}} \log \left(\frac{z}{z_m} \right) \right] \right\} \exp \left[-\frac{a z^4}{z_m^4 - z^4} \right] \\
&+ \gamma_1 \left(1 - \frac{z}{z_m} \right)^{2.77} \exp \left[-\frac{a (z_m - z)^4}{z_m^4 - (z_m - z)^4} \right], \\
\tilde{\Psi}_2 &= \left\{ C_{21} \left(\frac{z}{z_m} \right)^{\frac{5}{6}} + C_{22} \left(\frac{z}{z_m} \right)^{\frac{1}{6}} + \sqrt{2} \xi \left[-\frac{1}{5} C_{11} \left(\frac{z}{z_m} \right)^{\frac{11}{6}} + 3 C_{12} \left(\frac{z}{z_m} \right)^{\frac{1}{2}} \right] \right. \\
&+ \left. \frac{1}{8} \xi^2 \left[\frac{27}{5} C_{21} \left(\frac{z}{z_m} \right)^{\frac{13}{6}} - C_{22} \left(\frac{z}{z_m} \right)^{\frac{3}{2}} \right] \right\} \exp \left[-\frac{a z^4}{z_m^4 - z^4} \right] \\
&+ \gamma_2 \left(1 - \frac{z}{z_m} \right)^{\frac{1}{2}} \exp \left[-\frac{a (z_m - z)^4}{z_m^4 - (z_m - z)^4} \right]. \tag{E.4}
\end{aligned}$$

We were forced to proceed to second order in ξ to eliminate all singular contributions to the mean value of the Hamiltonian. As before, and for similar reasons, we worked with $\gamma_1 = \gamma_2 = 0$, exploring values of a of order one.

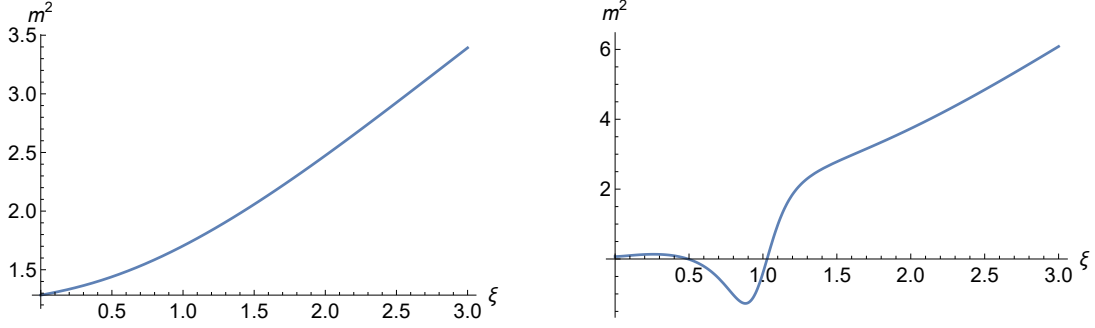


Figure 24: Estimates for the lowest $m^2(\xi)$ (in units of $\frac{1}{z_0^2}$) for non-singlet scalar modes obtained for $(\theta_1, \theta_2, \rho) = (-\frac{\pi}{2}, \frac{\pi}{2}, 0)$ (left panel), and for $(\theta_1, \theta_2, \rho) = (1.2\pi, 0.3\pi, 2)$ (right panel).

In this sector we found again self-adjoint boundary conditions leading to no unstable modes for all values of ξ_0 , as in the left panel of fig. 24, or for values of ξ_0 larger than a few units, as in the right panel of fig. 24. However, unstable boundary conditions were more difficult to find in this sector.

In all cases, our tests convey useful information only for low-enough values of ξ , since the test functions contain higher-order corrections in ξ that we left out. However, the formal arguments in Section 10.2 indicate that the large- ξ behavior leads to positive $m^2 \sim |\mathbf{k}|^2$, due to the diagonal terms in the Hamiltonians.

References

- [1] For reviews see: M. B. Green, J. H. Schwarz and E. Witten, “Superstring Theory”, 2 vols. Cambridge, UK: Cambridge Univ. Press (1987); J. Polchinski, “String theory”, 2 vols. Cambridge, UK: Cambridge Univ. Press (1998); C. V. Johnson, “D-branes,” USA: Cambridge Univ. Press (2003) 548 p; B. Zwiebach, “A first course in string theory” Cambridge, UK: Cambridge Univ. Press (2004); K. Becker, M. Becker and J. H. Schwarz, “String theory and M-theory: A modern introduction” Cambridge, UK: Cambridge Univ. Press (2007); E. Kiritsis, “String theory in a nutshell”, Princeton, NJ: Princeton Univ. Press (2007).
- [2] R. Rohm, Nucl. Phys. B **237** (1984), 553; C. Kounnas and M. Porrati, Nucl. Phys. B **310** (1988), 355; S. Ferrara, C. Kounnas, M. Porrati and F. Zwirner, Nucl. Phys. B **318** (1989), 75; C. Kounnas and B. Rostand, Nucl. Phys. B **341** (1990), 641; I. Antoniadis and C. Kounnas, Phys. Lett. B **261** (1991), 369; E. Kiritsis and C. Kounnas, Nucl. Phys. B **503** (1997), 117 [arXiv:hep-th/9703059 [hep-th]].
- [3] I. Antoniadis, E. Dudas and A. Sagnotti, Nucl. Phys. B **544** (1999), 469 [arXiv:hep-th/9807011 [hep-th]]; I. Antoniadis, G. D’Appollonio, E. Dudas and A. Sagnotti, Nucl. Phys. B **553** (1999), 133 [arXiv:hep-th/9812118 [hep-th]]; I. Antoniadis, G. D’Appollonio, E. Dudas and A. Sagnotti, Nucl. Phys. B **565** (2000), 123 [arXiv:hep-th/9907184 [hep-th]].
- [4] A. Sagnotti, in Cargese ’87, “Non-Perturbative Quantum Field Theory”, eds. G. Mack et al (Pergamon Press, 1988), p. 521, arXiv:hep-th/0208020; G. Pradisi and A. Sagnotti, Phys. Lett. B **216** (1989) 59; P. Horava, Nucl. Phys. B **327** (1989) 461, Phys. Lett. B **231** (1989) 251; M. Bianchi and A. Sagnotti, Phys. Lett. B **247** (1990) 517; M. Bianchi and A. Sagnotti, Nucl. Phys. B **361** (1991) 519; M. Bianchi, G. Pradisi and A. Sagnotti, Nucl. Phys. B **376** (1992) 365; A. Sagnotti, Phys. Lett. B **294** (1992) 196 [arXiv:hep-th/9210127]. For reviews see: E. Dudas, Class. Quant. Grav. **17** (2000) R41 [arXiv:hep-ph/0006190]; C. Angelantonj and A. Sagnotti, Phys. Rept. **371** (2002) 1 [Erratum-ibid. **376** (2003) 339] [arXiv:hep-th/0204089].
- [5] L. J. Dixon and J. A. Harvey, Nucl. Phys. B **274** (1986) 93; L. Alvarez-Gaume, P. H. Ginsparg, G. W. Moore and C. Vafa, Phys. Lett. B **171** (1986) 155.

- [6] A. Sagnotti, [arXiv:hep-th/9509080 [hep-th]], Nucl. Phys. B Proc. Suppl. **56** (1997), 332 [arXiv:hep-th/9702093 [hep-th]].
- [7] S. Sugimoto, Prog. Theor. Phys. **102** (1999) 685 [arXiv:hep-th/9905159]; I. Antoniadis, E. Dudas and A. Sagnotti, Phys. Lett. **B 464** (1999) 38 [arXiv:hep-th/9908023]; C. Angelantonj, Nucl. Phys. **B 566** (2000) 126 [arXiv:hep-th/9908064]; G. Aldazabal and A. M. Uranga, JHEP **9910** (1999) 024 [arXiv:hep-th/9908072]; C. Angelantonj, I. Antoniadis, G. D’Appollonio, E. Dudas and A. Sagnotti, Nucl. Phys. **B 572** (2000) 36 [arXiv:hep-th/9911081]. For recent reviews, see: J. Mourad and A. Sagnotti, [arXiv:1711.11494 [hep-th]], LHEP **2021** (2021), 219 [arXiv:2107.04064 [hep-th]].
- [8] E. Dudas and J. Mourad, Phys. Lett. B **514** (2001) 173 [hep-th/0012071]; G. Pradisi and F. Riccioni, Nucl. Phys. B **615** (2001) 33 [hep-th/0107090]; N. Kitazawa, JHEP **1804** (2018) 081 [arXiv:1802.03088 [hep-th]].
- [9] S. S. Gubser and I. Mitra, JHEP **07** (2002), 044 [arXiv:hep-th/0108239 [hep-th]].
- [10] J. Mourad and A. Sagnotti, Phys. Lett. B **768** (2017) 92 [arXiv:1612.08566 [hep-th]].
- [11] S. Raucci, Phys. Lett. B **837** (2023), 137663 [arXiv:2209.06537 [hep-th]].
- [12] Z. K. Baykara, D. Robbins and S. Sethi, [arXiv:2212.02557 [hep-th]].
- [13] I. Basile, J. Mourad and A. Sagnotti, JHEP **01** (2019), 174 [arXiv:1811.11448 [hep-th]].
- [14] J. Mourad and A. Sagnotti, JHEP **08** (2023), 041 [arXiv:2305.09587 [hep-th]].
- [15] E. Dudas and J. Mourad, Phys. Lett. **B 486** (2000) 172 [arXiv:hep-th/0004165].
- [16] J. H. Schwarz, Nucl. Phys. B **226** (1983), 269; P. S. Howe and P. C. West, Nucl. Phys. B **238** (1984), 181.
- [17] J. Mourad and A. Sagnotti, JHEP **12** (2021), 137 [arXiv:2109.06852 [hep-th]].
- [18] J. Mourad and A. Sagnotti, JHEP **12** (2021), 138 [arXiv:2109.12328 [hep-th]].
- [19] J. Mourad and A. Sagnotti, JHEP **08** (2022), 301 [arXiv:2206.03340 [hep-th]].
- [20] D. Z. Freedman, P. van Nieuwenhuizen and S. Ferrara, Phys. Rev. **D 13** (1976) 3214; S. Deser and B. Zumino, Phys. Lett. **B 62** (1976) 335. For recent reviews see: D. Z. Freedman and A. Van Proeyen, “Supergravity,” (Cambridge, Cambridge Univ. Pr.,2012) 607 p.;

- G. Dall'Agata and M. Zagermann, “Supergravity: From First Principles to Modern Applications,” *Lect. Notes Phys.* **991** (2021), 1-263 2021.
- [21] M. Henneaux and C. Teitelboim, *Phys. Lett. B* **206** (1988), 650.
- [22] J. Mourad and A. Sagnotti, *Phys. Lett. B* **804** (2020), 135368 [arXiv:2002.05372 [hep-th]].
- [23] C. Vafa, [arXiv:hep-th/0509212 [hep-th]]; N. Arkani-Hamed, L. Motl, A. Nicolis and C. Vafa, *JHEP* **06** (2007), 060 [arXiv:hep-th/0601001 [hep-th]]; T. Banks and N. Seiberg, *Phys. Rev. D* **83** (2011), 084019 [arXiv:1011.5120 [hep-th]]. For a review see: E. Palti, *Fortsch. Phys.* **67** (2019) no.6, 1900037 [arXiv:1903.06239 [hep-th]].
- [24] K. M. Case, *Phys. Rev.* **80** (1950) 797; M. A. Naimark, “Linear Differential Operators”, vols. I and II (London, Ge.C. Harrap & C, 1968); N. I. Akhiezer and I. Glazman, “Theory of Linear Operators in Hilbert Space”, parts I and II (New York, Dover Publications, 1993); C. Lanczos, “Linear Differential Operators” (Philadelphia, SIAM, 1996).
- [25] D. M. Gitman, I. V. Tyutin and B. L. Voronov, “Self-Adjoint Extensions in Quantum Mechanics” (Hiedelberg, Birkhauser-Springer, 2010); B. C. Hall, “Quantum Theory for Mathematicians” (New York, Springer, 2013).
- [26] See, for example, D. M. Gitman, I. V. Tyutin and B. L. Voronov, “Self-Adjoint Extensions in Quantum Mechanics” (Heidelberg, Birkhauser-Springer, 2010); B. C. Hall, “Quantum Theory for Mathematicians” (New York, Springer, 2013).
- [27] NIST Handbook of Mathematical Functions, eds. F.W. J. Olver et al (Cambridge, Cambridge Univ. Press, 2015).
- [28] J. Mourad and A. Sagnotti, “Effective Orientifolds from Broken Supersymmetry”, to appear.
- [29] E. Bergshoeff, R. Kallosh, T. Ortin, D. Roest and A. Van Proeyen, *Class. Quant. Grav.* **18** (2001) 3359 [hep-th/0103233].
- [30] L. J. Dixon, J. A. Harvey, C. Vafa and E. Witten, *Nucl. Phys. B* **261** (1985), 678-686; L. J. Dixon, J. A. Harvey, C. Vafa and E. Witten, *Nucl. Phys. B* **274** (1986), 285-314
- [31] P. Horava and E. Witten, *Nucl. Phys. B* **460** (1996), 506-524 [arXiv:hep-th/9510209 [hep-th]]; P. Horava and E. Witten, *Nucl. Phys. B* **475** (1996), 94-114 [arXiv:hep-th/9603142 [hep-th]].

- [32] L. Randall and R. Sundrum, Phys. Rev. Lett. **83** (1999), 3370 [arXiv:hep-ph/9905221 [hep-ph]]; L. Randall and R. Sundrum, Phys. Rev. Lett. **83** (1999), 4690 [arXiv:hep-th/9906064 [hep-th]].
- [33] J. McNamara and C. Vafa, [arXiv:1909.10355 [hep-th]]; M. Montero and C. Vafa, JHEP **01** (2021), 063 [arXiv:2008.11729 [hep-th]]; G. Buratti, M. Delgado and A. M. Uranga, JHEP **06** (2021), 170 [arXiv:2104.02091 [hep-th]]; G. Buratti, J. Calderón-Infante, M. Delgado and A. M. Uranga, JHEP **10** (2021), 037 [arXiv:2107.09098 [hep-th]]; R. Blumenhagen, N. Cribiori, C. Kneissl and A. Makridou, JHEP **08** (2022), 204 [arXiv:2205.09782 [hep-th]]; S. Raucci, Nucl. Phys. B **985** (2022), 116002 [arXiv:2206.06399 [hep-th]]; R. Blumenhagen, C. Kneissl and C. Wang, JHEP **05** (2023), 123 [arXiv:2303.03423 [hep-th]].
- [34] E. Cremmer, “Supergravities in 5 Dimensions,” in “Superspace and supergravity”, eds S. Hawking and M. Rocek (Cambridge Univ. Press, 1981), LPTENS-80-17; M. Gunaydin, L. J. Romans and N. P. Warner, Phys. Lett. B **154** (1985), 268.
- [35] For reviews see: M. Grana, Phys. Rept. **423** (2006), 91 [arXiv:hep-th/0509003 [hep-th]]; A. Tomasiello, “Geometry of String Compactifications” (Cambridge Univ. Press, 2021).